DONALDSON, ROBERT W.
--Frequency assignment for land mobile radio system in the 900 MHz band : suitability of new modulation techniques over land mobile channels.

FINAL REPORT

FREQUENCY ASSIGNMENT FOR LAND MOBILE RADIO SYSTEM IN THE 900 MHz BAND: SUITABILITY OF NEW MODULATION TECHNIQUES OVER LAND MOBILE CHANNELS

by

Dr. Robert W. Donaldson, Professor

Department of Electrical Engineering

Faculty of Applied Science

The University of British Columbia

for

Department of Communications

Ottawa, Ontario, CANADA

under

Department of Supply and Services Contract Serial No: OSU81-00123

Period: July 1, 1981 - February 28, 1982

ABSTRACT

To assess the suitability of narrowband land mobile communication channels for digital transmission requires knowledge of bit-error rate behaviour in the presence of Rayleigh fading, shadowing and mobile-base distance changes. The bit-error probability $\bar{p}$ averaged over Rayleigh fading is determined in terms of co-channel and adjacent-channel interference levels. Co-channel levels depend on the assignment of channels to cells. Adjacent-channel levels depend on the ratio of bit rate R to channel separation Δ, as well as on the digital signalling format for data or the transmitted spectrum for analog FM. Adjacent-channel levels are determined for easily implemented signalling schemes including staggered quadrature differential PSK and FSK.

Distribution and density functions for $\bar{p}$ are determined for interference-limited systems in terms of the propagation factor n and shadowing variance σ (typically, $n \simeq 3.5$ and $\sigma \simeq 9$ dB). It is found that variations in $\bar{p}$ from shadowing are more severe than are variations from distance separations. The distribution for $\bar{p}$ enables determination of the probability that $\bar{p}$ exceeds any given value. The density function permits the average of $\bar{p}$ over the radio coverage area to be calculated. The number of groups of channels needed in a cellular plan to obtain any desired average $\bar{p}$ value is then obtainable, as well as the maximum R/Δ value for a given data signalling format. The spectrum efficiency can then be determined, and is determined for several fixed channel-assignment schemes. A 7-cell pattern with 120° sectoral illumination proposed by American Telephone and Telegraph is found to have a maximum efficiency of 0.20 bits/sec/Hz/cell.

Spread spectrum multiple access (SSMA) systems are described, and their spectrum efficiencies are compared with those of narrowband systems. SSMA systems with isotropic antennae at cell-centre have maximum efficiencies of 0.17 bits/sec/Hz/cell. Use of 120° sectoral antennae at cell corners would increase this efficiency threefold. SSMA advantages include substantial reduction of Rayleigh fading effects, unrestricted system access, message privacy, absence of channel switching as users cross cell boundaries, and potential for co-existence with other systems. Primary disadvantages include complexity and cost, and synchronization delays.

All spectrum efficiencies determined excluded overheads from synchronization, retransmissions, acknowledgements and in the case of narrowband systems, channel scanning. Of particular importance is SSMA synchronization, which can involve times comparable to message transmission times. Further study to determine and minimize these overheads is recommended, in order that final comparisons of obtainable spectrum efficiencies can be determined.

TABLE OF CONTENTS

LIST OF ILLUSTRATIONS

LIST OF TABLES

I. INTRODUCTION

I-1 Scope and Objectives of the Study

This report presents the results of a Communications Canada Contract study whose motivation, purpose and general approach are summarized below.

MOTIVATION

Recent advances in Land Mobile system development has provided increasing evidence that digital transmission of dispatch data as well as other digitally encoded information will constitute an important part of Land Mobile communication traffic. The need for the development of guidelines identifying transmission characteristics, requirements, and limitations of digital transmission is becoming increasingly urgent. These guidelines would lead to the development of new regulations and standards governing the technical characteristics and operation of equipment and systems employing digital transmission of information over Land Mobile communication channels.

The following items are of specific interest.

1) Comparison of spread spectrum techniques with conventiona analog FM over Land Mobile channels.
2) Bit error rate analysis over digital mobile channels; effect of noise, interference, fading, and mobile base distance.
3) FM noise interference into digital mobile channels; different types of voice models.
4) Equipment complexity for digital mobile communication systems for modulation techniques not covered in previous contracts.

PURPOSE

To produce technical data in support of the development of guidelines for the use and operation of Land Mobile radio equipment and systems in the 900 MHz band for communication over Land Mobile channels utilizing digital modulation techniques.

At the outset it was recognized that an important part of the study would involve selection of an approach which woiuld provide useful technical data consistent with the study's motivation and purpose.

GENERAL APPROACH AND RESULTS

Proper assessment of systems for digital transmission over conventional narrowband channels requires accurate determination of bit-error rate (BER) as described in item 2 above. Considerable effort was therefore devoted to BER determination. The method developed here involves calculation of bit-error probability $\bar{p}$ averaged over Rayleigh fading of both the signal and interference levels, followed by determination of the probability distribution of $\bar{p}$ which results from shadowing and mobile-base distance separation changes. Our approach enables direct computation of $\bar{p}$, its distribution, and its average $\langle\bar{p}\rangle$ over shadowing and distance variations, in terms of the shadowing variance, propagation constant, digital modulation format, bit-rate, channel separation and co-channel and adjacent-channel interference levels. Both types of interference are treated in a unified way, whether from transmission of data or FM voice.

Distributions and $\langle\bar{p}\rangle$ are actually determined for those modulation formats suitable for land mobile channels, and for some cellular system channel

assignment schemes. Sectrum efficiencies in bits/sec/Hz are obtained, for various blocking probabilities (or delay) and $\langle\bar{p}\rangle$ values. The overall result is an accurate and meaningful basis for system design, evaluation, performance assessment and performance comparison with other systems including SSMA.

An earlier report in January, 1980 detailed FM voice interference calculations, based on a Gaussian speech model. It was shown that the pre-modulation signal processing together with the speech spectrum determines the transmitted FM spectrum and its spectral attenuation rate. Once the transmitted FM spectrum has been calculated the approach developed in this report is readily used to determine $\bar{p}$, its distribution and $\langle\bar{p}\rangle$.

Spectrum efficiencies for SSMA systems are available in the literature. These results were used for comparisons with narrowband systems. All comparisons assume that all bits transmitted are message information bits. Overhead from synchronization, retransmissions and acknowledgement reduces the spectrum efficiency, and final comparisons should include these overheads. Of particular importance is SSMA synchronization, which can involve times comparable to message transmission times.

Equipment complexity considerations are incorporated throughout the report.

I-2 Executive Summary

Chapter 2 begins with a brief summary of the functional parts of digital communication systems. Three basic types of information to be transmitted over land mobile radio channels are identified, including speech, text and control information. The speed vs. accuracy requirements for each of these

is different. Speech transmission is in real-time at a high data rate with non-stringent accuracy requirements, while control information requires high accuracy but not real-time transmission.

Chapter 2 also reviews the physical characteristics of conventional narrowband land mobile radio channels, which include signal level variations resulting from fading, shadowing and base-mobile distance changes. These variations can exceed 90 dB, and result in orders of magnitude variations in bit-error probability over a radio coverage area. Various alternatives to reduce the effects of these variations are summarized. Spectrum efficiency O/N in bits/sec/Hz is defined, and the effects of message traffic parameters, channel assignments, channel codes, bit rate, channel separation and other factors on spectrum efficiency are described. The way in which channel access delay or channel blocking probability relates to spectrum efficiency is explained.

Chapter 3 deals with relationships between modulation formats, adjacent-channel and co-channel interference, bit-error probability, and channel encoding. The interference-to-signal power ratio SNR^{-1} is determined for coherently detected binary PSK, staggered quadrature PSK (SQPSK) and MSK (a type of FSK). SQPSK and FSK are constant-envelope signals, with implementation advantages. The approach is then extended to include non-coherently detected FSK, which has a simple receiver structure. The approach permits SNR^{-1} to be determined in terms of the receiver filter characteristic, the basic modulator pulse shape and Δ/R where Δ is the channel spacing in Hz and R the bit rate. The approach also permits a unified treatment of co-channel and adjacent-channel interference, whether from other data or FM voice

signals. Modulator design to reduce both types of inteference is discussed.

When many interfering signals are present, the bit-error probability p can be determined in terms of SNR, and averaged over Rayleigh fading. For high signal-to-interference ratios, $\bar{p} \sim \overline{SNR}^{-1}$ where $\overline{SNR}$ is the average signal to average interference power ratio.

The benefits of channel encoding for forward error correction and/or error detection are sumarized. Appropriate design values for $\bar{p}$ are considered. The choice $\bar{p} \simeq 10^{-3}$ is deemed adequate for speech, with some channel encoding required for text and control messages. For $\bar{p} \simeq 10^{-2}$, some coding would likely be needed for speech transmission.

Chapter 4 presents a detailed examination of the variation of $\bar{p}$ as a result of shadowing and distance variations between transmitter and receiver. The probability distribution and density functions for $\bar{p}$ are determined with shadowing variance σ (in dB) and distance propagation factor n as variables. Variations in $\bar{p}$ from shadowing tend to be larger than variations caused by distance changes. Variations are largest for one interfering signal, and decrease as the number of interferers increase.

The distribution for $\bar{p}$ enables the required $\overline{SNR}$ value to be determined such that $\bar{p}$ is less than any given value, with any specified probability. For narrowband cellular systems which reuse frequency channels, this $\overline{SNR}$ limitation translates into a minimum Δ/R value to limit adjacent-channel interference, and a minimum number of channel groups G to limit co-channel interference. The resulting spectrum efficiency obtainable is then readily determined.

In Chapter 5 the density function for $\bar{p}$ is used to determine $\langle\bar{p}\rangle$, the bit-error probability averaged over shadowing and distance separation. This result is then used to determine G and R/Δ in cellular plans, given $\langle\bar{p}\rangle$. Typically $\sigma \simeq 9$ and $n = 4$ in a large urban area. For $\langle\bar{p}\rangle \simeq 3\times10^{-3}$, $G \cong 43$ for SODPSK (D ~ differential), DMSK, and FSK-PSK and $G > 63$ for FSK, with a single isotropic base antenna at cell centre. The maximum spectrum efficiency in bits/sec/Hz/cell which results for a 16-cell system is $O/N \simeq 0.033$, 0.078, 0.039 for SODPSK, DMSK and FSK-PSK respectively. For a 21-cell system using FSK, $O/N \simeq 0.053$. These results are obtained by requiring that adjacent-channel interference levels not exceed co-channel levels.

Spectrum efficiency can be increased by use of directional antennae at cell corners, and by the use of channel encoding. The 7-cell system of American Telephone and Telegraph, for example, yields $O/N \simeq 0.20$ with $\langle\bar{p}\rangle \simeq 3\times10^{-3}$ when $\sigma = 6$ and 2×10^{-2} when $\sigma = 9$. In the case $\sigma = 9$ a (31,21) double-error-correcting Hamming code reduces the average bit-error probability after decoding to $\langle\bar{p}_i\rangle \simeq 3\times10^{-3}$, with a 33% reduction in spectrum efficiency. If a (31,26) single-error-correcting code is used for error-detection with retransmission, $\langle\bar{p}_i\rangle \simeq 10^{-4}$ with a 55% reduction in maximum spectrum efficiency to 0.09 bits/sec/Hz/cell when $\sigma = 9$. Coding results are based on an independent-error channel, implying totally effective interleaving of bits which could not always be achieved in practise.

Actual spectrum efficiencies would be reduced from maximum values in accordance with the delay or blocking probability P_B and the number of channels per mobile m. For the AT&T system, m = 96 channels/mobile/cell. With $P_B = 0.02$ the actual efficiency is 85% of the maximum; with $P_B = 0.20$ this

value is 96%. The reduction factor increases with G, which should be minimized.

Spread spectrum systems are considered in Chapter 6. Advantages of SSMA include substantial reduction of Rayleigh fading effects, no hard limits on system access, some message privacy, absence of channel switching upon crossing of cell boundaries, and potential for coexistence with other systems. The primary disadvantage is the cost and complexity of mobile transceiver hardware. Existing spectrum efficiency results available in the literature are described and compared with each other, and with the results obtained for narrowband systems.

Spectrum efficiencies Q/N for the 7-cell AT&T system with 120° sectoral illumination and SSMA cellular systems with isotropic antennae are comparable. However, 120° sectoral illumination improves Q/N threefold for SSMA. Channel encoding and/or switched diversity improves Q/N for narrowband systems. All of these comparisons assume negligible overhead bits for synchronization, retransmissions, acknowledgements and in the case of narrowband systems, channel scanning. In cases involving communication of short, interactive messages overheads may be considerable, particularly when SSMA synchronization is involved. Final spectrum efficiency comparisons require analysis and minimization of these overheads.

Chapter 6 includes some policy considerations, including appropriate choices for (narrowband) channel spacing Δ and bit rate R. Part of the band could have $\Delta \simeq R \simeq 12$ kHz with $R \simeq \Delta \simeq 30$ kHz over the rest of the band. Such an arrangement together with channel encoding would make narrowband systems practically as flexible in data rates as SSMA.

II INFORMATION SOURCES, LAND MOBILE CHANNELS AND SPECTRUM EFFICIENCY

II-1 Digital Communication Transceivers

Fig. 2-1 shows in block diagram a digital communication link, whose component subsystems perform the following tasks [G1, L1]:

1. Source encoder: converts the message source which may be either analog or digital into a binary digit stream which ideally has no redundancy.
2. Channel encoder: maps source digit sequences into channel digit sequences which contain controlled amounts of redundancy to combat channel transmission errors, either by means of forward error correction, or error detection and retransmission, or both.
3. Modulator: converts binary digit sequences from the channel encoder into signals suitable for transmission over the physical waveform channel.
4. Demodulator: extracts from the received signal r(t) a replica of the channel-encoded digits.
5. Channel Decoder: maps the demodulated binary digits into source digits.
6. Source Decoder: uses the channel decoder output bits to reconstruct a replica of the original message.

The term digital communication implies a fundamental constraint on the transmitter and receiver in Fig. 2-1, namely that the transmitted signal consists of a superposition of time-translates of a few basic signals [L1]. For land mobile applications, binary signalling is particularly attrative [D1], and particular emphasis is placed on signals which minimize adjacent-channel interference.

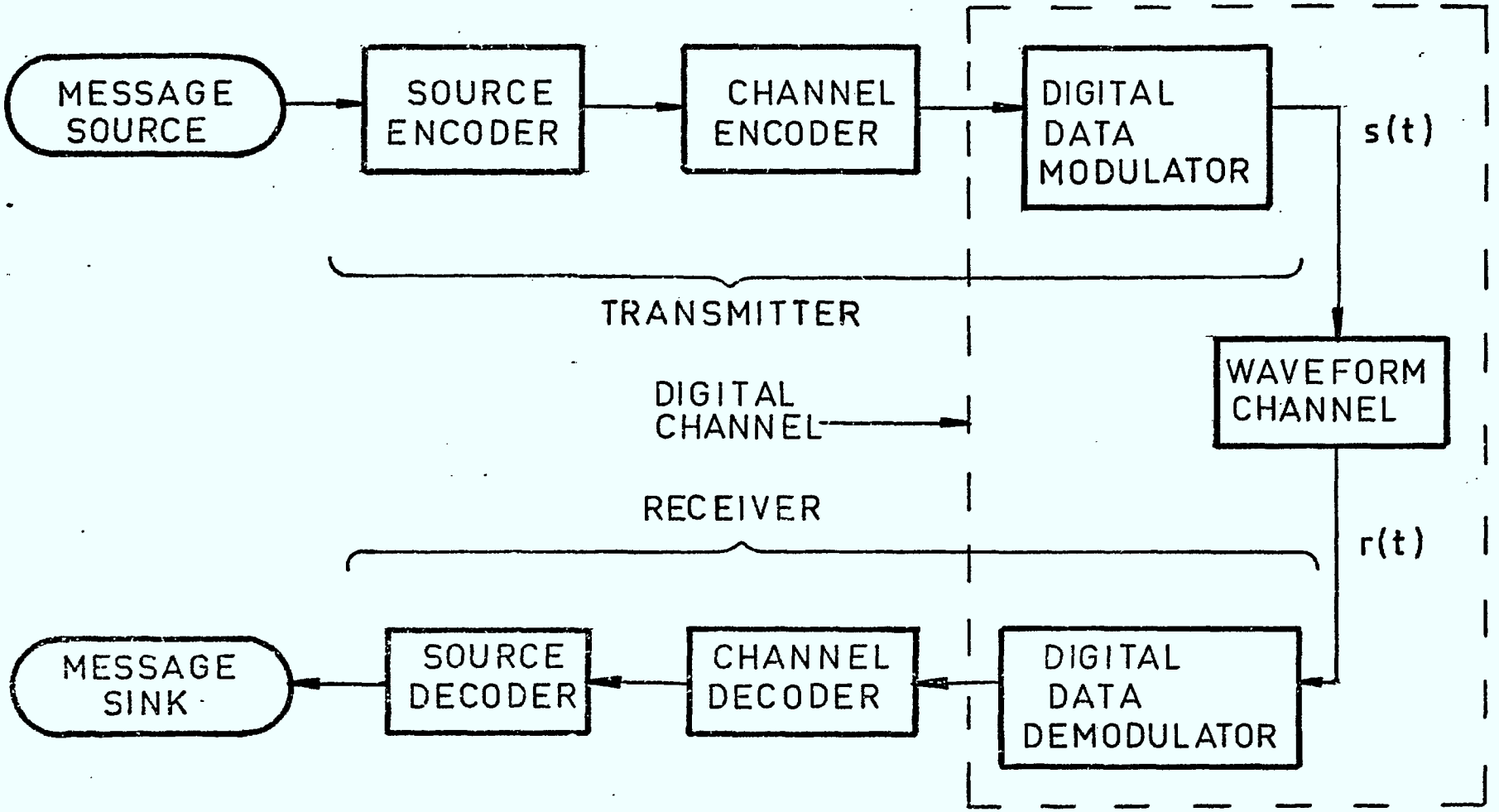

Fig. 2-1 Block diagram of a digital communication link.

The restriction to digital signalling is for ease of system implementation. Even with this constraint, the bit-error probability can be made arbitrarily small by proper channel encoder/decoder design provided that the rate at which source digits are transmitted does not exceed the capacity in bits/sec of the digital channel [L1, G1, W1]. Simplicity of implementation as well as symbol synchronization capability is an added consideration in modulator and demodulator design [L2, S1].

Effective channel encoders can be implemented using linear feedback shift registers [G1, L3, P1]. Decoding is more difficult and, except for some selected (but very useful) codes, requires decoding algorithms whose implementation is often prohibitively expensive. Design and performance analysis of channel encoders and decoders requires knowledge of the bit-error statistics of the digital channel in Fig. 2-1, including bit-error dependencies. Further discussion appears in Section 3-4.

The continuing cost/benefit trend of micro-circuits promises improved source encoding. Such improvements are needed for highly redundant sources such as speech and video data if significant reductions in transmitted bit rates (and therefore in required channel bandwidth) are to be realized. The various types of information sources are described below.

II-2 Information Sources for Land Mobile Radio Channels

Three types of information can be identified as requiring transmission over land mobile radio channels, as follows:

1. Speech is real-time information with considerable natural redundancy. In the absence of a prohibitively larger storage buffer, speech requires

transmission as it is generated; i.e. real-time transmission. The actual source information rate is less than 100 bits/sec. However, conventional 7-bit PCM transmission of speech sampled at 8 KMZ requires 56 Kb/s. Three-bit DPCM, which is equivalent in quality to 4-bit PCM requires 24 Kb/s [Y1]. Adaptive DPCM at 16 Kb/s is comparable to 4- or 5-bit DPCM [H1, C1, C5]. Coding based on analysis/synthesis methods at rates as low as 2400 bits/s [F2] may soon be practical.

2. Text information like voice contains redundancy. Shannon [S2] estimated that English text is approximately 50% redundant in that random deletion of up to half of the message does not prevent reconstruction (possibly with difficulty) of the remainder. Text does not normally require real-time transmission. Transmission errors are annoying in that they may cause "spelling" errors upon reconstruction of the received text. However, these errors are normally correctable by the reader provided they don't occur too frequently. Video facsimile would fall into the text information category because of its redundant and non-real-time nature, although buffer storage limitations may require a scanning rate commensurate with average data transmission rate.

3. Control information includes vehicle status reports, vehicle dispatch orders and street addresses. Because control information contains minimal redundancy, accuracy of its transmission is essential. Although real-time transmission of control data is seldom necessary, prompt transmission is normally required.

Fortunately, information sources requiring accurate transmission do not normally require high data transmission rates; conversely, information requiring high speed transmission does not normally carry stringent accuracy requirements.

Communication in a mobile environment often involves two or all three types of information. It may be advantageous to provide for two or more digital transmission modes, one of which would favour speed while another would favour accuracy.

II-3 Physical Behaviour of Land Mobile Radio Channels

Land mobile radio channels are dispersive in time, frequency, and space [J1, C2, K1]. Relative motion between the transmitter and receiver causes the level of received narrow-band signal to fluctuate rapdily, as indicated in Fig. 2-2. These level changes are due to scattering and multipath, and vary with the receiver's spatial location and with the frequency band occupied by the signal. The rate of signal level change depends on the velocities of the mobile transceiver, which velocity is itself variable. Adjacent peaks in the signal envelope correspond to changes in the relative separation between transmitter and receiver of one-half the (narrow-band) signal's wavelength.

The amplitude probability density $f_r(\alpha)$ of the received signal level r is reasonably well approximated by the Rayleigh distribution, as follows [W1, F1]:

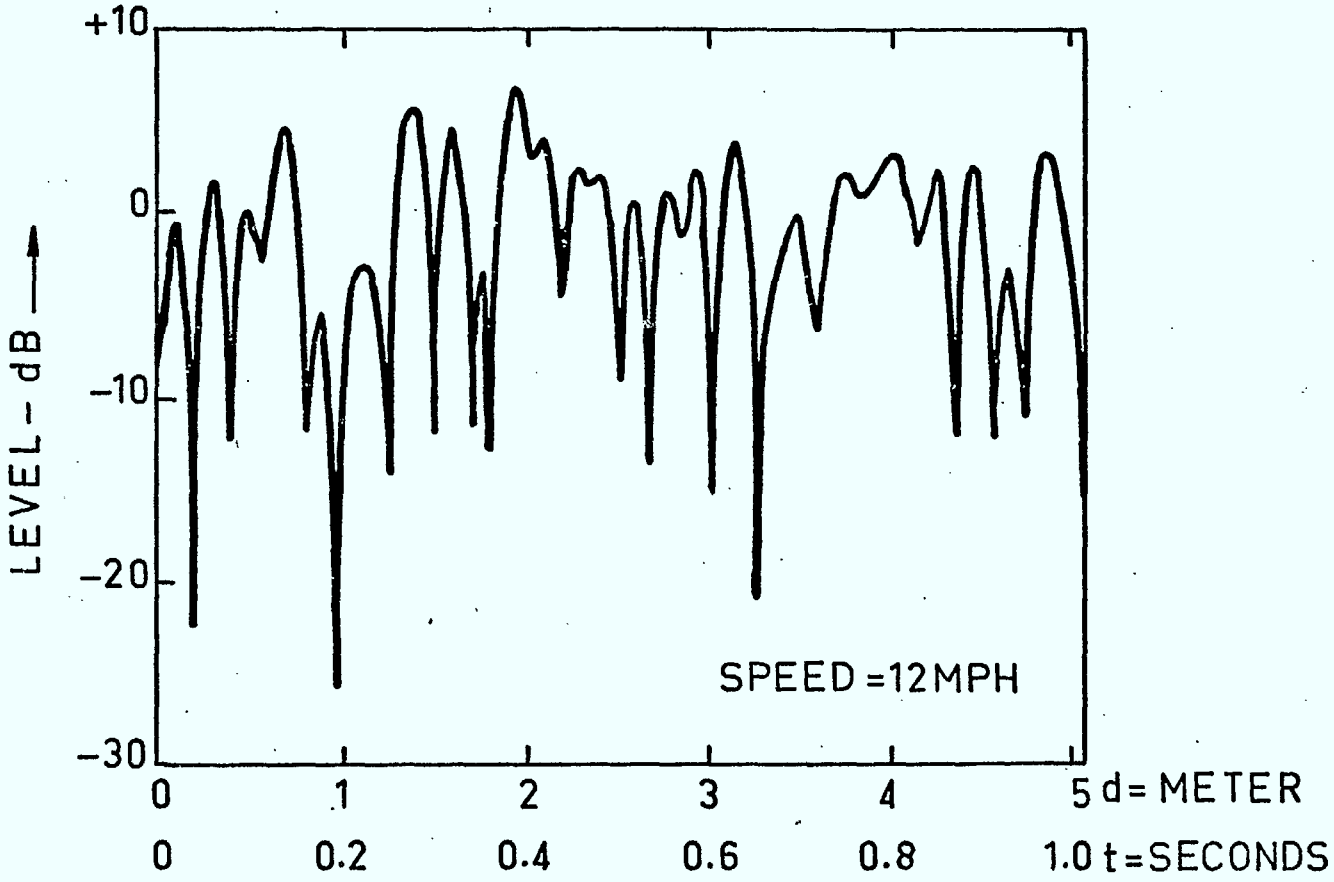

Fig. 2-2 Received signal level vs. time in an urban environment. Vehicle speed: 12 mph. Carrier frequency: 850 MHz. (after Arredondo and Smith [A1]).

$$f_r(\alpha) = \begin{cases} (2\alpha/r_o)\ \exp\ (-\alpha^2/r_o) & \alpha \geq 0 \\ 0 & \alpha < 0 \end{cases} \qquad (2\text{-}1)$$

where $s = \sqrt{\pi r_0/2}$ is the local mean level of the received signal and r_0 is the average energy in the received signal. The distribution of r^2 the received signal energy is [W1, F1]:

$$f_{r^2}(\alpha) = \begin{cases} (1/r_0)\exp(-\alpha/r_0) & \alpha \geq 0 \\ 0 & \alpha < 0 \end{cases} \qquad (2\text{-}2)$$

The local mean signal level s varies slowly over several wavelengths as a result of gradual changes in path transmission characteristics. These changes result from variations in shadowing caused by topographical features such as street width, building height and hills. The amplitude probability density of s in dB is reasonably well approximated by the log-normal distribution, as follows [J1, F1]:

$$f_s(\alpha) = \frac{1}{\sqrt{2\pi}\sigma} \exp\ (-(\alpha-m)^2/2\sigma^2) \qquad (2\text{-}3)$$

In (2-3) m is the mean signal level in dB averaged over several wavelengths (typically 50 m), and σ is the standard deviation in dB of the local mean; σ has been quated as 6 dB in London [F1] and as 8-12 dB in Japan and the U.S.A. [F1, J1].

The local mean m varies over the mobile coverage areas as the distance D between transmitter and receiver changes. This variation (in linear coordinates) is proportional to D^{-n} where $2 < n < 4$ [J1, O1] for $D \lesssim 40$ km (25 miles). The rate of attenuation of n tends to increase with D. A recent

study shows that $n \simeq 3.7$ in urban Philadelphia [01].

The rate of signal level variation relative to vehicle speed affects the performance of various digital transmission schemes. The carrier signal wavelength $\lambda = c/f$ where c is the velocity of light (3×10^8 m/sec) and f the carrier frequency. At 900 MHz, $\lambda \simeq$ 1ft. Thus, fading minima in Fig. 2-2 correspond to vehicle movements of 1/2 ft. (1/6 m). At 15 mph (22'/sec) a mobile moves 44 half-wavelengths in one sec. For data rates of 10 Kb/s, 227 bits are transmitted as a vehicle moving at 15 mph moves one-half wavelength. For data rates of 1 Kb/s, 11 bits are transmitted as a vehicle moving at 30 mph moves one-half wavelength. Thus, at 10 Kb/s and 15 mph a 100 bit data block is transmitted as the vehicle moves one-quarter wavelength. At 1 Kb/s and 30 mph a 100 bit block is transmitted as the vehicle moves 5 wavelengths. If follows that the received signal level ios relatively constant over one bit period, but not necessarily during the transmission of once data block when using conventional 30 kHz channels. The mean signal level, however, being relatively constant over 50 m, is relatively constant over one transmitted data block.

The random doppler shifts in signal frequency caused by vehicle motion also broadens the power spectral density of the radiated signal on the order of 50 Hz at 20 mph. Because radiated spectra normally have bandwidths in excess of 10 kHz, this spectrum broadening can be neglected below 1 GHz, for spectral occupancy calculations.

The signal level variations resulting from fading, local mean variations, and variations in transmitter-receiver separation D can exceed 20 dB, 10 dB and 60 dB, respectively, which together can cause a total received

signal level variation in excess of 90 dB. One way to combat these large fluctuations is to use one or more types of diversity, based on the fact that these variations are not uniform over time, space or frequency. For example, spatial diversity utilizes several base station antennas located at the edge of the radio coverage area to reduce fluctuations in base-station received signal level resulting from all these of the above-noted causes [J1]. By switching these antennas during transmission from the base station, variations in mobile receiver signal level due to shadowing and D^{-n} loss can also be reduced considerably [J1]. Space diversity systems utilize the fact that the probability of two or more transmission paths being poor at the same time is considerably less than the corresponding probability for any individual path. Forward error correcting [L1, G1] codes involve use of time diversity. Frequency diversity is an inherent part of recently proposed spread spectrum systems, in which each transceiver makes full use of the available spectrum.

An alternative to diversity involves transmitting information at a rate which depends either directly or indirectly on the signal-to-noise ratio (SNR) at the receiver. Transmission rates are high when SNR is high, and conversely. Variable-rate transmission normally implies a two-way channel between transmitter and receiver. The receiver may estimate its signal-to-noise ratio and transmit this estimate to the transmitter, whose information transmission rate is adjusted accordinly [C3, C4]. Alternatively, the decoder in the receiver may detect, rather than correct errors in transmitted bit sequences, and request retransmission of those sequences recieved in error. Retransmission probability is highest and information throughput is

lowest when SNR is low; thus, the actual information rate adjusts automatically to the state of the channel.

Again, it should be emphasized that Fig. 2-2 corresponds to a signal whose bandwidth is sufficiently narrow that the level of all frequency components vary in unison (flat fading). Conventional 30 kHz land mobile channels meet this narrow-band criterion; as indicated earlier, spread spectrum systems do not.

II-4 Spectrum Efficiency

Spectrum efficiency Q denotes the number of information bits per second carried by a system of total bandwidth B. In terms of the symbols defined in the Appendix, Q for a conventional narrowband cellular system with N cells is [D1]:

$$Q = \frac{R}{\Delta} \cdot \phi \cdot \frac{k}{n} \cdot f \cdot g(P_c) \cdot \frac{N}{G} \qquad (2\text{-}4)$$

The channel occupancy ϕ equals the expected fraction in use of the total number of available channels. This factor depends on the channel blocking probability P_B in an Erlang B environment (blocked cells cleared) or on the average message delay D in an Erlang C environment (blocked cells queued) [J1, K2]. The larger the allowed value for P_B or D, the larger is ϕ. The factor ϕ also increases as the number of channels per mobile m increases. Fig. 2-3 shows ϕ vs. the traffic carried $(\rho/m)(1-P_B)$ for various values of P_B and normalized delay d/m where

$$d/m = \mu RD \qquad (2\text{-}5)$$

This curve is obtained from those in Fig. 2-4 and 2-5, which show P_B and d

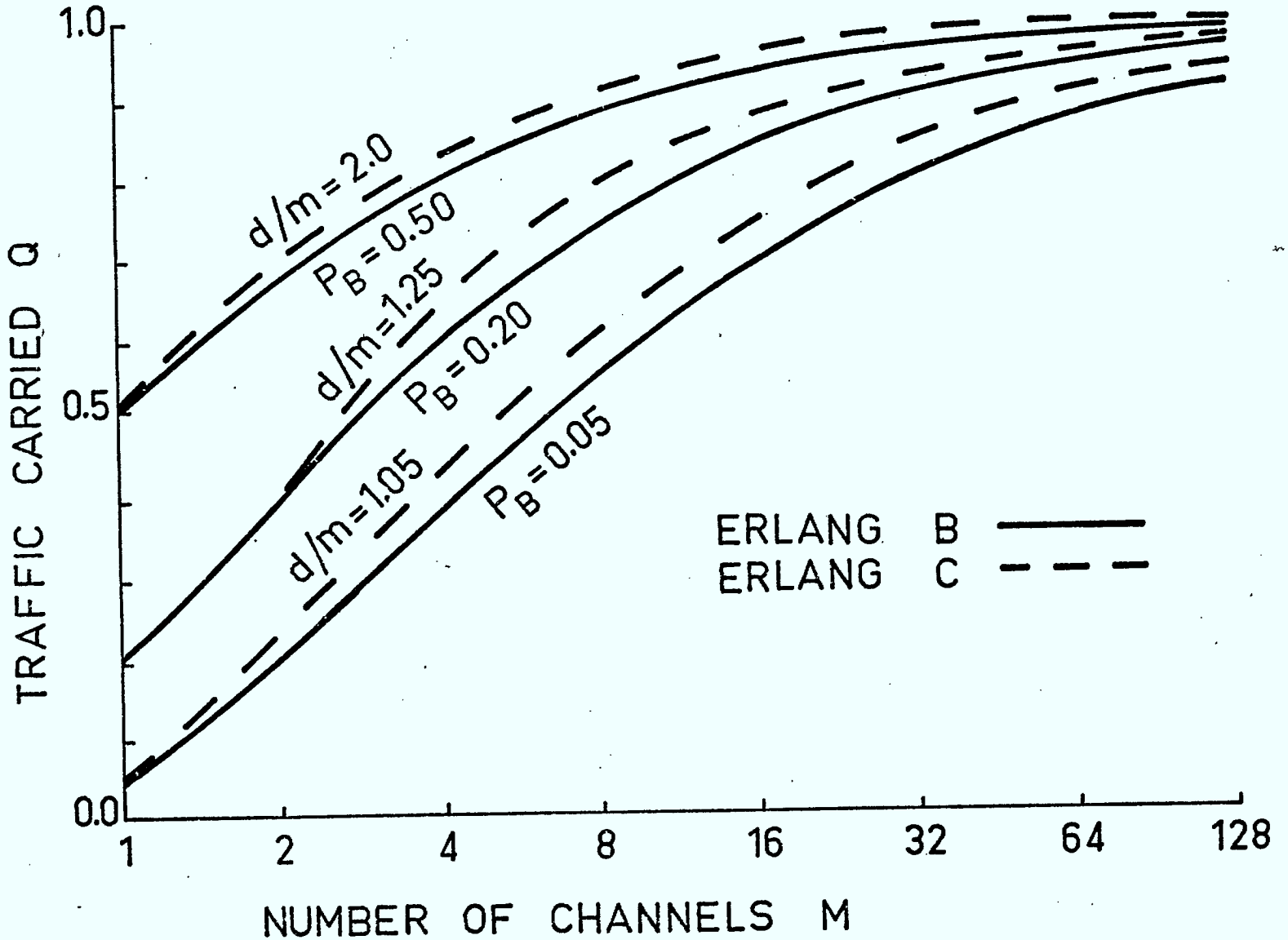

Fig. 2-3 Traffic carried (per channel) vs. number of channels m.

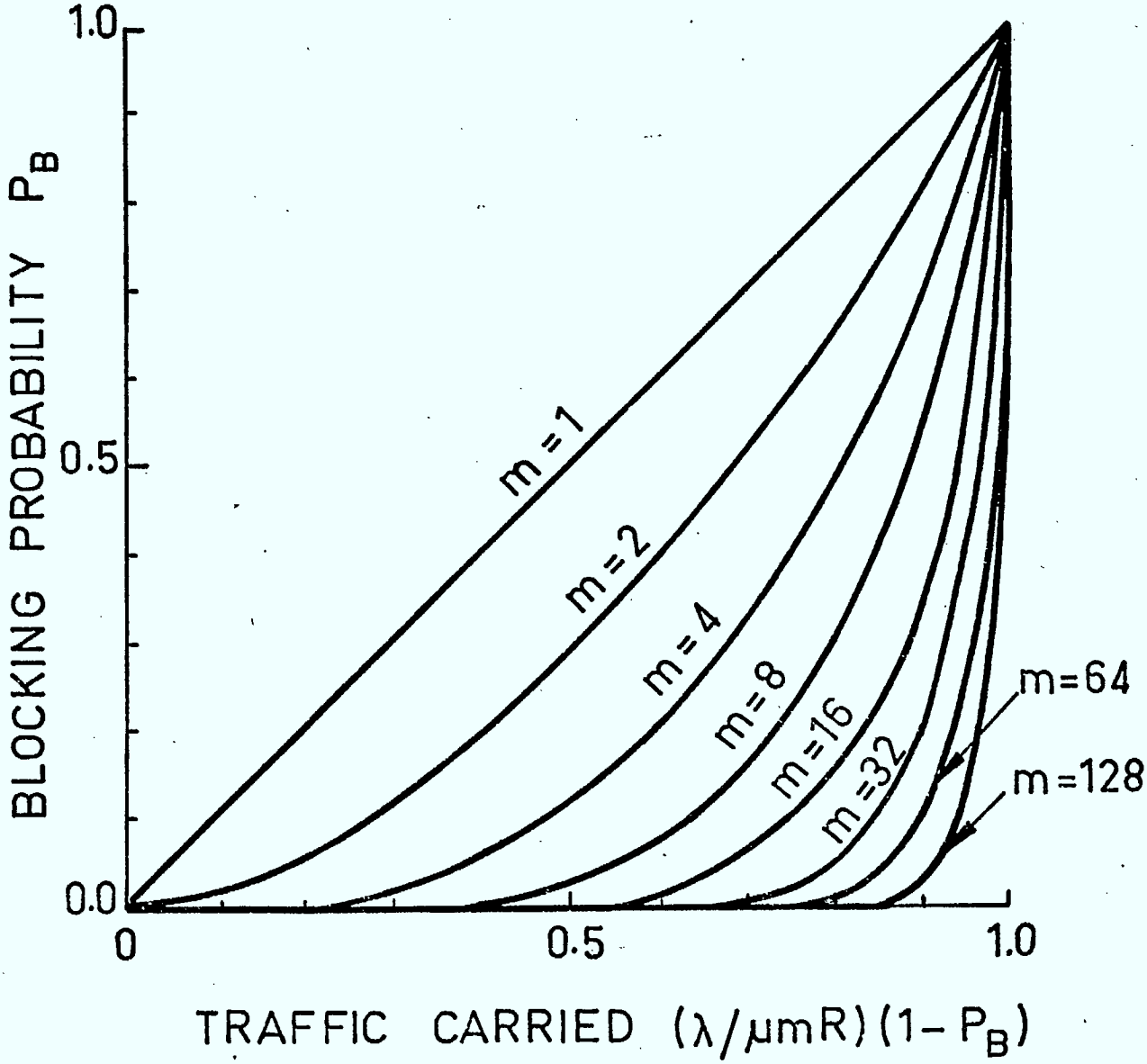

Fig. 2-4 Blocking probability P_B for an m-server system vs. traffic carried, $\rho(1-P_B)/m$ (Erlang B).

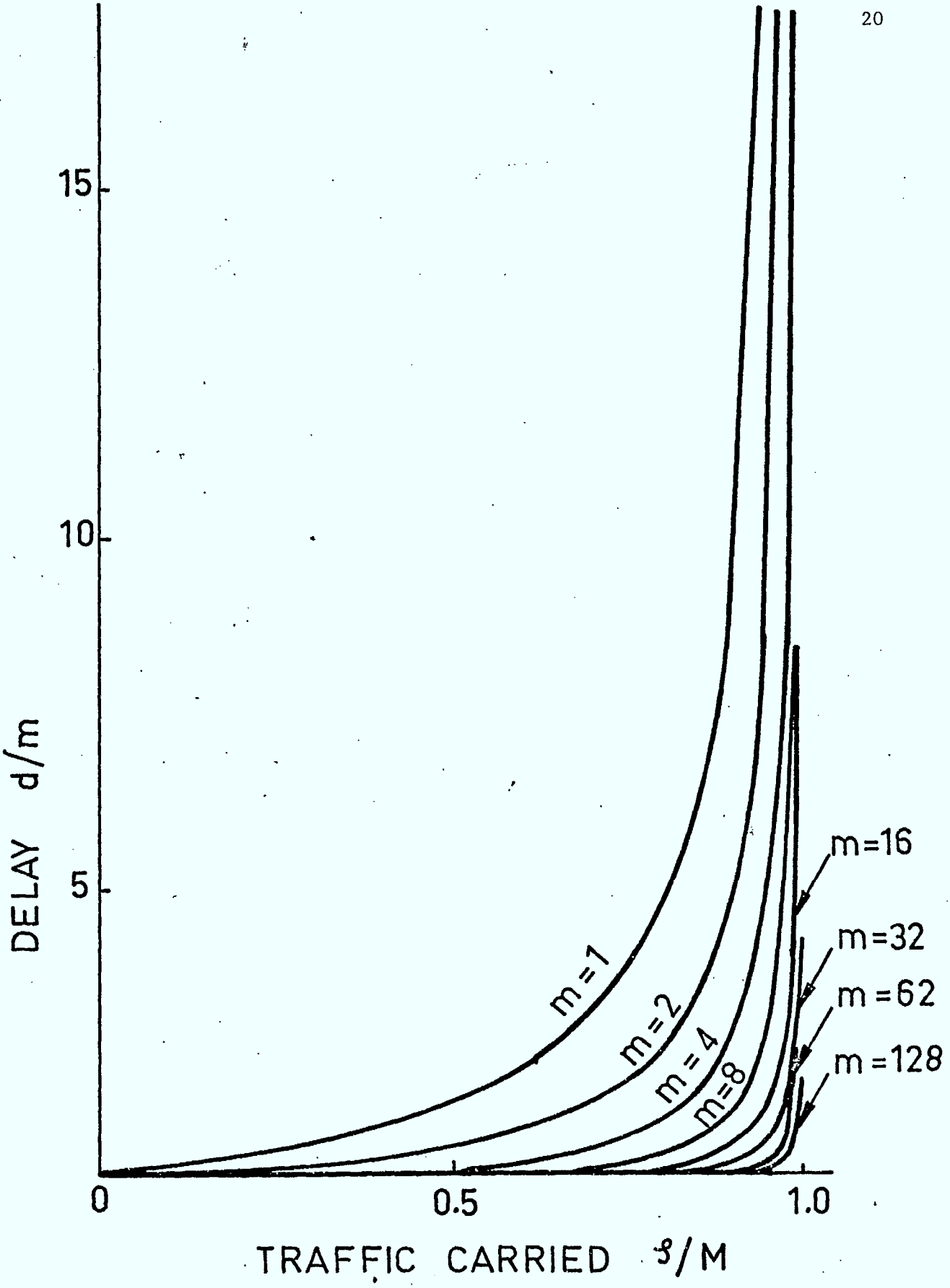

Fig. 2-5 Queuing delay (normalized) d/m for an m-server system vs. traffic carried ρ/m (Erlang C).

vs. $(\rho/m)(1-P_B)$. For Erlang C, $P_B = 0$.

For Erlang B

$$P_B = \left[\sum_{k=0}^{m} \rho^k/k!\right]^{-1} \rho^m/m! \qquad (2\text{-}6)$$

For Erlang C

$$d = m + P_m/[1 - (\rho/m)] \qquad (2\text{-}7a)$$

$$P_m = \{c_0/[1 - (\rho/m)]\}\ \rho^m/m! \qquad (2\text{-}7b)$$

$$c_0/[1 - (\rho/m)] = \{\rho\ /m! + [1 - (\rho/m)] \sum_{k=0}^{m} \rho^k/k!\}^{-1} \qquad (2\text{-}7c)$$

The utilization factor

$$\rho = \lambda/\mu R \qquad (2\text{-}8)$$

where λ is the call-attempt rate in the region A covered by the m channels. Thus,

$$\lambda = \lambda_v \int_A n(x,y)dx\ dy \qquad (2\text{-}9)$$

The size of region A and hence the value of λ decreases as the number of cells increases.

The function $g(P_c) = 1$ in (2-4) for systems which use either no channel encoding or forward error correction. In systems where message acknowledgements are sent via a return channel $g(P_c) = \overline{P}_c$ represents the probability of correct reception of a digital word, averaged over the entire coverage area. Determination of this average requires that the bit-error probability distribution be determined, since P_c depends on bit-error probability.

The factor N/G indicates the number of times a channel is reused over a coverage area. An increase in N/G increases Q directly, and also indirectly through an increase in ϕ which tends to grow with the number of channels per mobile per cell. However, either R/Δ would have to decrease to offset increased co-channel interference, or else k/n would decrease to combat channel errors, or P_c would increase. The net effect on Q depends on the parameter values, and is different in different situations.

The factor f depends on the channel control scheme and equals the fraction of the time that the channel is actually being used for successful transmission of information bits.

Channel assignments, number of cells, and modulation formats determine co-channel and adjacent-channel interference levels, which in turn determine signal-to-noise ratio, bit-error rate, P_c and required code rate k/n. Adjacent-channel interference determines the allowable R/Δ value, which directly affects Q. Choice of modulation format is important here; Chapter 3 shows that a 30 dB signal to adjacent-channel interference level requires $\Delta/R \simeq 7.5$ for conventional PSK against $\simeq 1.8$ for MSK. Similarly, choice of premodulation filters for FM voice to yield favourable R/Δ values is also of interest.

II-5 References for Chapter 2

[A1] G.S. Arrendondo and J.I. Smith, "Voice and data transmission in a mobile radio channel at 850 MHz", IEEE Trans. Veh. Technol., vol. VT-26, pp. 94-105, Feb. 1977.

[C1] D.L. Cohn and J.L. Melsa, "The residual encoder - an improved ADPCM system for speech digitization", IEEE Trans. Commun., vol. COM-23, pp. 935-941, Sept. 1975.

[C2] G.R. Cooper and R.W. Nettleton, "Spectral efficiency in cellular land-mobile communications: A spread-spectrum approach", School of Elec. Eng. Purdue Univ. Tech. Rpt. TR-EE 18-44, 1978.

[C3] J.K. Cavers, "Variable rate transmission for Rayleigh fading channels", IEEE Trans. Commun., vol. COM-20, pp. 15-22, Feb. 1972.

[C4] J.K. Cavers and S.K. Lee, "A simple buffer control for variable-rate communication systems", IEEE Trans. Commun., vol. COM-24, pp. 1045-1048, Sept. 1976.

[C5] R.V. Cox, "A comparison of three speech coders to be implemented on the digital signal processor", Bell Syst. Tech. J., vol. 60, pp. 1411-1421, Sept. 1981.

[D1] R.W. Donaldson, "Frequency assignment for land mobile radio system in the 900 MHz Band: Digital transmission over land mobile channels - Spectrum usage considerations", Report to Dept. of Communications, Ottawa, Canada, Feb. 1981.

[F1] R.C. French, "Error rate predictions and measurements in the mobile radio data channel", IEEE Trans. Veh. Technol., vol. VT-27, pp. 110-117, Aug. 1978.

[F2] J.L. Flanagan, M.R. Schroeder, B.S. Atal, R.E. Crochiere, N.S. Jayant, and J.M. Tribolet, "Speech coding", IEEE Trans. Commun., vol. COM-27, pp. 710-737, April 1979.

[G1] R.G. Gallager, Information Theory and Reliable Communication. New York, N.Y.: Wiley, 1968.

[H1] B.A. Hanson and R.W. Donaldson, "Subjective evaluation of an adaptive differential voice encoder with oversampling and entropy encoding", IEEE Trans. Commun., vol. COM-26, pp. 201-208, Feb. 1978.

[J1] W.C. Jakes, Microwave Mobile Communications. New York: Wiley, 1974.

[K1] R.S. Kennedy, Fading Dispersive Communication Channels. New York: Wiley, 1969.

[K2] L. Kleinrock, Queueing Theory, vol. 2: Computer Applications. New York: Wiley, 1976.

[L1] R.W. Lucky, J. Salz and E.J. Weldon, Jr., Principles of Communication Engineering. New York, N.Y.: McGraw-Hill, 1968.

[L2] W.C. Lindsay and M.K. Simon, Telecommunication Systems Engineering. Englewodd Cliffs, N.J.: Prentice-Hall, 1973.

[L3] S. Lin, An Introduction to Error-Correcting Codes. Englewood Cliffs, N.J.: Prentice-Hall, 1970.

[O1] G.D. Ott, "Urban path-loss characteristics at 820 MHz", IEEE Trans. Veh. Technol., vol. VT-27, pp. 189-198, Nov. 1978.

[P1] W.W. Peterson and E.J. Weldon, Jr., Error-Correcting Codes, 2nd Ed., Cambridge, MA: The MIT Press, 1972.

[S1] J.J. Stiffler, Theory of Synchronous Communications. Englewood Cliffs, N.J.: Prentice-Hall, 1971.

[S2] C.E. Shannon and W. Weaver, The Mathematical Theory of Communication. Urbana, IS: University of Illinois Press, 1962; also in Bell Syst. Tech. J., July 1949 and Oct. 1949 and Scientific American, July 1949.

[W1] J.M. Wozencraft and I.M. Jacobs, Principles of Communication Engineering. New York, N.Y.: 1965.

[Y1] J. Yan and R.W. Donaldson, "Subjective effects of channel transmission errors on PCM and DPCM voice communication systems", IEEE Trans. Commun., vol. COM-20, pp. 281-290, June 1972.

III. INTERFERENCE, CODING AND BIT ERROR PROBABILITY

III-1 Interference for Binary PSK and MSK Signalling

This section summarizes both the approach used and the results obtained in an earlier [D1] detailed analysis of signal-to-noise and signal-to-interference ratios for binary PSK and MSK signalling. Our approach differs from one used earlier by Kalet [K1] and permits extension in the following section to other signalling formats and detection schemes.

With reference to Fig. 3-1, the received signal

$$r(t) = \sqrt{2P_s}\, p(t) \cos(2\pi f_c t+\theta) + n_c(t) + i_c(t) \qquad (3\text{-}1)$$

where P_s is the power in r(t) due to the transmitted signal, p(t) is the baseband data signal, θ is a random phase angle uniformly distributed between 0 and 2π, $n_c(t)$ is white Gaussian noise with power spectral density $N_o/2$ and $i_c(t)$ is interference consisting of other data signals and/or voice modulated FM. The input x(t) to the filter is

$$x(t) = \sqrt{P_s}\, p(t)[1+\cos(4\pi f_c t+2\theta)] + \sqrt{2}\,(n_c(t)+i_c(t)) \cos(2\pi f_c t+\theta) \qquad (3\text{-}2)$$

For cases of interest in this section,

$$p(t) = \sum_k a_k\, g(t-kT) \qquad (3\text{-}3)$$

where $a_k = \pm 1$ and g(t-kT) is the basic modulator pulse shape. It is convenient to scale g(t) and $g_T(t)$ as follows:

$$\int_{-\infty}^{\infty} |G(f)|^2 df = T \qquad (3\text{-}4)$$

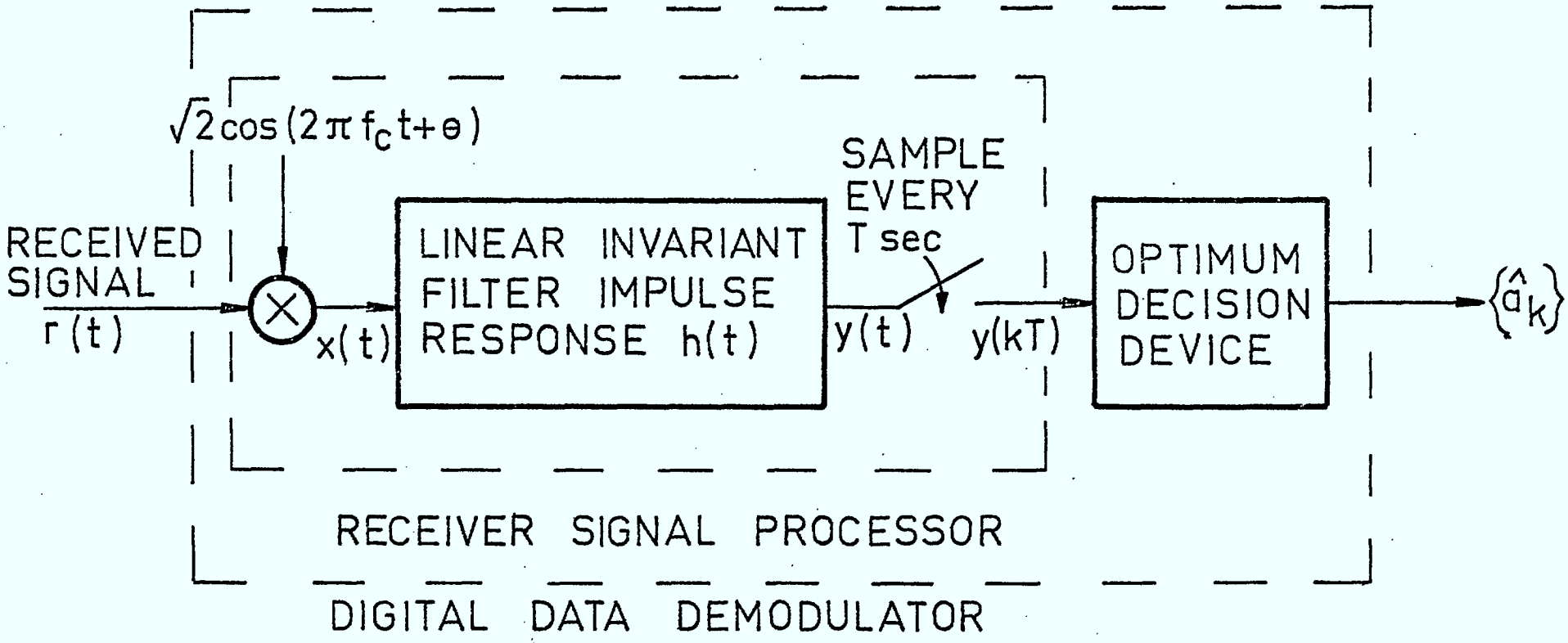

Fig. 3-1 Receiver for coherent demodulation of PAM signals with zero intersymbol interference.

$$\int_{-\infty}^{\infty} |G_T(f)|^2 = 1 \tag{3-5}$$

where G(f) and $G_T(f)$ are Fourier transforms of g(t) and $g_T(t)$, respectively.

For conventional PSK

$$g_T(t) = \begin{cases} 1/\sqrt{T} & |t| < T/2 \\ 0 & |t| > T/2 \end{cases} \tag{3-6}$$

The response y(t) in Fig. 3-1 is

$$y(t) = x(t-\tau)h(\tau)d\tau \tag{3-7a}$$

The filter removes signals outside the data signal baseband, with the result that the response y(kT) due to the data signal alone at k=0 is

$$y(0) = \sqrt{P_s} \int_{-\infty}^{\infty} p(-\tau)h(\tau)d\tau \tag{3-7b}$$

For reasons cited earlier [D1], g(t) is selected such that y(0) contains no intersymbol interference, in which case

$$y(0) = \sqrt{P_s} \int_{-\infty}^{\infty} a_k\, g(-\tau)h(\tau)d\tau \tag{3-8a}$$

$$= \sqrt{P_s} \int_{-\infty}^{\infty} a_k\, G(f)H(f)df \tag{3-8b}$$

where H(f) is the Fourier transform of h(t).

Thus, the output power S solely from the data signal is

$$S = y^2(0)$$

$$= P_S T\left[\int_{-\infty}^{\infty} G_T(f)H(f)df\right]^2 \qquad (3\text{-}9a)$$

$$= P_S T\left[\int_{-\infty}^{\infty} g_T(\tau)h(-\tau)d\tau\right]^2 \qquad (3\text{-}9b)$$

The output power I_i due to noise or interference with power spectral density $S_i(f)$ at the input to filter $H(f)$ is

$$I_i = \int_{-\infty}^{\infty} S_i(f)|H(f)|^2 df \qquad (3\text{-}10)$$

In the present context three choices for $S_i(f)$ are of interest: white Gaussian noise with $S_i(f) = N_o/2$; voice interference of power P_v and baseband power density spectrum $V(f)$ on a channel Δ Hz from the wanted channel at f_c; and data interference at $f_c+\Delta$, with power P_d and baseband power spectral density $P_i(f)$. For the data signal interference, in the band of $H(f)$

$$S_i(f) = (P_d/4)[P_i(f+\Delta) + P_i(f-\Delta)] \qquad (3\text{-}11)$$

In the case of a data signal with zero intersymbol interference $P_i(f) = |G_T(f)|^2$. For voice signal interference $P_i(f)$ is replaced in (3-11) by $V(f)$.

Relative to S, the power outputs in these interfering signals are as follows:

$$N/S = (N_o/2P_s)T^{-1}\int_{-\infty}^{\infty}|H(f)|^2 df / \left[\int_{-\infty}^{\infty} G_T(f)H(f)df\right]^2 \qquad (3\text{-}12)$$

$$I_v/S = \frac{1}{2}(P_v/P_s)T^{-1}\int_{-\infty}^{\infty} V(f)|H(f-\Delta)|^2 df / \left[\int_{-\infty}^{\infty} G_T(f)H(f)df\right]^2 \quad (3\text{-}13)$$

$$I_d/S = \frac{1}{2}(P_d/P_s)T^{-1}\int_{-\infty}^{\infty} |P_i(f-\Delta)|^2|H(f)|^2 df / \left[\int_{-\infty}^{\infty} G_T(f)H(f)df\right]^2 \quad (3\text{-}14)$$

The above equations are quite general, and apply even when the data signal on the interfering channel is not of a form given by (3-3), or when its data rate differs from that of the wanted signal. Simplification occurs when the interfering and wanted signal have the same format and data rate and when $H(f) = G_T^*(f)$ (matched filtering). In this case

$$\int_{-\infty}^{\infty} |H(f)|^2 df = 1 \quad (3\text{-}15)$$

$$\int_{-\infty}^{\infty} G_T(f)H(f)df = 1 \quad (3\text{-}16)$$

and

$$N/S = (N_o/2P_sT) \quad (3\text{-}17)$$

$$I_v/S = (P_v/P_s)C_v(\Delta T, B, g) \quad (3\text{-}18)$$

$$I_d/S = (P_d/P_s)C_d(\Delta T, g) \quad (3\text{-}19)$$

where, with $\lambda = fT$ and $x = \tau/T$

$$C_v(\Delta T,B,g) = (2T)^{-1}\int_{-\infty}^{\infty} V(f)|G_T(f-\Delta)|^2 df \tag{3-20a}$$

$$= (1/2T^2)\int_{-\infty}^{\infty} V(\lambda)|G_T(\lambda-\Delta T)|^2 d\lambda \tag{3-20b}$$

$$= \frac{1}{T}\int_{o}^{\infty} v(\tau)\rho_g(\tau)\cos 2\pi\Delta\tau d\tau \tag{3-20c}$$

$$= \int_{o}^{\infty} v(x)\rho_g(x)\cos 2\pi\Delta Tx dx \tag{3-20d}$$

$$C_d(\Delta T,g) = (2T)^{-1}\int_{-\infty}^{\infty} |G_T(f-\Delta)|^2|G_T(f)|^2 df \tag{3-21a}$$

$$= (1/2T^2)\int_{-\infty}^{\infty} |G_T(\lambda-\Delta T)|^2|G_T(\lambda)|^2 d\lambda \tag{3-21b}$$

$$= \frac{1}{T}\int_{o}^{\infty} \rho_g{}^2(\tau)\cos 2\pi\Delta\tau d\tau \tag{3-21c}$$

$$= \int_{o}^{\infty} \rho_g{}^2(x)\cos 2\pi\Delta Tx dx \tag{3-21d}$$

In (2-21) $v(\tau)$ is the inverse Fourier transform of $V(f)$ and

$$\rho_g(\tau) = \int_{-\infty}^{\infty} g_T(t)g_T(t-\tau)dt \tag{3-22}$$

In obtaining (3-20c) and (3-21c) we have used

$$\int_{-\infty}^{\infty} A(f)B^*(f-y)df = \int_{-\infty}^{\infty} a(t)b(t)e^{j2\pi yt}dt \tag{3-23}$$

where $A(f)$ and $B(f)$ are the Fourier transforms of $a(t)$ and $b(t)$,

respectively, as well as the fact that $v(x)$ and $\rho_g(x)$ are even functions.

For conventional PSK signals on all channels, the above simplifying assumptions apply, and one obtains

$$\rho_g(\tau) = \begin{cases} 1 - \frac{|\tau|}{T} & |\tau| < T \\ 0 & |\tau| > T \end{cases} \tag{3-24}$$

$$C_d = \int_0^1 (1-x)^2 \cos(2\pi\Delta T x)\,dx$$

$$= \frac{1}{2(\pi\Delta T)^2}\left[1 - \frac{\sin 2\pi\Delta T}{2\pi\Delta T}\right] \tag{3-25}$$

For $\Delta T=0$, $C_d = 1/3$.

MSK can be regarded as staggered quadrature PAM [K1,S1,G1], where each data stream consists of baseband PSK-type pulses with duration 2T and shape

$$g_{2T}(t) = \begin{cases} \frac{1}{\sqrt{T}} \cos \pi t/2T & |t| < T \\ 0 & |t| > T \end{cases} \tag{3-26}$$

The optimum coherent quadrature receiver appears in Fig. 3-2. Each data stream has power $P_s/2$. From either receiver filter, the output power S due to the data signal only is

$$S = (P_s/2)2T\left[\int_{-\infty}^{\infty} G_{2T}(f)H(f)df\right]^2 \tag{3-27a}$$

$$= P_s T\left[\int_{-\infty}^{\infty} g_{2T}(\tau)h(-\tau)d\tau\right]^2 \tag{3-27b}$$

Each interfering MSK signal consists of two uncorrelated PSK-type data

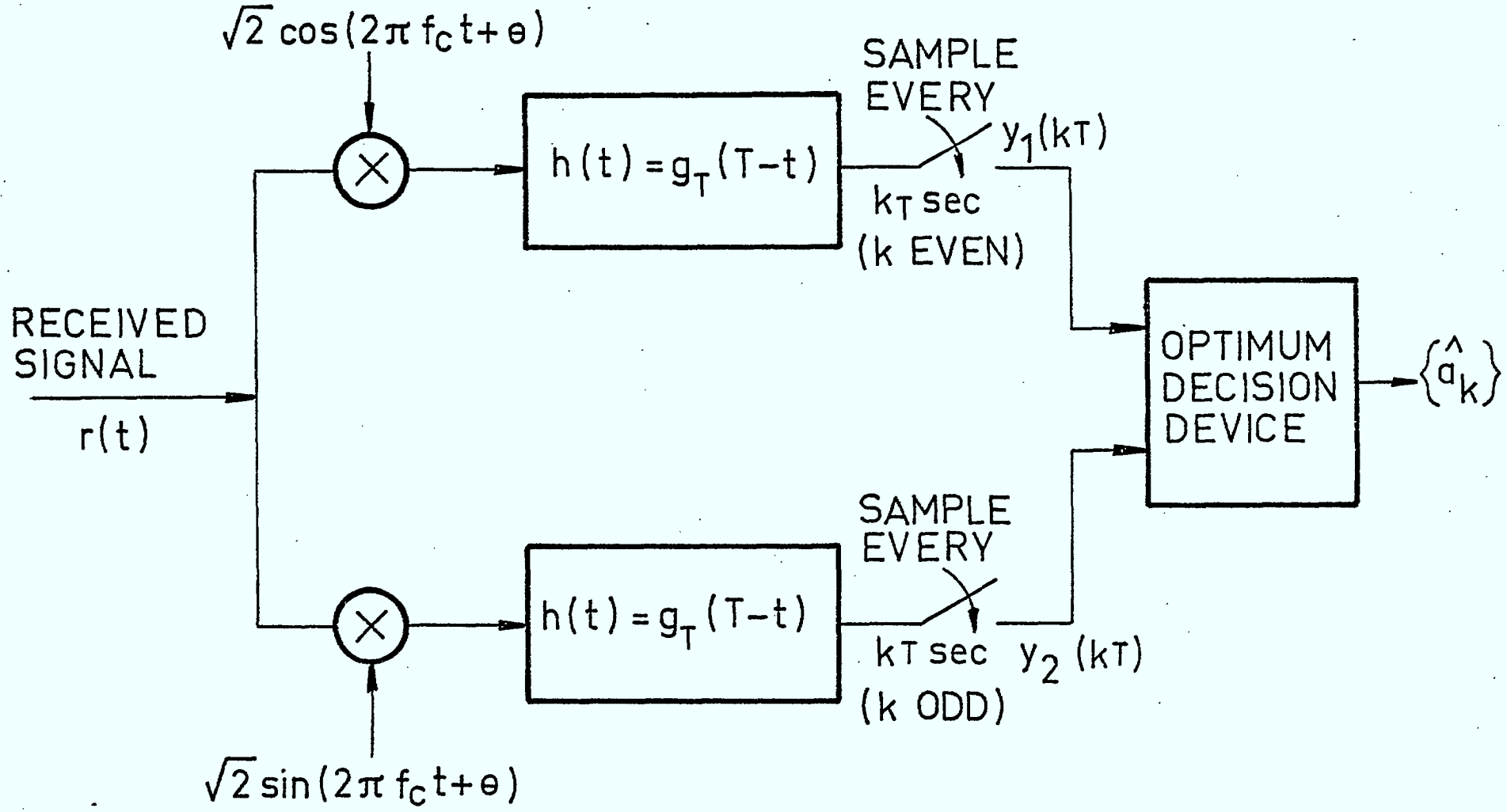

Fig. 3-2 Optimum binary MSK receiver.

streams each of power $P_d/2$, with identical spectra $P_i(f) = |G_{2T}(f)|^2$. Thus, for MSK with matched filters in each quadrature arm N/S is again given by (3-18) and

$$I_d/S = (P_d/2P_sT)\int_{-\infty}^{\infty} |G_{2T}(f-\Delta)|^2 |G_{2T}(f)|^2 df \tag{3-28}$$

$$= (P_d/P_s)C_d(\Delta T, g) \tag{3-29}$$

where

$$C_d(\Delta T, g) = \frac{1}{T}\int_0^{\infty} \rho^2_g(\tau)\cos 2\pi\Delta\tau d\tau \tag{3-30}$$

and

$$\rho_g(\tau) = \int_{-\infty}^{\infty} g_{2T}(\tau) g_{2T}(\tau - t)dt \tag{3-31}$$

In this case

$$\rho_g(\tau) = \begin{cases} \frac{1}{\pi}\sin\frac{\pi|\tau|}{2T} + \left(1-\frac{|\tau|}{2T}\right)\cos\frac{\pi|\tau|}{2T} & |\tau| < 2T \\ 0 & |\tau| \geq 2T \end{cases} \tag{3-32}$$

Thus, C_d can be written as follows

$$C_d(\Delta T) = \int_0^2 \left[\frac{1}{\pi}\sin\frac{\pi x}{2} + \left(1-\frac{x}{2}\right)\cos\frac{\pi x}{2}\right]^2 \cos 2\pi\Delta T x dx \tag{3-33a}$$

$$C_d(\Delta T) = 2\int_0^1 \left[\frac{1}{\pi}\sin \pi y + (1-y)\cos \pi y\right]^2 \cos 4\pi\Delta T y dy \tag{3-33b}$$

A similar approach yields $C_v(\Delta T)$ for MSK [D2].

Figure 3-3 shows $C_d(\Delta T)$ for MSK and SQPSK *; $C_d(\Delta T)$ for SQPSK is obtained by adding 3 dB to $C_d(2\Delta T)$ for PSK. For SQPSK, $C_d \sim (\Delta T)^{-2}$. For MSK, $C_d \sim (\Delta T)^{-4}$.

An earlier report [D2] shows $C_v(\Delta T)$ for two different (Gaussian) voice models. One model is based on the long-term average spectrum [D2,F1] of speech into a pre-emphasis audio filter normally used with FM transmission; for this model the spectral roll-off rate is no faster than $(\Delta T)^{-2}$, and $C_v(\Delta T) \sim (\Delta T)^{-2}$ for both PSK and MSK. The other model assumes an ideal low-pass modulating spectrum [J1], flat in the pass band and having zero energy in the stop band. For this latter model the spectral roll-off rate is at least as fast as $(\Delta T)^{-4}$, since $C_v \sim (\Delta T)^{-2}$ for PSK and $\sim (\Delta T)^{-4}$ for MSK.

The rate of decrease of C_d (and also C_v) with ΔT is equal to rate of decrease of either the interfering signal spectrum, or of $|H(f)|^2$, whichever is slower [R1]. The roll-off rate of $|H(f)|^2$ is often chosen to be equal to that of the baseband data signal.

Clearly, adjacent-channel interference depends very much on the choice of the data signal format. The voice model chosen for FM spectrum calculations clearly affects the interference levels through C_v. It is desirable to pre-filter the voice signal prior to modulation to yield an FM spectral roll-off rate equal to or better than that of the wanted data signal. Some results of work currently underway at the University of British Columbia indicate that prefiltering of speech to achieve an FM spectral roll-off rate

---

* SOPSK consists of two quadrature PSK data streams of equal power, offset by one-half a bit period [K1]. SOPSK, like MSK, results in a constant envelope signal which facilitates implementation.

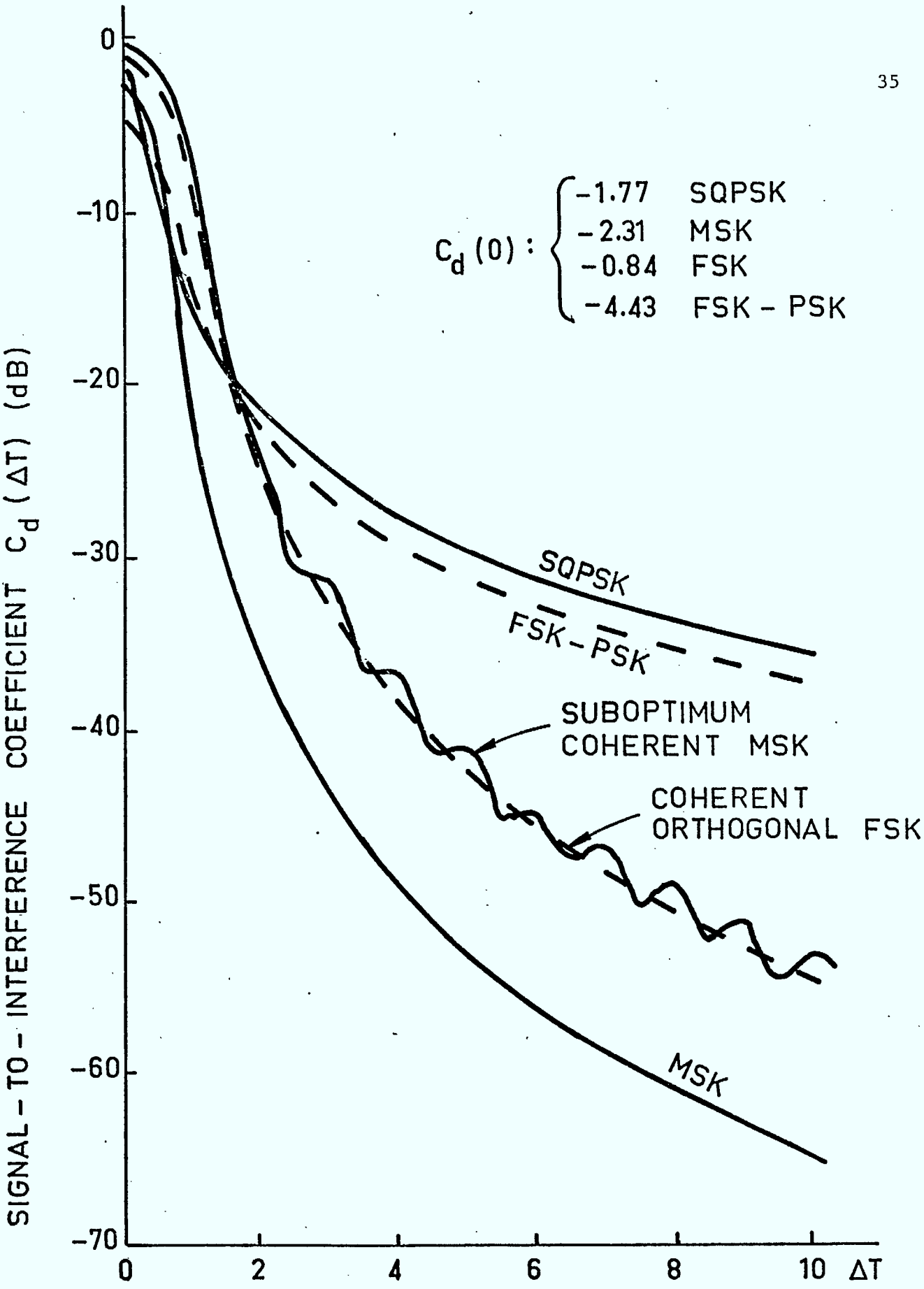

Fig. 3-3 Crosstalk function C_d vs. ΔT for SQPSK, MSK and FSK.

as good as that for MSK is possible. The quality of the received voice signals is currently being assessed.

III-2 Suboptimum MSK Receiver Performance

The quadrature receiver in Fig. 3-2 has two disadvantages. First, two filters and samplers, rather than one are required. Second, coherent detection which requires carrier recovery, is employed. Under Rayleigh fading, carrier tracking is difficult, and differential detection or incoherent detection is often employed instead.

By using a receiver filter with

$$h(t) = \sqrt{2}\, g_{2T}(2t) \tag{3-34}$$

where $g_{2T}(t)$ is given by (3-26), the first problem can be alleviated; the impulse response of the above filter is non-zero for T rather than 2T sec., and a single filter can be used with sampling at T sec. intervals. In this case

$$C_d = \frac{1}{T}\int_0^T \rho_g(\tau)\rho_h(\tau)\cos 2\pi\Delta\tau\, d\tau \Big/ \left[2\int_0^{T/2} g_{2T}(-\tau)h(\tau)d\tau\right]^2 \tag{3-35}$$

where $\rho_g(\tau)$ is given by (3-31) and $\rho_h(\tau) = 2\rho_g(2\tau)$. Equation (3-35) can be written as follows:

$$C_d(\Delta T) = \frac{2}{L_{gh}^2}\int_0^1 \left[\frac{1}{\pi}\sin\frac{\pi x}{2} + \left(1-\frac{x}{2}\right)\cos\frac{\pi x}{2}\right]\left[\frac{1}{\pi}\sin \pi x + (1-x)\cos\pi x\right]\cos 2\pi\Delta T x\, dx \tag{3-36a}$$

where

$$L_{gh} = 2\sqrt{2}\int_0^{1/2} \cos(\pi x/2)\cos(\pi x)dx \qquad (3\text{-}36b)$$

$$= 8/3\pi \qquad (3\text{-}36c)$$

The value $8/3\pi$ equals the -1.43 dB obtained by Kalet and White [K2] using a different approach. Fig. 3-3 shows C_d, which is seen to be approximately 10 dB worse than C_d for the optimum MSK receiver, for $\Delta T \gtrsim 2$. The analysis procedure in the previous section can be used to determine the interference ratios for detection of MSK using conventional FSK receivers. Consider the coherent case in Fig. 3-4. Using the filter of (3-34), yields

$$I_d/S = (P_d/P_s)\bar{C}_d(\Delta T) \qquad (3\text{-}37)$$

where

$$\bar{C}_d(\Delta T) = [C_d(\Delta T + \tfrac{1}{4}) + C_d(\Delta T - \tfrac{1}{4})]/2 \qquad (3\text{-}38)$$

Function C_d is given by (3-36) with

$$L_{gh} = 2\sqrt{2}\int_0^{1/2} \cos \pi x dx \qquad (3\text{-}39a)$$

$$= 2\sqrt{2}/\pi \qquad (L_{gh}^2\ 0.90 = -0.91\ \text{dB}) \qquad (3\text{-}39b)$$

The result for L_{gh} follows from the fact that the output signal power S from the filter corresponding to the signal's bit frequency is based on (3-27), where $g_{2T}(\tau)$ is a rectangular pulse. The averaging in (3-38) is with C_d expressed in actual units (not dB) and occurs because the interference is on a channel $\Delta \pm \Omega$ Hz from the wanted signal's bit frequencies, which are

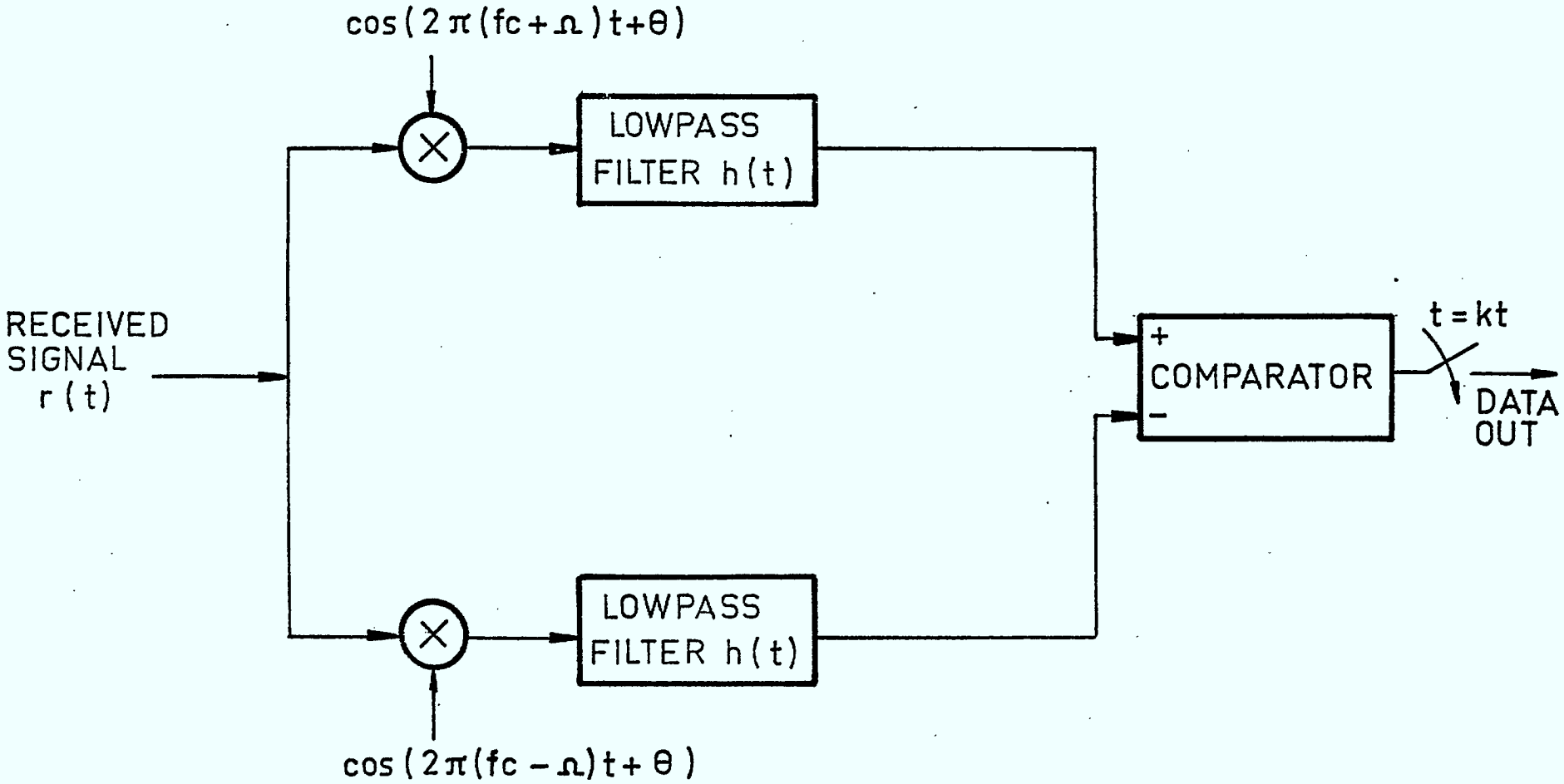

Fig. 3-4 Coherent FSK receiver.

equiprobable. For MSK $\Omega T = 1/4$. To a first approximation, $\bar{C}_d(\Delta T) \simeq C_d(\Delta T)$ for $\Delta T \gtrsim 1/2$. The dotted curve in Fig. 3-3 shows $\bar{C}_d(\Delta T)$ in (3-38). The need to carefully select the receiver bandpass filter roll-off rate cannot be over-emphasized. Use of a PSK-type receiver filter with lowpass equivalent $h(t) = g_T(t)$ in (3-6), which is optimum for FSK detection in white Gaussian noise, would yield a $\bar{C}_d$ value which would fall off as $(\Delta T)^{-2}$, rather than ΔT^{-4}, as shown by the MSK-PSK curve in Fig. 3-3.

It is seen that the procedures developed earlier for PSK-type signals can be extended to conventional FSK receivers with an arbitrary frequency deviation. It is also seen that this analysis is useful in selecting appropriate bandpass filters and for analysis of their performance.

The same analysis procedure is also used to obtain C_v for FSK receivers, once V(f) is known.

The value of N/S is given as before by (3-12).

To obviate the need for carrier tracking incoherent detection may be employed. In this case each local oscillator in Fig. 3-4 is replaced by a bandpass filter centered at $f_c \pm \Omega$, a squarer and an integrator. Replacing a coherent FSK receiver with an incoherent counterpart involves some loss in detectability (up to 3 dB in white Gaussian noise) [W1,L1]. However, the two detectors give equal performance at high signal-to-noise ratios.

Differential detection of PSK signals also obviates the need for carrier tracking, and thereby simplifys the receiver [W1,L1]. Differential detection of MSK signals, based on the receiver in Fig. 3-1, has also been

demonstrated [K3]. At high signal-to-noise ratios differential PSK (DPSK) performance is virtually identical to PSK [W1].

The effects of incoherent and differential detection on bit error probability are discussed in the next section.

III-3 Channel Bit-Error Rates

For binary antipodal signalling on white Gaussian noise channels, the bit-error probability p with optimum (matched filter) receivers is [W1,L1]

$$p = \operatorname{erfc}\left(\sqrt{SNR}\right) \tag{3-40}$$

where

$$SNR = 2P/RN_o \tag{3-41}$$

$$\operatorname{erfc}(x) = \frac{1}{\sqrt{2\pi}} \int_x^\infty \exp(-y^2/2)dy \tag{3-42}$$

and P, R and $N_o/2$ denote, respectively, the received signal power, noise power spectral density and bit rate. Binary PAM and binary PSK are examples of binary antipodal signalling, as are binary MSK and 4-phase PSK when viewed as quadrature streams of binary PAM data. In the case of 4-phase PSK, P is the power in each stream.

With binary orthogonal signalling on white Gaussian channels, optimum (coherent) reception yields

$$p = \operatorname{erfc}\left(\sqrt{SNR/2}\right) \tag{3-43}$$

Binary orthogonal signalling results when MSK is coherently detected as FSK.

As p becomes small, twice the power (3 dB) is seen to be needed if orthogonal signalling is to match the performance of binary antipodal signalling.

For reasons of either implementation simplicity or necessity, the receiver may operate incoherently and ignore carrier phase. For optimum incoherent reception of binary orthogonal FSK in white Gaussian noise

$$p = 0.5 \exp(-SNR/4) \tag{3-44}$$

Incoherent and coherent detection are "exponentially equivalent", however a penalty of up to 3 dB results when incoherent detection is used; the penalty reduces as p decreases, and is less than 1.5 dB for $\bar{p} < 10^{-3}$.

For binary antipodal DPSK

$$p = 0.5 \exp(-SNR/2) \tag{3-45}$$

The degredation in performance which results in comparison with PSK is negligible for practical values of p. However errors tend to occur in pairs, since an error in one bit implies a poor phase reference for the following bit.

When the signal level is subject to Rayleigh fading, SNR varies and p must be averaged over the SNR levels. For binary orthogonal (incoherent) signalling,

$$\begin{aligned} \bar{p} &= (2 + \bar{P}/RN_o)^{-1} \\ &= (2 + [\overline{SNR}/2])^{-1} \end{aligned} \tag{3-46}$$

where the overbar represents an average.

Non-white Gaussian noise, multi-level signalling or suboptimum receivers change the above values for p and $\bar{p}$. However, in all cases, p

decreases exponentially with SNR for Gaussian channels, while $\bar{p}$ decreases linearly with $\overline{SNR}$ for Rayleigh channels. In the case of differential PSK $\overline{SNR}/2$ in (3-46) is replaced by $\overline{SNR}$, in accordance with (3-45).

In land mobile channels interfering signals with Rayleigh varying levels often constitute the primary disturbance. Consider for the moment that all mobiles are stationary. If the interference plus noise could be modelled as white Gaussian noise, then SNR would be given by (3-41), with N_o replaced by

$$N_e = N_o + 2T \sum_i P_i C_i(\Delta T) \tag{3-47}$$

assuming independent interference sources. If the signal only is subject to Rayleigh fading then averaging (3-46) yields

$$\bar{p} = \left[2 + \frac{\bar{P}_s T}{N_o + 2T \sum_i P_i C_i(\Delta T)} \right]^{-1} \tag{3-48}$$

In those cases where $\bar{p} << 1$,

$$\bar{p} \simeq \frac{N_o}{\bar{P}_s T} + 2 \sum_i \frac{P_i}{\bar{P}_s} C_i(\Delta T) \tag{3-49}$$

If the interference is also varying in level from bit-to-bit, then for $\bar{p} << 1$

$$\bar{p} \simeq \frac{N_o}{\bar{P}_s T} + 2 \sum_i \frac{\bar{P}_i}{\bar{P}_s} C_i(\Delta T) \tag{3-50}$$

In those cases where the assumption $\bar{p} << 1$ is violated, (3-50) upper

bounds $\bar{p}$, and the bound become increasingly tight as $\bar{p}$ decreases.

In interference limited systems (3-48) becomes

$$\bar{p} = \left[2 + \frac{\bar{P}_s}{2 \sum_i \bar{P}_i C_i(\Delta T)} \right]^{-1} \tag{3-51}$$

If many interfering signals are each varying about their average $\bar{P}_i$, and if each of these interferers has channel occupancy ϕ then

$$\bar{p} = \left[2 + \frac{\bar{P}_s}{2\phi \sum_i \bar{P}_i C_i(\Delta T)} \right]^{-1} \tag{3-52}$$

In conventional narrowband land mobile radio systems which do not reuse channels there are one or two predominant sources of interference from adjacent channels. In this case $\bar{p}$ in (3-51) should be averaged over the Rayleigh varying interference levels.

For a single interfering signal, the probability density for the interference power level is

$$f_i(\alpha) = (1-\phi)\,\delta(\alpha) + \frac{\phi}{\bar{P}_i} \exp(-\alpha/\bar{P}_i) U(\alpha) \tag{3-53}$$

where $U(\alpha)$ is the unit step function and

$$\bar{p}_1 = \int_0^\infty \left[\frac{\phi}{2 + (\bar{P}_s / 2C_i \alpha)} \right] \frac{\exp(-\alpha/\bar{P}_i)\, d\alpha}{\bar{P}_i}$$

$$= \frac{\phi}{2} \int_0^\infty \left[\frac{\beta}{\beta + a} \right] \exp(-\beta)\, d\beta \tag{3-54}$$

where n_i is the number of interfering signals (here $n_i=1$) and

$$a = (\overline{P}_s/\overline{P}_i)/4n_iC_i \tag{3-55}$$

In (3-54) the subscript on $\overline{p}_1$ denotes one interfering signal.

When there are two interfering signals of equal average strength $\overline{P}_i$ with the same values for ϕ and C_i, $\overline{p}$ can be calculated as above, provided the density function is for the sum of the interfering signals. This density function is obtained by convolution of (3-53) with itself to yield:

$$f_i(\alpha) = (1-\phi)^2\delta(\alpha)+\{[\frac{2\phi(1-\phi)}{\overline{P}_i}]\exp(-\alpha/\overline{P}_i)+[\frac{\phi}{\overline{P}_i}]^2\alpha\exp(-\alpha/\overline{P}_i)\}U(\alpha) \tag{3-56}$$

The last term in (3-56) results from the fact that the self-convolution of $e^{-at}U(t)$ yields $te^{-at}U(t)$.

Application of (3-56) together with (3-51) yields the average $\overline{p}_2$ (here $n_i=2$):

$$\overline{p}_2 = \frac{2\phi(1-\phi)}{\overline{P}_i}\int_0^\infty \frac{\exp(-\alpha/\overline{P}_i)}{2+(\overline{P}_s/4C_i\alpha)}\,d\alpha + (\frac{\phi}{\overline{P}_i})^2\int_0^\infty \frac{\alpha\exp(-\alpha/\overline{P}_i)}{2+(\overline{P}_s/4C_i\alpha)}\,d\alpha$$

$$= 2(1-\phi)\overline{p}_1 + \frac{\phi^2}{2}\int_0^\infty (\frac{\beta^2\exp(-\beta)}{\beta+a})d\beta \tag{3-57}$$

The integrals in (3-54) and (3-57) can be determined in terms of the integral

$$I(pq) = \int_0^\infty \frac{\exp(-pt)}{q+t}\,dt \tag{3-58}$$

Thus,

$$\overline{p}_1 = \frac{\phi}{2} \left[1-a \int_0^\infty \frac{\exp(-\beta)}{\beta+a} \, d\beta\right]$$

$$= \frac{\phi}{2} \left[1-aI(a)\right] \tag{3-59}$$

$$\overline{p}_2 = 2(1-\phi)\overline{p}_1 + \frac{\phi^2}{2} \left\{\int_0^\infty (\beta-a)\exp(-\beta)d\beta + a^2 \int_0^\infty \frac{\exp(-\beta)}{\beta+a} \, d\beta\right.$$

$$= 2(1-\phi)\overline{p}_1 + \frac{\phi^2}{2} \left[1-a+a^2 I(a)\right]$$

$$\overline{p}_2 = 2(1-\phi)\overline{p}_1 + \phi\left[\frac{\phi}{2} - a\overline{p}_1\right] \tag{3-60}$$

Fig. 3-5 shows $\overline{p}_1$ and $\overline{p}_2$ plotted vs. a for ϕ=0.5 and ϕ=1.0. Also shown for comparison purposes is $\overline{p}$ for the case of many interferers, where

$$\overline{p} = \frac{1}{2} \left(\frac{1}{1 + (a/\phi)}\right) \tag{3-61}$$

where

$$a = (\overline{P}_s / 4 \sum_i C_i \overline{P}_i) \tag{3-62}$$

If all P_i and C_i values are equal then (3-62) reduces to (3-55).

Fig. 3-5 shows that $\overline{p}_1$ and $\overline{p}_2$ are bounded above by $\overline{p}$ as given by (3-61). For large values of a, $\overline{p}_1$, $\overline{p}_2$ and $\overline{p}$ all approach the value

$$\overline{p} \simeq \phi/2a$$

$$\simeq 2\phi \sum_i C_i (\Delta T) \overline{P}_i / \overline{P}_s \qquad (\overline{p} \ll 1) \tag{3-63}$$

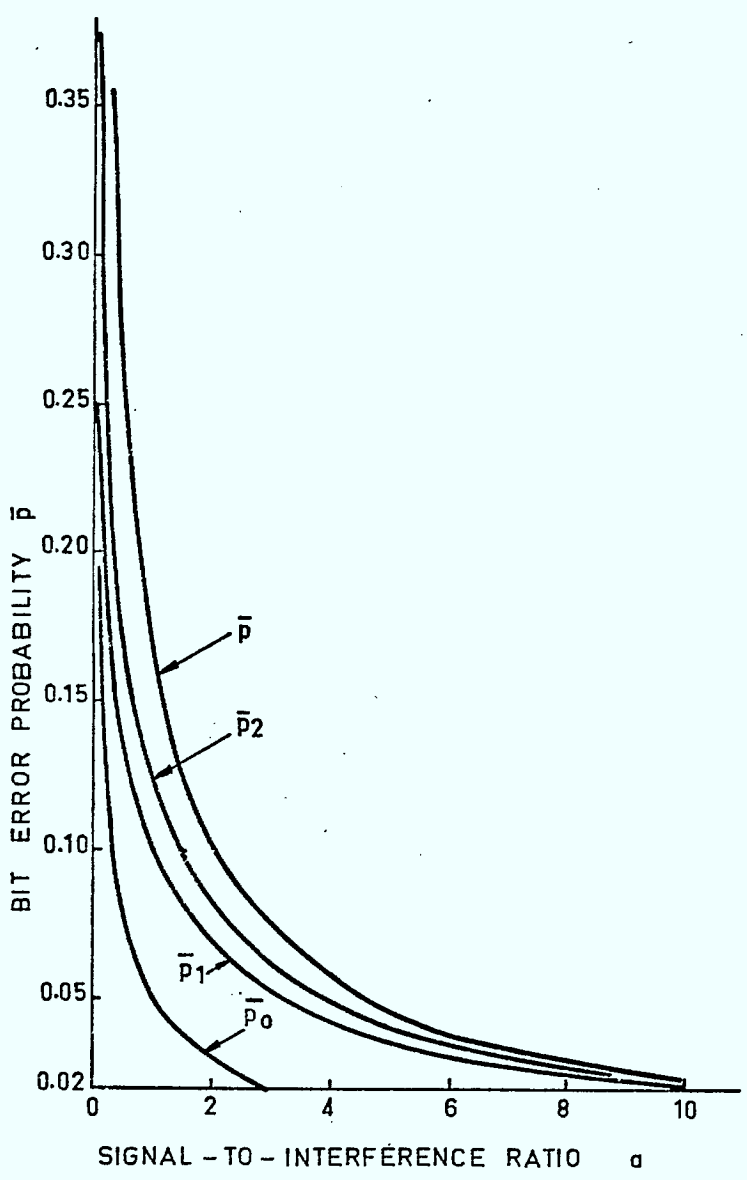

(a) $\phi = 0.5$

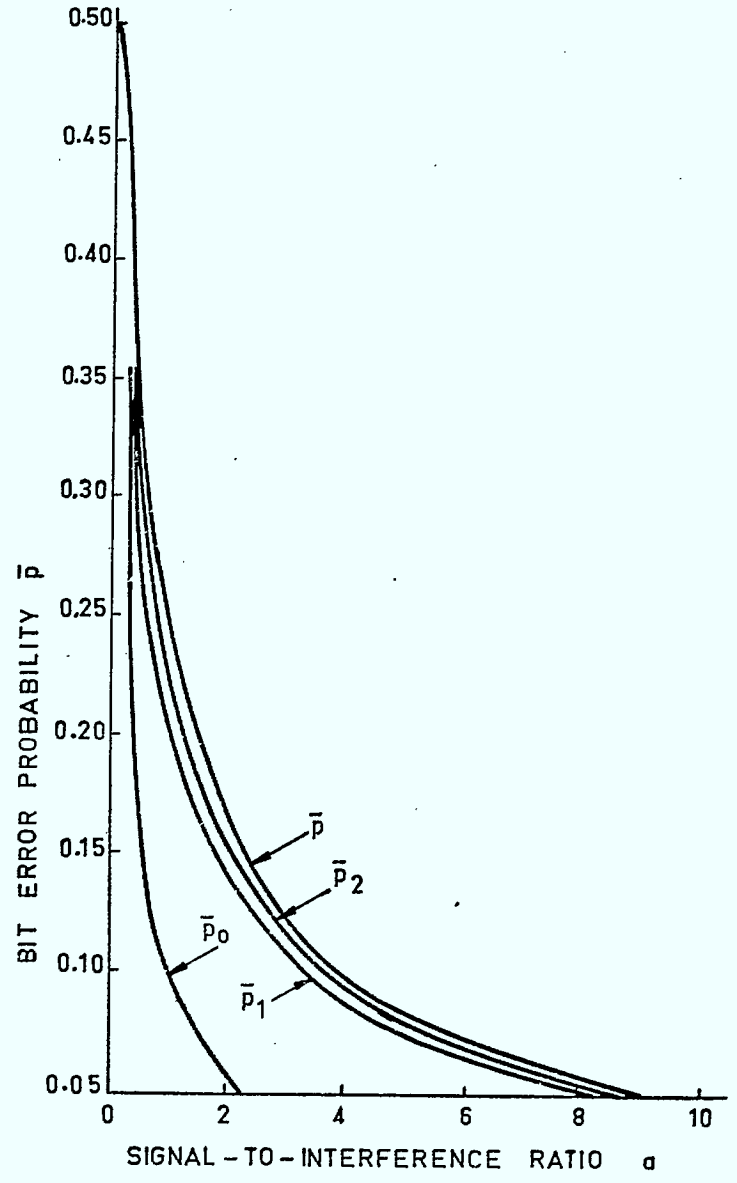

(b) $\phi = 1.0$

Fig. 3-5 Bit-error probability $\bar{p}$ averaged over Rayleigh fading.

Equations (3-48) to (3-63) inclusive apply to binary orthogonal incoherent FSK. These same results apply to binary DPSK provided $\overline{P}_s$ is replaced by $2\overline{P}_s$. In particular, for DPSK

$$\overline{p} \simeq \phi \sum_i C_i(\Delta T)\overline{P}_i/\overline{P}_s \qquad (\overline{p} \ll 1) \tag{3-64}$$

All of the above analysis is based on the assumption that interference has the same effect in determining p in (3-40) to (3-45), inclusive, as does white Gaussian noise. When there are many interfering signals making a significant contribution to the total interference, the assumption is appropriate, because of the central limit theorem [W1]. When there are one or two interfering signals only, the Gaussian assumption cannot be defended; however, it does not follow that p in (3-40) to (3-45) is grossly inaccurate. In fact existing studies [E1] on the effects of co-channel interference show that

$$\overline{p} \simeq K\phi\overline{P}_i/\overline{P}_s \quad (p \ll 1) \tag{3-65}$$

where for duobinary MSK $K \simeq 1$ for discriminator detection and $K \simeq 1/2$ for differential detection. Below, we demonstrate that for a single co-channel interfering signal $K \simeq 1/2$ for binary orthogonal incoherent FSK and $K \lesssim 1/\pi$ for binary coherent PSK. For adjacent channel interference, preliminary results [K3] suggest that the use of formulas based on Gaussian noise of power equal to the averaged interference power may yield bit-error results which are reasonably accurate. However additional work on the effects of a few interfering signals on bit-error probability, particularly for adjacent-channel signals, would be useful.

When the wanted signal (s) and interfering signal (i) in binary coherent FSK differ over an entire bit period (event A), then an error occurs if $P_s < P_i$. The probability p_s of this event is

$$p_s = \int_{\beta=0}^{\infty} \int_{\alpha=0}^{\beta} f_s(\alpha) f(\beta) d\alpha d\beta \tag{3-66}$$

where

$$f_s(\alpha) = [\exp(-\alpha/\bar{P}_s)]/\bar{P}_s \tag{3-67}$$

$$f_i(\beta) = [\exp(-\beta/\bar{P}_i)]/\bar{P}_i \tag{3-68}$$

Integration yields

$$p_s = \bar{P}_i/(\bar{P}_i+\bar{P}_s) \tag{3-69}$$

When the wanted and interfering signal differ over a fraction f ($0 < f < 1$) of a bit period (event B) then the probability of error $p_d \leq p_s$, and equality applies only if the carrier phases of the interfering and wanted bits cancel over that part of the bit period where the two bit streams are equal.

Since $P(A) = \phi/4$, and $P(B) = \phi/2$ and $\bar{p} = p_s\, P(A) + p_d\, P(B)$,

$$\frac{\phi}{4}\left(\frac{\bar{P}_i}{\bar{P}_s+\bar{P}_i}\right) < \bar{p} < \frac{3\phi}{4}\left(\frac{\bar{P}_i}{\bar{P}_s+\bar{P}_i}\right) \tag{3-70}$$

Thus, (3-70) suggests the following approximation for binary orthogonal incoherent FSK:

$$\bar{p} \simeq \frac{\phi}{2}\left[\frac{1}{1+(\bar{P}_s/\bar{P}_i)}\right] \tag{3-71}$$

$$\bar{p} \simeq \phi[\bar{P}_i/\bar{P}_s]/2 \qquad (p \ll 1) \tag{3-72}$$

From (3-63), on the other hand, one obtains $\bar{p} \simeq 2\phi(\bar{P}_i/\bar{P}_s)C_i(0)$. For MSK detected as coherent FSK $C_i(0) \simeq C_d(1/4) \simeq 2/3$ (see Section 3-2, Fig. 3-3), and $\bar{p} \simeq (4/3)\phi\bar{P}_i/\bar{P}_s$. Incoherent detection increases $\bar{p}$ further, and the approximation in (3-63) gives a value of $\bar{p}$ which is too high, by a factor of at least 2.7. Fig. 3-5 shows that $\bar{p}$ in (3-71) (shown as $\bar{p}_o$) is bounded above by $\bar{p}$ in (3-61).

A similar analysis applies to PSK signals with a single co-channel interfering signal. In Fig. 3-1,

$$r(t) = \sqrt{2P_s}\cos\omega_c t + \sqrt{2P_i}\cos(\omega_c t+\psi) \tag{3-73}$$

$$x(t) = 2P_s\cos^2\omega_c t + 2P_i\cos\omega_c t\cos(\omega_c t+\psi) \tag{3-74}$$

$$y(kT) = P_s T + P_i T\cos\psi \tag{3-75}$$

where ψ is the phase of the interfering signal relative to that of the wanted signal. The output energy due to the interference exceeds that from the signal if $\pi/2 < |\psi| < \pi$ and if $P_s < P_i|\cos\psi|$. From (3-69) one sees that the probability of this event is

$$P(P_s < P_i|\cos\psi|) = \frac{1}{2}\frac{\bar{P}_i|\cos\psi|}{\bar{P}_s + \bar{P}_i|\cos\psi|} \tag{3-76}$$

Since $|\cos\psi| \leq 1$

$$P\left(P_s < P_i|\cos\psi|\right) \leq \frac{1}{2}\left(\frac{\overline{P}_i|\cos\psi|}{\overline{P}_s + \overline{P}_i}\right) \tag{3-77}$$

Averaging over $|\cos\psi|$ yields the following bound on the bit error probability $\bar{p}$:

$$\bar{p} \leq \frac{1}{\pi}\frac{\overline{P}_i}{\overline{P}_s + \overline{P}_i} \tag{3-78}$$

Eqn. (4-78) suggests $\bar{p}$ as given by (3-71) with ϕ/π replacing $\phi/2$.

III-4 Channel Coding and Error Control

Channel coding is a form of time diversity which can be highly effective on fading channels, either in a forward error correction (FEC) or error detection and retransmission (ARQ) mode.

Block codes and convolutional codes are available for FEC [L2, G1, P1]. Block coders augment k-bit source-digit sequences with r redundant check bits, to correct up to t errors in an n-bit block, where,

$$t = \begin{cases} (d-1)/2 & d \quad \text{odd} \\ (d/2)-1 & d \quad \text{even} \end{cases} \tag{3-79}$$

and d is the minimum Hamming distance between two transmitted codewords.

Block codes are easily generated using feedback shift registers. Decoding of selected codes is possible using feedback shift register circuits or majority logic gates. In particular, all single-bit error correcting Hamming codes (a subclass of BCH codes) can be decoded using either

approach. Selected multiple-error correcting BCH codes can also be decoded using one or both types of decoders. Convolutional codes seem to offer no clear advantage over block codes for transmission of short messages.

A useful measure of block code performance is P_e, the probability of a block (or word) error. Define P(m,n) as the probability of m errors in a block of n bits. For a FEC code which corrects all errors in t or fewer bits,

$$P_e = \sum_{m=t+1}^{n} P(m,n) \tag{3-80}$$

For a binary symmetric memoryless channel with bit-error probability p

$$P(m,n) = \binom{m}{n} p^m (1-p)^{n-m} \tag{3-81}$$

where

$$\binom{m}{n} = \frac{m!}{n!(n-m)!} \tag{3-82}$$

Equation (3-81) can be used to calculate error performance for land mobile channels, provided bit interleaving is used to make errors independent. Otherwise, more complex models must be used for P(m,n) [A1].

Also of interest is p_b, the probability of error of a decoded information bit, where

$$p_b = P_w P_e \tag{3-83}$$

In (3-83), P_w denotes the probability of an error in the k information bits, given an error in the n-bit word, and depends on the code. Errors would normally cause the closest (in the Hamming sense) codeword to the one trans-

mitted to be decoded, in which case $P_w \simeq d/n$. For lower density codes such as orthogonal codes $P_w \simeq \frac{1}{2}$ [L2, S2].

When error detection is employed using block codes, the probability of a detectable block error P_d is of interest, along with the probability of a block decoding error P_e and the probability P_c that the block is decoded correctly.

In the absence of any error correction [L1]:

$$P_c = P(m = 0,n) \tag{3-84}$$

$$P_e \simeq 2^{-(n-k)} \sum_{m=d}^{n} P(m,n) \tag{3-85}$$

$$P_d = 1 - P_c - P_e \tag{3-86}$$

The factor 2^{n-k} in (3-81) together with the lower limit d rather than $t \simeq d/2$ for FEC makes P_e much lower for error detection than for FEC. However, the converse is true of P_c since one or more errors in a block results in retransmission rather than decoding. As the channel degrades the number of retransmissions increases, and the actual information throughput adjusts automatically to match channel quality. It has been shown that use of some FEC can reduce P_c to acceptable levels ($\simeq 5\%$). The remaining check bits are then used for error detection [L4, F2].

Under FEC coding, the actual information throughput is k/n times the total number of bits transmitted. When ARQ is used, additional delay as well as throughput reductions occur as a result of retransmissions, depending on

the type of ARQ protocol used. Basic ARQ protocols are summarized below [B1, B2, B3, F2, S3]:

1. Send-and-wait ARQ: Following transmission of a block, the sending terminal waits for either a positive acknowledgement (ACK) or a negative acknowledgement (NACK) from the receiving terminal before sending the next block or retransmitting the same block.
2. Continuous (Go-Back-N) ARQ: The transmitter continues to send blocks until it receives a NACK, at which point it retransmits the current block as well as the previously transmitted N-1 blocks. A transmitter buffer is needed to save N blocks for possible retransmission. Following detection of one or more errors in a block, the receiver ignores all subsequent blocks prior to receiving the retransmitted block. Transmission delays and receiver decoding delays require $N \geq 2$.
3. Selective ARQ: The transmitter operates continuously, but retransmits only those blocks in which errors have been detected.

Send-and-wait ARQ is advantageous because of its implementation simplicity and is particularly suited to half-duplex channels [B1]. However, considerable idle channel time may occur and reduce information throughput. Selective repeat systems have the highest overall system throughput but require numbering of the data blocks to facilitate identification for retransmission.

Variations of each of the above schemes are possible [K4, M1, S4, S5]. For example, send-and-wait ARQ may involve transmission of a sequence of relatively short blocks (which may be numbered), and only those in which errors are detected are included for retransmission in the next sequence.

This option appears particularly suitable on land mobile channels, where bursts of noise may cause many errors in some blocks while others remain error-free. ACK's only may be returned to the transmitter, with retransmission occurring after a time-out period. The time-out period must be long enough to accommodate round-trip delays, otherwise unnecessary retransmissions may occur. Long time-out periods imply reduced overall system information throughput for the send-and-wait protocol and increased transmitter buffer storage for the other two protocols. Another variation results if NACK's only are sent to the transmitter. The advantage here is that acknowledgement traffic is considerably reduced, since NACK's would normally occur much less frequently than ACK's. In a situation in which data traffic flows regularly in each direction, ACK's or NACK's can be embedded in data blocks. However, when data flow is predominately one-way, acknowledgement information would have to be sent in its own block which would contain the usual overheads. There is an advantage to sending acknowledgement information separately, however; when queueing delays occur acknowledgement blocks can be given priority over regular data blocks, thereby reducing retransmission delays [S4, P2].

The throughput efficiency η for a data link may be defined as the number of the information bits decoded relative to the total number of bits transmitted. Thus, for an (n,k) FEC code $\eta = k/n$. For an (n,k) code used in ARQ situations [S3]

$$\eta = \frac{k}{n} \frac{1}{1+N\left[P_d/(1-P_d)\right]} \tag{3-87}$$

where N denotes the value applicable to the go-back-N protocol.

Equation (3-81) also applies to both send-and-wait and selective ARQ in which cases N=1 and

$$\eta = (k/n)(1-P_d) \tag{3-88}$$

Normally $P_e << P_d$, $1-P_d \simeq P_c$ and, for N=1

$$\eta \simeq P_c\, k/n \tag{3-89}$$

The delay D from the time that a message is presented to the transmitter until it is processed by the receiver depends on various component delays including those for queueing for channel access, bit transmission, propagation, decoding, and modem start-up or turn-around. Let T_1 and T_2 denote the one-way and round-trip delays, respectively (often $T_2 \simeq 2T_1$); then

$$D = T_1 + T_2 (P_d + 2P_d^2 + 3P_b^3 + ... + iP_d^i + ...)$$

$$D/T_1 = 1 + (T_2/T_1)\,[P_d/(1-P_d)^2] \tag{3-90}$$

For $1-P_d \simeq P_c$ the increase in D relative to T_1 is $(T_2/T_1)(P_d/P_c^2)$ which is normally small. For $T_2/T_1 = 2$ and $P_d = 10^{-2}$ the relative delay increase is 2%.

It is seen that for channels which are "good" most of the time, retransmissions are infrequent and η and D are not reduced significantly below k/n. However, when the channel degrades increased retransmissions and delays together with reduced values of η is the price paid for low decoded bit-error probabilities under an ARQ protocol.

III-5 Selection of Bit-Error Rate $\bar{p}$

The higher the acceptable channel bit error rate $\bar{p}$, the higher the allowable bit rate R in a noise-limited land mobile radio system, and the higher the R/Δ value allowed in an interference-limited system. In either case, increasing R causes a direct increase in spectrum efficiency, although this increase may be offset somewhat by a decrease in $\bar{P}_c$ under an ARQ protocol.

Consider the choice $\bar{p} = 10^{-3}$. For differential PCM transmission of speech with previous-sample feedback on a memoryless channel [M2, D3] with no coding, the output signal-to-noise ratio

$$\overline{SNR}_0^{-1} \simeq (1-a^2)\, 4^{-L} + 4\,\bar{p} \qquad (3\text{-}91)$$

where feedback coefficient $a \simeq 0.89$ for speech [D3, C2], and L is the number of bits of quantization. The first term results from quantization noise, and the second from channel transmission errors. For 3-bit DPCM, the quantization noise equals $(0.2)/64 = 3.13\times10^{-3}$, while the channel noise equals 4×10^{-3}. In this case $\overline{SNR}_0 \simeq 10^3/7.13 \simeq 21.5$ dB. The sampling rate r(kHz) might lie in the range $6 \lesssim r \lesssim 8$ which implies a bit rate $18 \lesssim R \lesssim 24$, where R is in Kb/s. Use of 4-bit PCM results in a quantization noise of 3.91×10^{-3} and $\overline{SNR}_0 \simeq 21$ dB, with $24 < r < 32$. To reduce the data rate below $R \lesssim 20$ without reducing $\overline{SNR}_0$ would require adaptive DPCM coding. Such coding yields acceptable speech quality at 16 Kb/s, and $\bar{p} = 10^{-3}$ does not significantly degrade the speech quality [H1, C1]. Even $\bar{p} = 5\times10^{-2}$ results in speech which is marginally intelligible [C1].

Reduction to $\bar{p} = 10^{-4}$ would improve $\overline{SNR}_0$ for 3-bit DPCM and 4-bit PCM to 25 dB and 24 dB, respectively. The $\overline{SNR}_0$ values could also be improved by increasing L, but such an increase would increase R and either increase $\bar{p}$ or reduce 0, or both. An increase to $\bar{p} = 10^{-2}$ would reduce $\overline{SNR}_0$ $^{-1}$ to 14 dB for both 3-bit DPCM and 4-bit PCM; in both cases channel noise dominates $\overline{SNR}_0$.

Consider next the transmission of text, when forward error correction might be used. If the "text" consists of video facsimilie, PCM transmission yields the same SNR values as for voice. For DPCM [C2], $a \simeq 0.95$, $(1-a^2) \simeq 0.10$, and for 3-bit DPCM, the quantization noise equals 1.56×10^{-3} and SNR $\simeq$ 22.6 dB. (Again, we have assumed $\bar{p} = 10^{-3}$). Use of channel encoding permits reduction of the information bit-error rate $\bar{p}_i$, in exchange for a reduced information bit rate $R_i = kR/n$. For example, for a (15,11) single error correcting Hamming code on a memoryless channel, $\bar{p}_i \simeq 2\times10^{-5}$. Use of a double-error correcting (15,7) BCH code yields $\bar{p}_i \simeq 1.5\times10^{-6}$. FEC coding could also be used in speech transmission, in those cases where channel errors limit $\overline{SNR}_0$.

A smaller value of the uncoded bit-error rate $\bar{p}$ enables use of a high-higher k/n value for a given value of $\bar{p}_i$. Obtaining a lower $\bar{p}$ value requires a reduction in the channel bit rate R. Whether or not the product (k/n)R increases or decreases depends on a variety of factors, as illustrated below.

Consider the use of MSK detected incoherently as orthogonal FSK, with the requirement $\bar{p}_i = 10^{-3}$. From (3-63), $\bar{p} \simeq 2C_i(\Delta T)$. With no coding $\bar{p}_i = \bar{p}$

and $10\log_{10}\bar{p} \simeq C_d(\Delta/R) + 3$ dB, which implies $C_d(\Delta/R) \simeq -33$ dB. From Fig. 3-3 we obtain $\Delta/R \simeq 3$.

An alternative is to use $\bar{p} = 10^{-2}$, which implies $\Delta/R \simeq 2$, together with a (31,21) double error correcting BCH code. In this case $\bar{p}_i = 0.6\times10^{-3}$. This bit rate is acceptable; however, the normalized information rate $R_i/\Delta = (21/31)(R/\Delta) \simeq 0.33$ which is not really any better than that for direct transmission.

However, use of differential PSK results in $\Delta/R \simeq 10$ for $C_d(\Delta/R) = -33$ dB. Reduction to $\bar{p} = 10^{-2}$ results in $\Delta/R \simeq 3$. Use of the (31,21) code now improves R_i/Δ from 0.10 for the uncoded case to $R_i/\Delta \simeq 0.22$ for the coded case, with an implied improvement factor of 260% in spectrum efficiency.

A similar analysis would show greater benefits for both cases above if the requirement were $\bar{p}_i = 10^{-4}$. In general, the raw information bit-error rate required, the signal format as described by $C_d(\Delta/R)$ and the code used all determine the extent to which FEC coding is helpful. In general, the lower $\bar{p}$ or the slower the roll-off rate for $C_d(\Delta T)$ the more beneficial is FEC coding.

In an environment where $\bar{p}$ fluctuates as a result of shadowing and mobile to base distance separation changes, FEC coding effects must be averaged in accordance with these fluctuations. Since $\bar{p}_i \sim (\bar{p})^{t+1}$, where t is the error-correcting power of the code, fluctuations in $\bar{p}$ cause larger fluctuations in $\bar{p}_i$.

Finally, we consider error detection, with $\bar{p} = 10^{-2}$. With a (31,26)

single error correcting Hamming code, $P_c = 0.73$, and $\bar{p}_i = 3\times10^{-4}$. With a (31,21) double-error correcting code, $P_c = 0.73$ and $\bar{p}_i = 2.7\times10^{-6}$.

If the above codes are used with $\bar{p} = 10^{-3}$, then $P_c = 0.97$ for both codes, and $\bar{p}_i = 3\times10^{-7}$ and 2.7×10^{-11} for the (31,26) and (31,21) code, respectively. In this case moderate redundancy results in dramatic improvements in information bit error rates.

In summary, $\bar{p} \approx 10^{-3}$ yields acceptable performance for transmission of speech, text and control messages, provided some channel encoding is used with text and control messages. Reduction to $\bar{p} \approx 10^{-2}$ would probably require some FEC coding to reduce channel noise effects in speech, and could cause excessive retransmissions of control messages, unless these were transmitted in short blocks, or some FEC were included to maintain the retransmission probability at an acceptable level.

III-6 References for Chapter III

[A1] T. Aulin, "Characteristics of a digital mobile radio channel", IEEE Trans. Veh. Technol., Vol. VT-30, pp. 45-53, May 1981.

[B1] H.O. Burton and D.D. Sullivan, "Errors and error control", Proc. IEEE, vol. 60, pp. 1293-1301, Nov. 1972.

[B2] R.J. Bernice and A.H. Frey, Jr., "An analysis of retransmission systems", IEEE Trans. Commun., vol. COM-12, pp. 135-145, Dec. 1964.

[B3] R.J. Bernice and A.H. Frey, Jr., "Comparison of error control techniques", IEEE Trans. Commun., vol. COM-12, pp. 146-154, Dec. 1964.

[C1] D.L. Cohn and J.L. Melsa, "The residual encoder - an improved ADPCM system for speech digitization", IEEE Trans. Commun., vol. COM-23, pp. 935-941, Sept. 1975.

[C2] K.Y. Chang and R.W. Donaldson, "Analysis optimization and sensitivity study of differential PCM systems operating on noisy communication channels", IEEE Trans. Commun., vol. COM-20, pp. 338-350, June 1972.

[D1] R.W. Donaldson, "Frequency assignment for land mobile radio system in the 900 MHz band: Digital transmission over land mobile channels - spectrum usage considerations", Rpt. to Dept. of Communications, Ottawa, Canada, Feb. 1981.

[D2] R.W. Donaldson, "Frequency assignment for land mobile radio system: Digital transmission over land mobile channels - Interference considerations", Rpt. to Dept. of Communications, Ottawa, Canada, Jan. 1980.

[D3] R.W. Donaldson and D. Chan, "Analysis and subjective evaluation of differential pulse-code modulation voice communication systems", IEEE Trans. Commun., vol. COM.17, pp. 10-19, Feb. 1969.

[E1] S. Elnoubi and S.G. Gupta, "Error rate performance of non-coherent detection of duobinary coded MSK and TFM in mobile radio communication systems", IEEE Trans. Veh. Technol., vol. VT-30, pp. 62-76, May 1981.

[F1] M. Fletcher, Speech and Hearing in Communication. New York, N.Y.: Van Nostrand, 1953.

[F2] C. Fujiwara, M. Kasahara, K. Yamashita and T. Namekawa, "Evaluations of error control techniques in both independent-error and dependent-error channels", IEEE Trans. Commun., vol. COM-26, pp. 785-794, June 1978.

[G1] R.G. Gallager, Information Theory and Reliable Communication. New York, N.Y.: Wiley, 1968.

[G2] S.A. Gronemeyer and A.L. McBride, "MSK and offset QPSK modulation", IEEE Trans. on Comm., vol. COM-24, pp. 809-820, Aug. 1976.

[H1] B.A. Hanson and R.W. Donaldson, "Subjective evaluation of an adaptive differential voice encoder with oversampling and entropy encoding", IEEE Trans. Commun., vol. COM-26, pp. 201-208, Feb. 1978.

[J2] W.C. Jakes, Microwave Mobile Communications. New York, N.Y.: Wiley, 1974.

[K1] I. Kalet, "A look at crosstalk in quadrature-carrier modulation systems", IEEE Trans. Commun., vol. COM-25, pp. 884-892, Sept. 1977.

[K2] I. Kalet and E. White, "Suboptimal continuous shift keyed (CSK) demodulation for efficient implementation of low crosstalk data communication", IEEE Trans. Commun., vol. COM-25, pp. 1037-1041, Sept. 1977.

[K3] I. Kalet and L. Weiner, "Close packing of PCSFSK signals-model and simulation results", IEEE Trans. Commun., Vol. COM-27, pp. 1234-1239, Aug. 1979.

[K4] L. Kleinrock, Queueing System, Vol. 2: Computer Applications. New York: J. Wiley, 1976, Ch. 5 and 6.

[L1] R.W. Lucky, J. Salz and E.J. Weldon, Jr., Principles of Communication Engineering. New York, N.Y.: McGraw-Hill, 1968.

[L2] S. Lin, An Introduction to Error-Correcting Codes. Englewood Cliffs, N.J.: Prentice-Hall, 1970.

[L3] W.C. Lindsay and M.K. Simon, Telecommunication Systems Engineering. Englewood Cliffs, N.J.: Prentice-Hall, 1973.

[L4] C.S.K. Leung and A. Lam, "Forward error correction for an ARQ scheme", IEEE Trans. Commun., vol. COM-29, pp. 1514-1519, October 1981.

[M1] J.M. Morris, "Optimal block lengths for ARQ error control schemes", IEEE Trans. Commun., vol. COM-27, pp. 488-493, Feb. 1979.

[M2] J.E. Max, "Quantizing for minimum distortion", IRE Trans. Inform. Theory, vol. IT-6, pp. 7-12, March 1960.

[P1] W.W. Peterson and E.J. Weldon, Jr., Error-Correcting Codes, 2nd Ed. Cambridge, MA: The MIT Press, 1972.

[P2] R.L. Pickholtz and C. McCoy, Jr., "Effects of a priority discipline in routing for packet-switched networds", IEEE Trans. Commun., vol. COM-24, pp. 506-516, May 1976.

[S1] M.K. Simon, "A generalization of minimum-shift-keying (MSK)-type signalling based on input data symbol pulse shaping", IEEE Trans. Commun., vol. COM-24, pp. 845-856, Aug. 1976.

[S2] J.J. Stiffler, Theory of Synchronous Communications. Englewood Cliffs, N.J.: Prentice-Hall, 1971.

[S3] A.R.K. Sastry, "Performance of hybrid error control schemes on satellite channels", IEEE Trans. Commun., vol. COM-23, pp. 689-695, July 1975.

[S4] M. Schwartz, Computer-Communication Network Design and Analysis. Englewood Cliffs, N.J.: Prentice-Hall, 1971.

[S5] C.A. Sunshine, "Efficiency of interprocess communication protocols for computer networks", IEEE Trans. Commun., vol. COM-25, pp. 287-293, Feb. 1977.

[W1] J.M. Wozencraft and I.M. Jacobs, Principles of Communication Engineering. New York, N.Y.: 1965.

IV BIT-ERROR PROBABILITY VARIATIONS

Any variation in $\bar{p}$ depends directly on the variation in $\bar{P}_i/\bar{P}_s$ in an interference-limited system. The present chapter includes a detailed study of how $\bar{P}_i/\bar{P}_s$ varies over the coverage area.

IV-1 Single-Cell Systems - Downstream Transmission

Transmission from a single base station to a mobile results in adjacent-channel interference. In a conventional narrowband FM system, interference level variations on immediately adjacent downstream channels which result from shadowing and distance changes are equal to those of the wanted signal. Thus, the ratio $\bar{P}_i/\bar{P}_s$ remains constant over the cell coverage area, when both the wanted and interfering signal are present.

In the following, we will be interested in the distribution function

$$F_i(\gamma) = \text{Prob}[\bar{P}_i < \gamma\bar{P}_s] \tag{4-1}$$

and in the density function

$$f_i(\gamma) = dF_i(\gamma)/d\gamma \tag{4-2}$$

For base-to-mobile transmission in single-cell systems, where all (narrowband) channels have equal transmitter power,

$$F_i(\gamma) = U(\gamma-1) \tag{4-3}$$

$$f_i(\gamma) = \delta(\gamma-1) \tag{4-4}$$

where $\delta(\gamma)$ and $U(\gamma)$ denote the unit impulse and unit step function, respectively. Equations (4-3) and (4-4) simply state that with probability one, the average powers in the wanted and interfering signal from the same base transmitter are equal at a mobile's antenna. The average is with respect to the fast Rayleigh fading, although transmissions on adjacent channels from the same base undergo Rayleigh fades which are highly correlated.

Also of interest is the distribution function for the output interference-to-signal ratio $F_o(\gamma)$ and its associated density $f_o(\gamma)$. For a single interfering data signal with data rate and modulation format the same as that of the wanted signal,

$$F_o(\gamma) = \text{Prob}\left(C\bar{P}_i < \gamma\bar{P}_s\right)$$

$$= F_i(\gamma/C) \qquad (4\text{-}5)$$

$$f_o(\gamma) = f_i[\gamma/C]/C \qquad (4\text{-}6)$$

where C is the interference coefficient; $C = C(\Delta T)$. From (4-3) and (4-4) one obtains

$$F_o(\gamma) = U\left(\frac{\gamma}{C} - 1\right)$$

$$= U(\gamma - C) \qquad (4\text{-}7)$$

$$f_o(\gamma) = \delta(\gamma - C) \qquad (4\text{-}8)$$

The functions in (4-7) and (4-8) were obtained assuming that interference is present whenever the signal is present. When such is not the case, they should be replaced by

$$f_o(\gamma) = (1-\phi)\delta(\gamma) + \phi\delta(\gamma-C) \tag{4-9}$$

$$F_o(\gamma) = (1-\phi)U(\gamma) + \phi U(\gamma-C) \tag{4-10}$$

where ϕ is the channel occupancy. When $\phi = 1$, (4-9) and (4-10) reduce to (4-7) and (4-8) respectively. Figure 4-1 shows $f_o(\gamma)$ and $F_o(\gamma)$ in (4-9) and (4-10).

The density function for the total output interference-to-signal power $f_{\overline{snr}^{-1}}(\gamma)$ is obtained by convolution of the output density functions for the individual interfering signals (assuming independent interferers). When the interference is primarily from the two adjacent channels, C is the same for each channel and

$$f_{\overline{snr}^{-1}}(\gamma) = (1-\phi)^2\delta(\gamma) + 2\phi(1-\phi)\delta(\gamma-C) + \phi^2\delta(\gamma-2C) \tag{4-11}$$

$$F_{\overline{snr}^{-1}}(\gamma) = (1-\phi)^2U(\gamma) + 2\phi(1-\phi)U(\gamma-C) + \phi^2\delta(\gamma-2C) \tag{4-12}$$

Figure 4-2 shows (4-11) and (4-12) for various values of ϕ. These results show that:

$$\overline{SNR}^{-1} = \begin{cases} 0 & \text{with probability } (1-\phi)^2 \\ C & \text{with probability } 2\phi(1-\phi) \\ 2C & \text{with probability } \phi^2 \end{cases} \tag{4-13}$$

With $\phi = 0.5$, $\overline{SNR}^{-1}$ is bounded above by C with 75% probability, but there is a 25% probability that $\overline{SNR}^{-1} = 2C$.

For any ϕ, the average $\overline{SNR}^{-1}$ value is $\langle \overline{SNR}^{-1} \rangle = 2\phi C$, where $\langle\rangle$

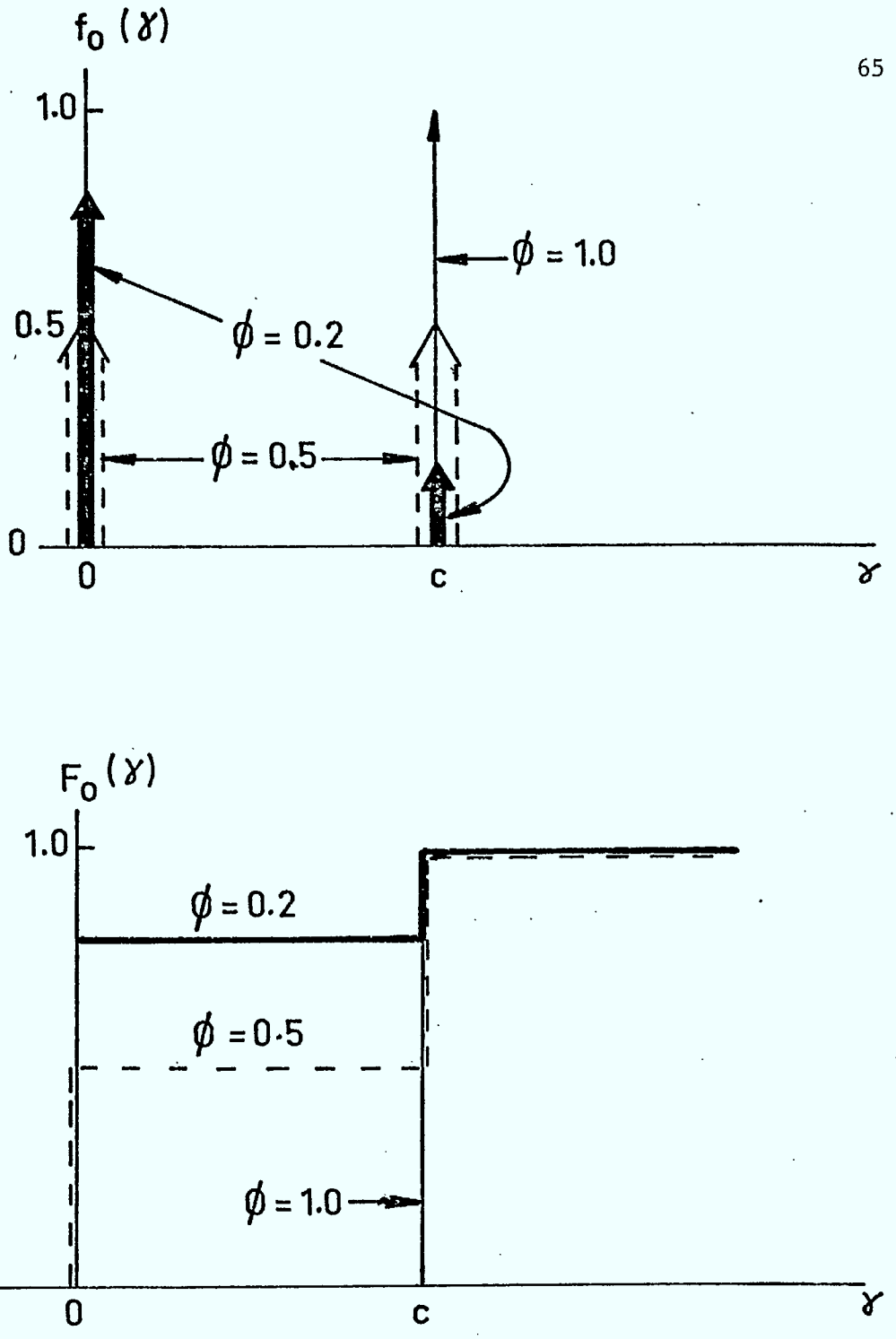

Fig. 4-1 Density and distribution functions for $f_o(\gamma)$ and $F_o(\gamma)$; downstream interference one-cell system.

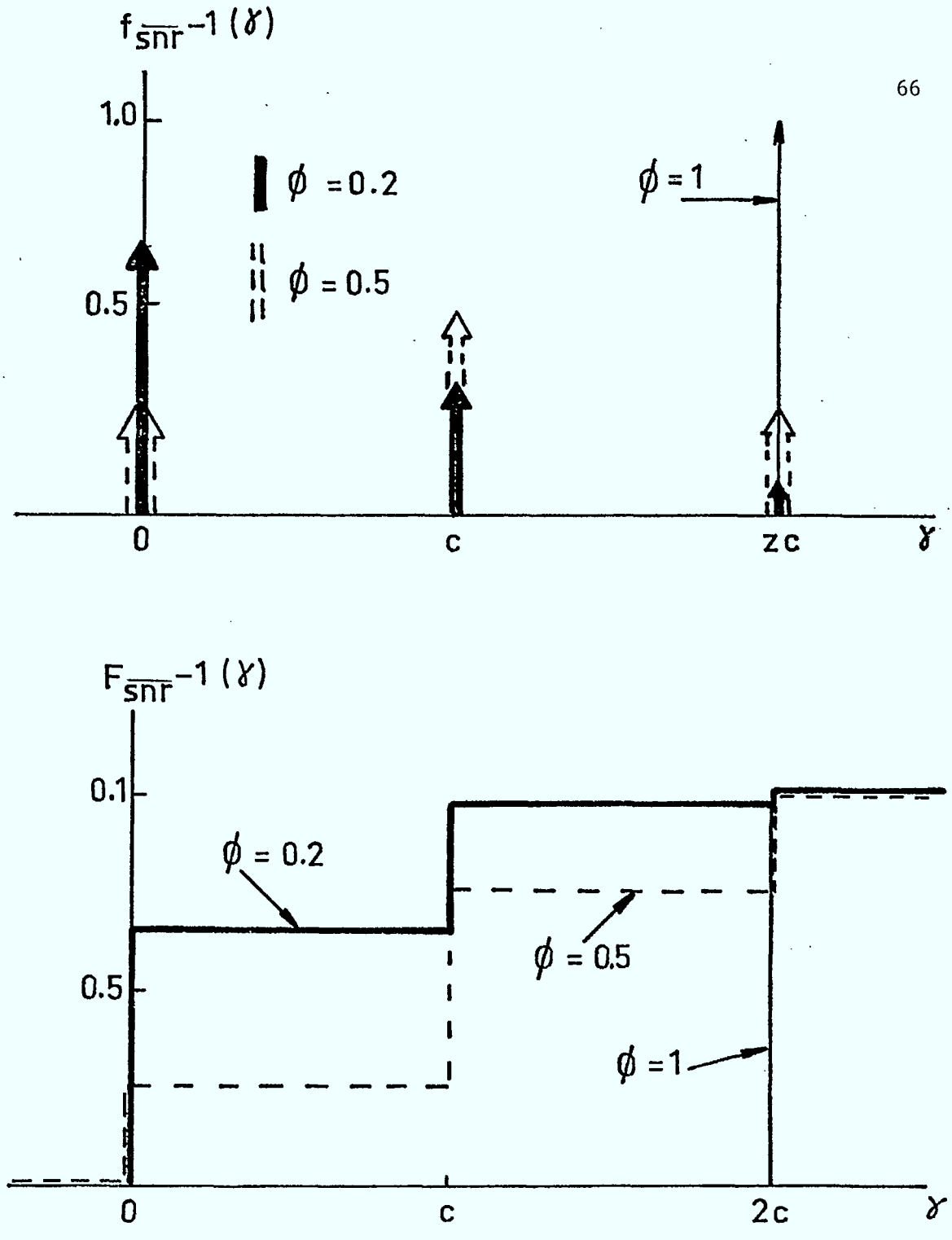

Fig. 4-2 Density and distribution functions $f_{\overline{snr}}{}^{-1}(\gamma)$ and $F_{\overline{snr}}{}^{-1}(\gamma)$; downstream interference, single-cell system.

denotes an average over shadowing and distance separation variations.

To the extent that $\bar{p} \simeq \overline{SNR^{-1}}$, these results can be used to determine the variation of $\bar{p}$.

These results are for interference-limited systems. When a large area is covered by a single base station, noise rather than interference may limit performance.

IV-2 Single-Cell System - Upstream Transmission

In transmissions from mobile-to-base, fading and distance separation for the wanted and interfering signals are statistically independent, and shadowing also tends to be independent.

Consider first the variation due to distance only with r_s and r_i denoting the separation between the base and the wanted and interfering signal, respectively. We determine below

$$F_r(\alpha) = \text{Prob}(r_s < \alpha r_i) \tag{4-14}$$

Define $f_{r_i}(\alpha)$ and $f_{r_s}(\alpha)$ as the radial density functions for r_i and r_s in a circular coverage region of radius R where vehicles are uniformly distributed over the coverage area. Then

$$f_{r_i}(\alpha) = f_{r_s}(\alpha)$$

$$= \begin{cases} 2\alpha/R^2 & 0 \leq \alpha \leq R \\ 0 & \alpha < 0 \ , \ \alpha > R \end{cases} \tag{4-15}$$

Thus, for $\alpha < 1$

$$F_r(\alpha) = \int_{y=0}^{R} \left[\int_{x=0}^{\alpha y} f_{r_s}(x)dx\right] f_{r_i}(y)dy$$

$$= \alpha^2/2 \qquad (\alpha \leq 1)$$

Symmetry arguments yield, for $\alpha > 1$

$$P(r_s < \alpha r_i) = 1 - P(r_s > \alpha r_i)$$

$$= 1 - 1/2\alpha^2$$

Therefore,

$$F_r(\alpha) = \begin{cases} \alpha^2/2 & \alpha \leq 1 \\ 1 - \dfrac{1}{2\alpha^2} & \alpha \geq 1 \end{cases} \tag{4-16}$$

$$f_r(\alpha) = \begin{cases} \alpha & \alpha \leq 1 \\ 1/\alpha^3 & \alpha \geq 1 \end{cases} \tag{4-17}$$

From these results one obtains, for any real number n,

$$F_{r^n}(\alpha) = P(r_s{}^n < \alpha r_i{}^n)$$

$$= P(r_s < \sqrt[n]{\alpha}\, r_i)$$

$$= F_r(\sqrt[n]{\alpha}) \tag{4-18}$$

$$f_{r^n}(\alpha) = n\sqrt[(n-1)]{\alpha}\, f_r(\sqrt[n]{\alpha}) \tag{4-19}$$

It is useful to express the above results in dB, by using

$$A = 20 \log_{10} \alpha \tag{4-20}$$

$$R_i = 20 \log_{10} r_i \tag{4-21}$$

$$R_s = 20 \log_{10} r_s \tag{4-22}$$

One thus obtains

$$F_R(A) = \text{Prob}(R_s < A + R_i)$$

$$= \begin{cases} [\exp(cA)]/2 & A < 0 \\ 1 - \frac{1}{2}[\exp(-cA)] & A \geq 0 \end{cases} \tag{4-23a}$$

where

$$c = (\log_e 10)/10 \tag{4-23b}$$

$$f_R(A) = (\tfrac{c}{2})\exp(-|cA|) \tag{4-24}$$

Similarly, by analogy with (4-18) and (4-19)

$$F_{nR}(A) = P(nR_s < A + nR_i)$$

$$= P(R_s < (A/n) + R_i)$$

$$= F_R(A/n) \tag{4-25}$$

$$f_{nR}(A) = \frac{1}{n} f_R(A/n) \tag{4-26}$$

To determine the distribution function $f_i(\gamma)$ which includes the effects of shadowing and distance separation, we use French's results [F1] for shadowing only, as follows, where ℓ_i and ℓ_s denote local mean voltage levels, m_i and m_s are area median voltage levels, and σ is the standard

deviation in dB of the local mean. (Note that eqn. (17) in [F1] should have lower limit $Z_d/\sigma\sqrt{2}$; also some minor errors appear in Appendix II, although the final result is correct.)

$$P(\ell_i < b\ell_s) = \frac{1}{\sqrt{2\pi}} \int_{Z/\sigma\sqrt{2}}^{\infty} \exp(-u^2/2)du \tag{4-27a}$$

$$Z = 20 \log_{10}(m_i/m_s b) \tag{4-27b}$$

With distance power loss factor n (typically, $n \simeq 3.5$)

$$m_i/m_s = (r_s/r_i)^{n/2} \tag{4-28}$$

Using $\bar{P}_i = \ell_i^2$ and $\bar{P}_s = \ell_s^2$ together with (4-27) yields

$$\begin{aligned} F_i(\gamma) &= P(\bar{P}_i < \gamma \bar{P}_s) \\ &= P(\ell_i < \sqrt{\gamma}\, \ell_s) \\ &= \int_{\beta=0}^{\infty} P(\ell_i/\ell_s < \sqrt{\gamma} \;\Big|\; \frac{r_s}{r_i} = \beta) f(\beta) d\beta \\ &= \int_{\beta=0}^{1} \beta G_i(\sqrt{\gamma} \;\Big|\; \frac{r_s}{r_i} = \beta) d\beta + \int_{1}^{\infty} \frac{1}{\beta^3} G_i(\sqrt{\alpha} \;\Big|\; \frac{r_s}{r_i} = \beta) d\beta \end{aligned} \tag{4-29}$$

where

$$G_i(\sqrt{\gamma} \mid \frac{r_s}{r_i} = \beta) = \frac{1}{\sqrt{2\pi}} \int_{\frac{20 \log_{10}(\beta^{n/2}/\sqrt{\gamma})}{\sigma\sqrt{2}}}^{\infty} \exp(-u^2/2)du \tag{4-30}$$

It now follows that

$$f_i(\gamma) = \int_0^1 \beta f_i\left(\gamma \mid \frac{r_s}{r_i} = \beta\right) d\beta + \int_1^\infty \frac{1}{\beta^3} f_i\left(\gamma \mid \frac{r_s}{r_i} = \beta\right) d\beta \qquad (4\text{-}31)$$

where

$$f_i(\gamma)\left|\frac{r_s}{r_i} = \beta\right. = dG_i\left(\sqrt{\gamma} \mid \frac{r_s}{r_i} = \beta\right)/d\gamma$$

$$= \left[\frac{5}{(\ln 10)\sqrt{\pi}\sigma\gamma}\right] \exp\left(\left[-\frac{50}{\sigma^2}(\log_{10}(\beta^n/\gamma)\right]^2\right) \qquad (4\text{-}32)$$

Substitution of

$$\Gamma = 10 \log_{10}\gamma \qquad (4\text{-}33a)$$

$$\gamma = 10^{\Gamma/10}$$

$$= e^{c\Gamma} \qquad (4\text{-}33b)$$

enables $f_i(\gamma)$ and $F_i(\gamma)$ to be plotted on a dB (power) scale. Thus,

$$f_I(\Gamma) = \left[\left(\frac{d\gamma}{d\Gamma}\right) f_i(\gamma)\right]_{\gamma = \exp(c\Gamma)}$$

$$= c\left[\gamma f_i(\gamma)\right]_{\gamma = \exp(c\Gamma)} \qquad (4\text{-}34)$$

Alternatively, it is possible to obtain $f_I(\Gamma)$ and $F_I(\Gamma)$ directly, as follows:

$$P(L_i < L_s + B) = \frac{1}{\sqrt{2\pi}} \int_{z/\sigma\sqrt{2}}^\infty \exp(-u^2/2)du \qquad (4\text{-}35a)$$

where

$$z = L_i - L_s - B \qquad (4\text{-}35b)$$

$$= \frac{n}{2}\left(R_s - R_i\right) - B \qquad (4\text{-}35c)$$

where R_i, R_s, L_i, L_s and B are the dB (level) equivalents of r_i, r_s, l_i, l_s, and B respectively; thus R_i and R_s are given by (4-21) and (4-22), respectively and

$$B = 20\log_{10} b \qquad (4\text{-}36)$$

Use of $\Gamma_i = 10\log_{10}\overline{P}_i = 10\log_{10} l_i^2 = L_i$, and similarly for L_s yields

$$\begin{aligned} F_I(\Gamma) &= P(\Gamma_i < \Gamma + \Gamma_s) \\ &= P(L_i < \Gamma + L_s) \\ &= \int_{-\infty}^{\infty} P(L_i - L_s < \Gamma \,|\, R_s - R_i = K)\; f_R(K)\,dK \\ &= \int_{-\infty}^{\infty} G_I(\Gamma \,|\, R_i - R_s = K)\left(\frac{c}{2}\right)\exp(-|cK|)\,dK \end{aligned} \qquad (4\text{-}37)$$

where

$$G_I(\Gamma \,|\, R_i - R_s = K) = \frac{1}{\sqrt{2\pi}} \int_{\left(\frac{n}{2}K - \Gamma\right)/\sigma\sqrt{2}}^{\infty} \exp(-u^2/2)\,du \qquad (4\text{-}38)$$

Differentiation of (4-37) with respect to Γ yields

$$f_I(\Gamma) = \frac{c}{4\sigma\sqrt{\pi}} \int_{-\infty}^{\infty} \exp\left[-\frac{\left(\frac{nK}{2} - \Gamma\right)^2}{4\sigma^2}\right] \exp(-|cK|)\,dK \qquad (4\text{-}39)$$

Density $f_I(\Gamma)$ can be integrated to yield $F_I(\Gamma)$.

Note that (4-39) is the convolution of the distance separation density

in dB and the shadowing density. This one would expect, sonce these two effects are additive when expressed in dB.

From (4-39) one obtains $f_i(\gamma)$ from

$$f_i(\gamma) = \left[\frac{d\Gamma}{d\gamma} \cdot f_I(\Gamma)\right]_{\Gamma=10\log_{10}\gamma}$$

$$= \left[\frac{10}{\gamma \ln 10} \; f_I(\Gamma)\right]_{\Gamma=10\log_{10}\gamma} \qquad (4\text{-}40)$$

The choice n = 0 leads to the shadowing-only case, in which case both (4-39) and (4-35) yield

$$f_I(\Gamma)\Big]_{n=0} = \frac{1}{2\sigma\sqrt{\pi}} \exp(-\Gamma^2/4\sigma^2) \qquad (4\text{-}41)$$

$$F_I(\Gamma)\Big]_{n=0} = \frac{1}{\sqrt{2\pi}} \int_{-\infty}^{\Gamma/\sigma\sqrt{2}} \exp(-u^2/2)du \qquad (4\text{-}42)$$

This reduces to French's result [F1], after correcting the error (replace $\sqrt{\sigma}$ by σ) in his eqn. (17).

Figs. 4-3 and 4-4 show $F_I(\Gamma)$ and $f_I(\Gamma)$ plotted on dB scales, for various values of n and σ. The case $\sigma = 0$ corresponds to no shadowing (or perfect shadowing correlation between the interfering and wanted signal). Note how the distribution and density functions disperse as n and/or σ increase.

Fig. 4-5 shows the densities for n = 0 (no distance variation) and $\sigma = 0$ (no shadowing). It is clear from these curves that in a single-cell system, the variation in signal level from shadowing causes a somewhat

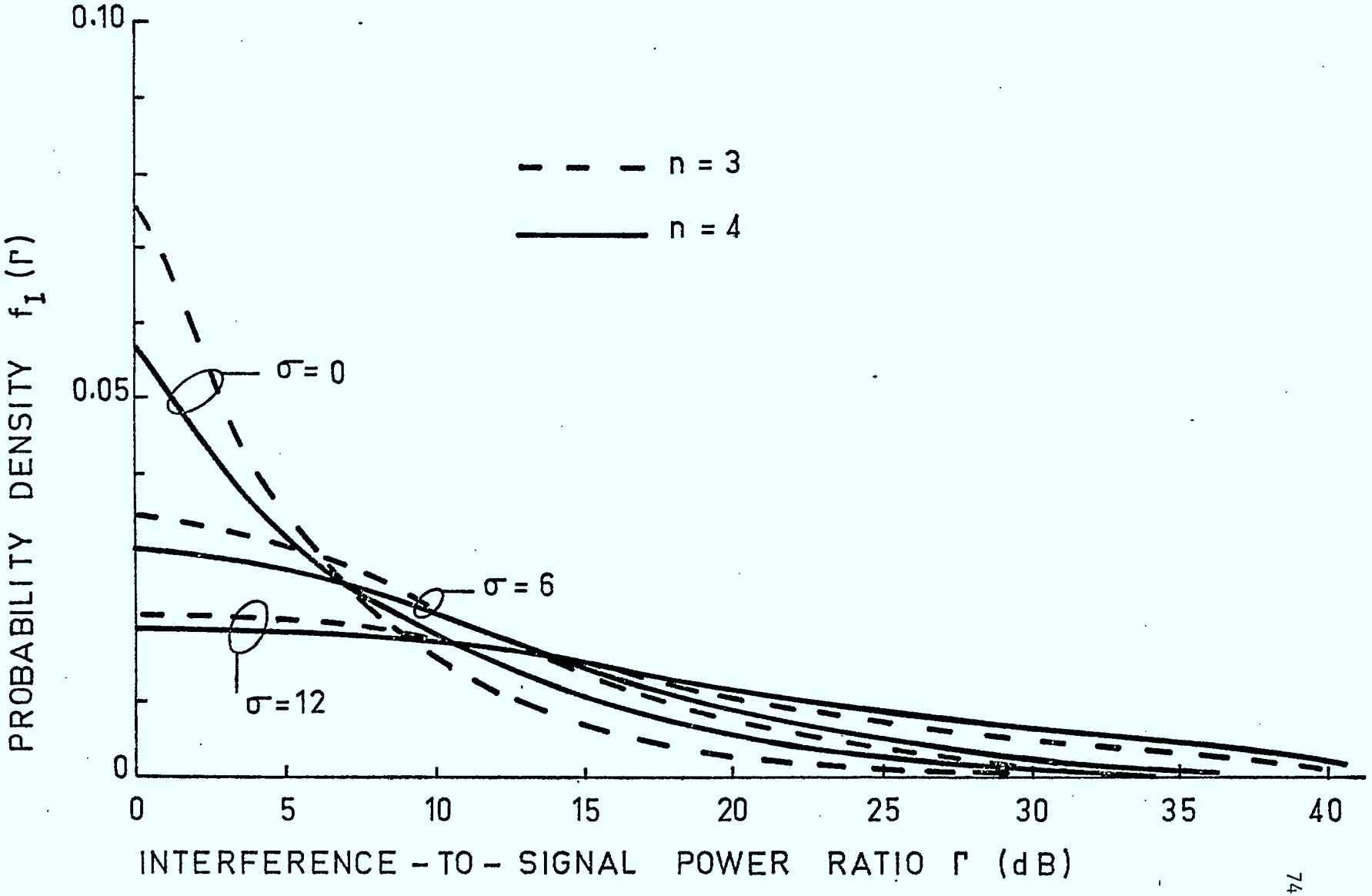

Fig. 4-3 Probability density $f_I(\Gamma)$ for a single interfering signal; upstream interference.

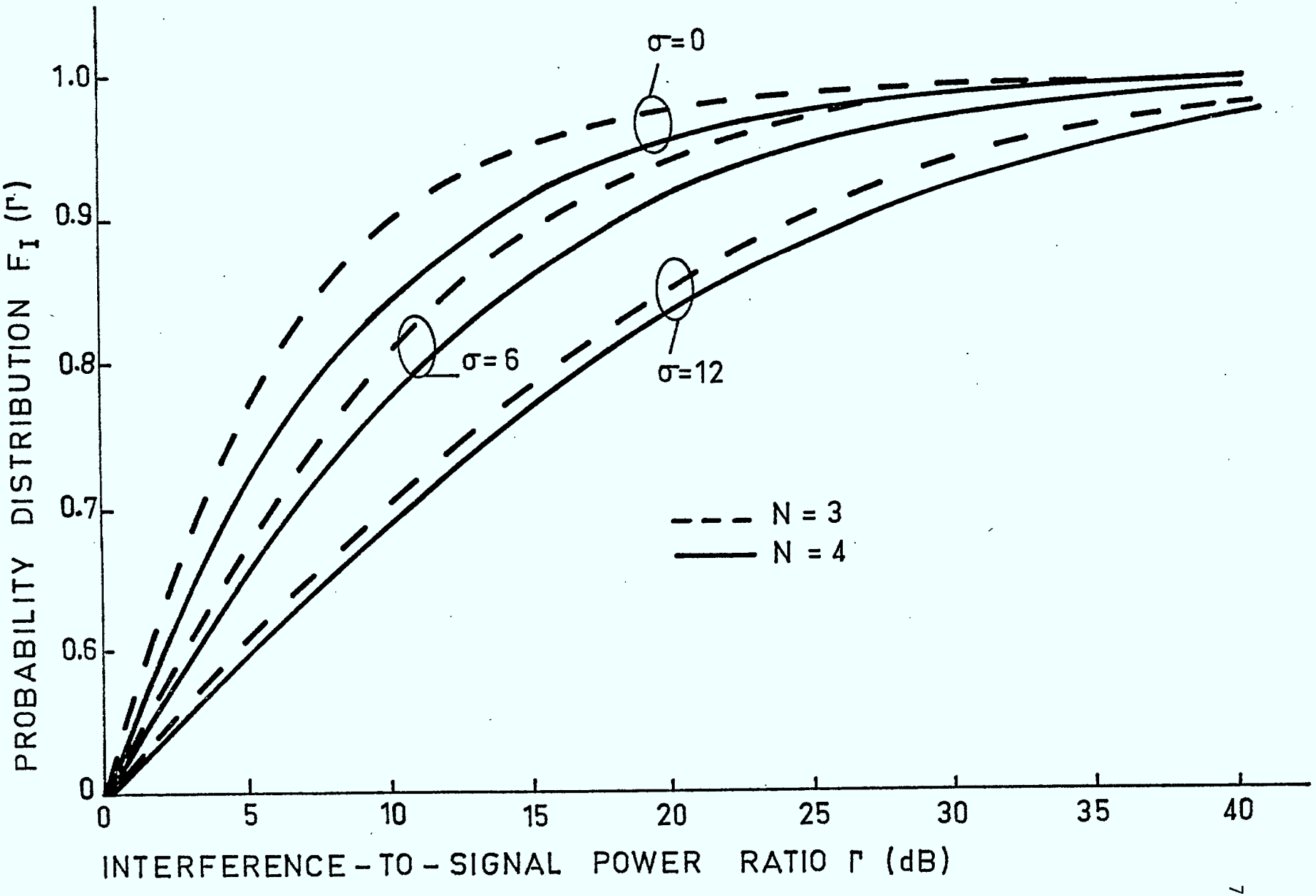

Fig. 4-4 Probability distribution $F_I(\Gamma)$ for a single interfering signal; upstream interference.

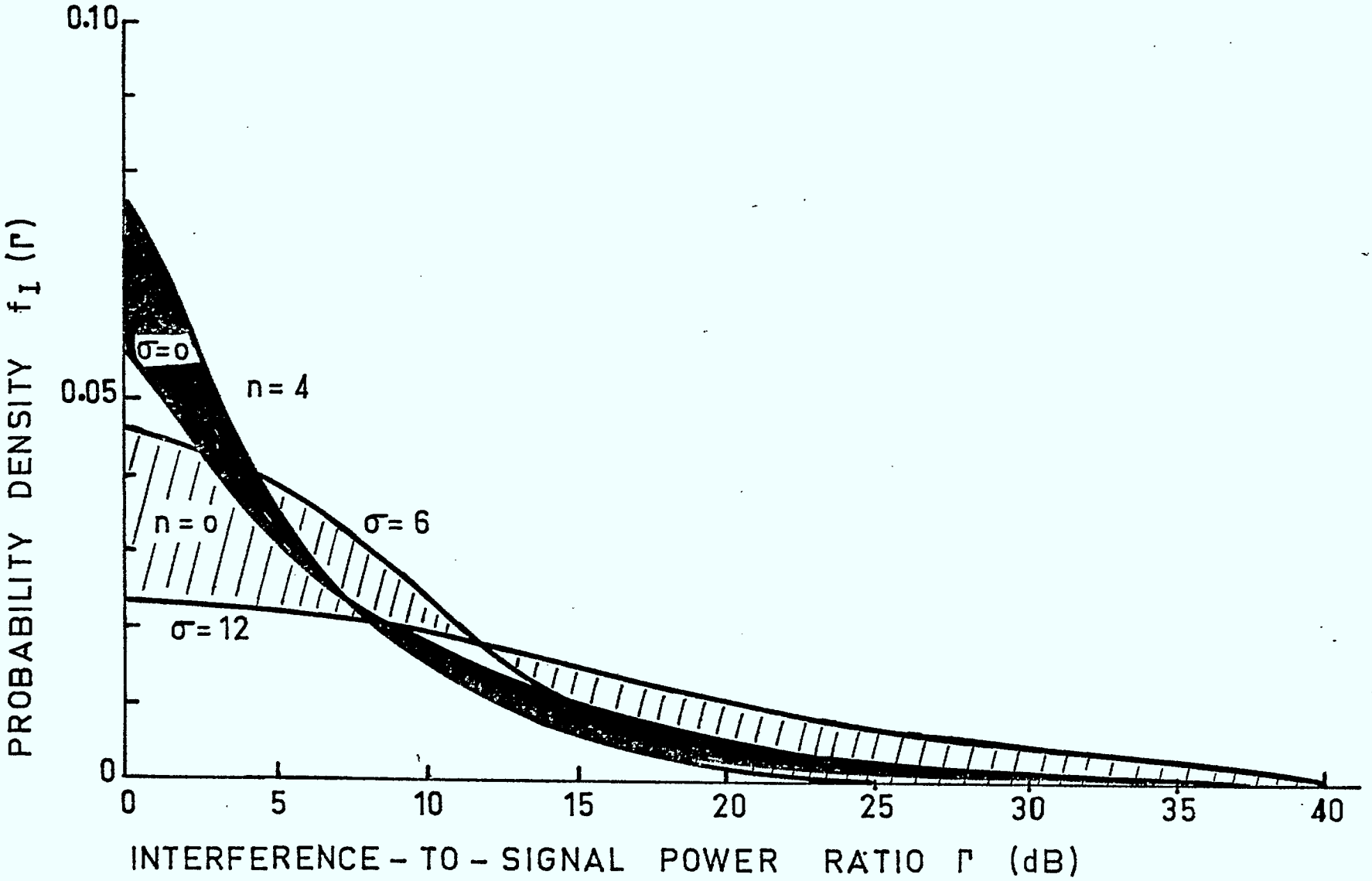

Fig. 4-5 Probability densities $f_I(\Gamma)$ for shadowing only (n=0) and and distance variation only (σ=0); upstream interference.

greater variation in interference-to-signal level than does variation in mobile-to-base distance separation.

The density and distribution function $h_I(\Gamma)$ and $H_I(\Gamma)$ which result when the interference consists of two independent signals of equal transmitted energy can now be determined. These would be signals on adjacent channels in a single cell system. The function $h_i(\gamma)$ is obtained by convolution of $f_i(\gamma)$ with itself; $h_I(\Gamma)$ is then obtained by using $\gamma = 10^{\Gamma/10}$. $H_I(\Gamma)$ is obtained by integration of $h_I(\Gamma)$. Thus;

$$H_I(\Gamma) = \int_{-\infty}^{\infty} h_I(\gamma)d\gamma \tag{4-43}$$

$$h_i(\gamma) = \int_{-\infty}^{\infty} f_i(x)f_i(x-\gamma)dx \tag{4-44}$$

$$h_I(\Gamma) = \left(\frac{d\gamma}{d\Gamma}\right) h_i(\gamma)\Big]_{\gamma=e^{c\Gamma}}$$

$$= c\left[\gamma h_i(\gamma)\right]_{\gamma=e^{c\Gamma}} \tag{4-45}$$

To determine the distribution function and density function when the mean power level of each interfering signal is $C = C(\Delta T)$, and channel occupancy is ϕ we use the following:

$$f_{\overline{snr}^{-1}}(\gamma) = (1-\phi)^2\delta(\gamma) + \frac{2\phi(1-\phi)}{C} f_i(\gamma/C) + \frac{\phi^2}{C} h_i(\gamma/C) \tag{4-46}$$

$$f_{\overline{SNR}^{-1}}(\Gamma) = (1-\phi)^2\delta(\Gamma+\infty) + 2\phi(1-\phi)f_I(\Gamma-C) + \phi^2 h_I(\Gamma-C) \tag{4-47}$$

$$F_{\frac{}{SNR}^{-1}}(\Gamma) = (1-\phi)^2+2\phi(1-\phi)F_I(\Gamma-C)+\phi^2H_I(\Gamma-c) \qquad (4\text{-}48)$$

A plot of (4-48) would be similar in some respects to Fig. 4-2, except that the sharp discontinuities would be replaced by smooth transitions. Such a plot for $\phi = 0.5$ is similar to one for $F_I(\Gamma-C)$ with $\phi = 1.0$.

IV-3 Intercell Interference

Consider the arrangement in Fig. 4-6, where the signal travels (in either direction) between base and mobile in the same cell, while the interference results from either the base or mobile in another cell. The distance between cell centres is d.

In Fig. 4-6, with $r_i = \alpha$

$$\phi = 2\cos^{-1}\left[\sqrt{\frac{1}{4}\frac{(\alpha+d+R)(\alpha+d-R)}{\alpha d}}\right] \qquad (4\text{-}49)$$

The density function $f_{r_i}(\alpha)$, obtained by dividing the shaded area in Fig. 4-6 by the area $\pi R^2 d\alpha$, is:

$$f_{r_i}(\alpha) = \frac{4\alpha}{\pi R^2}\cos^{-1}\left[\frac{1}{2}\sqrt{\frac{(\alpha+d+R)(\alpha+d-R)}{\alpha d}}\right] \qquad (4\text{-}50)$$

which yields, with $\beta = \alpha/R$ and $D = d/R$

$$Rf_{r_i}(\beta) = \frac{4\beta}{\pi}\cos^{-1}\left[\frac{1}{2}\sqrt{\frac{(\beta+D+1)(\beta+D-1)}{\beta D}}\right] \qquad (4\text{-}51)$$

Fig. 4-7 shows $Rf_{r_i}(\beta)$ vs. β for various values of D. The curves are reasonably insensitive to changes in D, particularly for $D \gtrsim 5$.

Note that (4-51) applies whether the interfering source is a mobile in

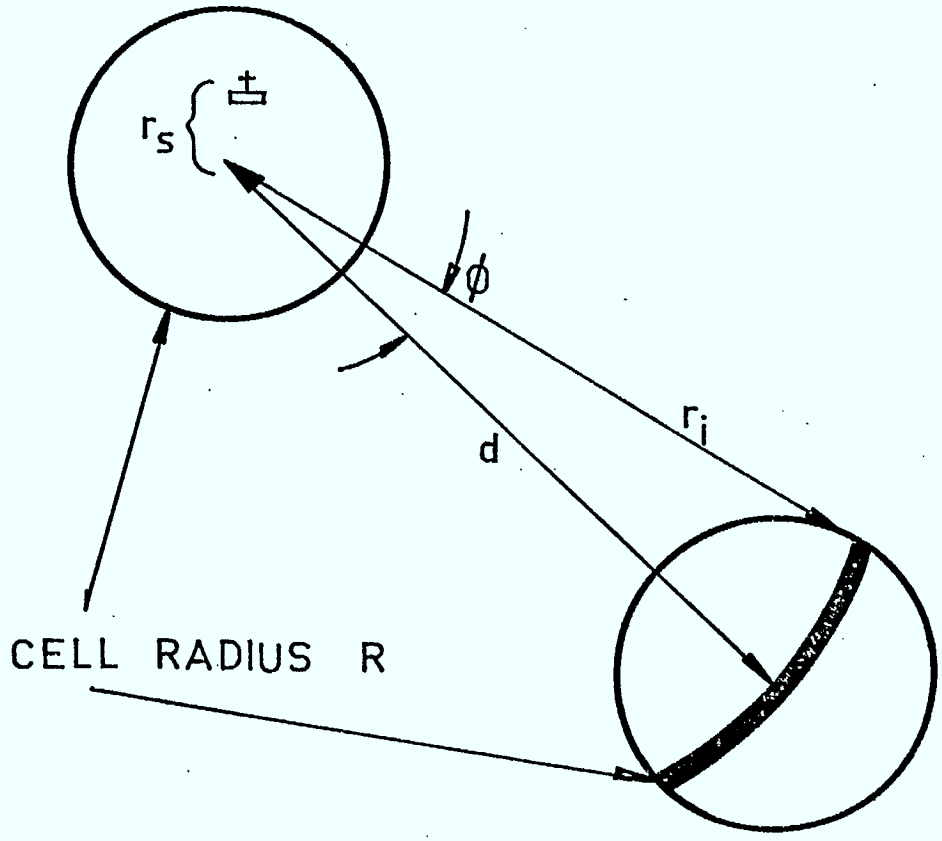

Fig. 4-6 Illustrating inter-cell interference density determination.

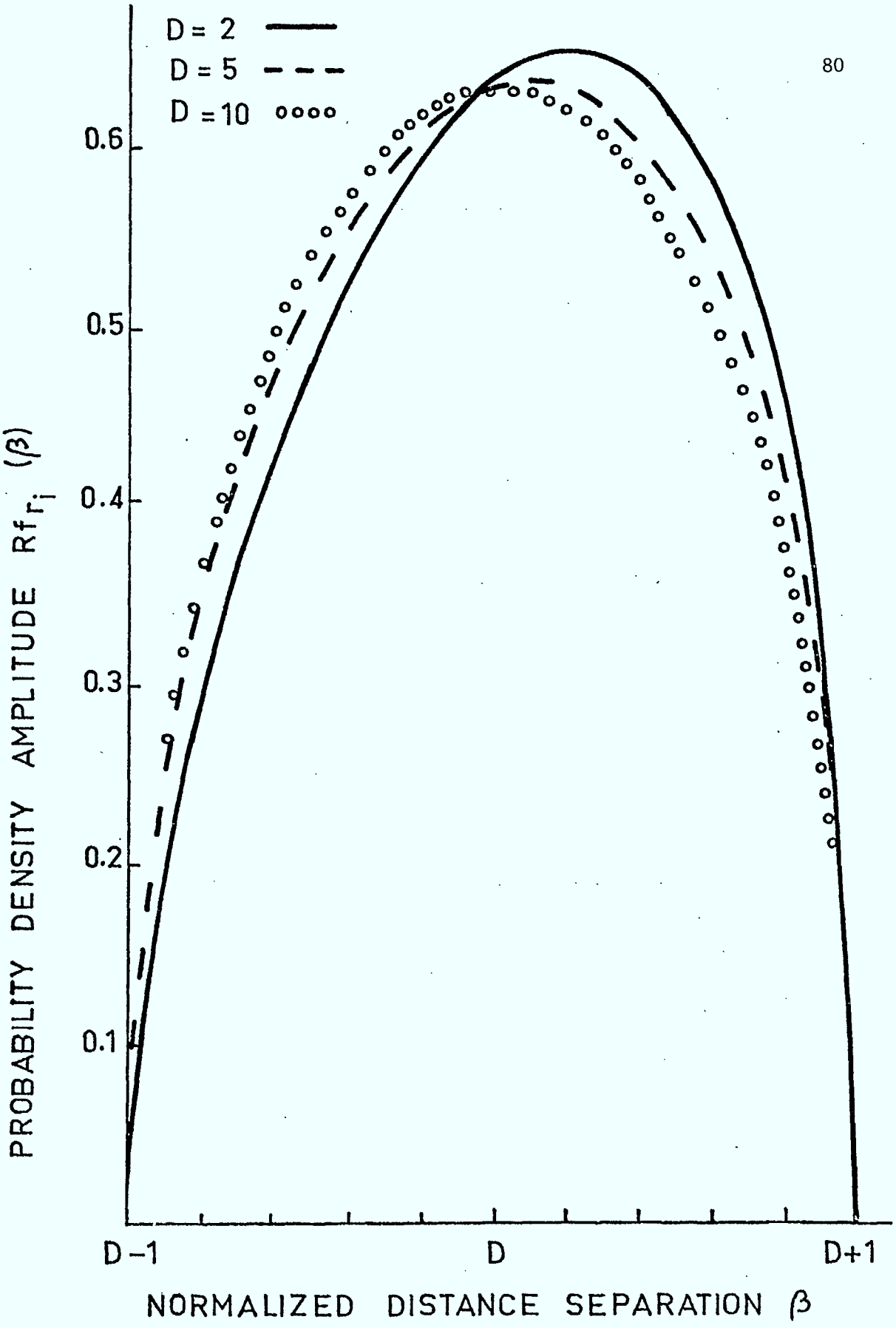

Fig. 4-7 Interference-to-signal density $Rf_{r_i}(\beta)$ for various D values.

another cell, or a base in another cell which interferes with the wanted base-to-mobile signal.

Fig. 4-8 illustrates calculation of

$$F_r(K) = P(r_s < Kr_i)$$

$$= \int f_{r_s}(y)\, f_{r_i}(x)\, dx\, dy \qquad (4\text{-}52)$$

The region of integration in (4-52) depends on K. For $0 \leq K \leq (d+R)^{-1}$, with $f_{r_s}(y)$ given by (4-15)

$$F_r(K) = \int_{x=d-R}^{d+R} f_{r_i}(x) \left[\int_{y=0}^{Kx} f_{r_s}(y)\, dy\right]dx$$

$$= \frac{4K^2}{\pi R^4} \int_{d-R}^{d+R} x^3 \cos^{-1}\left[\frac{1}{2}\sqrt{\frac{(x+d+R)(x+d-R)}{xd}}\right]dx$$

$$= K^2 I(D-1, D+1) \qquad 0 \leq K \leq \frac{1}{D+1} \qquad (4\text{-}53)$$

where $z = x/R$ and

$$I(A,B) = \frac{4}{\pi}\int_A^B z^3 \cos^{-1}\left[\frac{1}{2}\sqrt{\frac{(z+D+1)(z+D-1)}{zD}}\right]dz \qquad (4\text{-}54)$$

For $(D+1)^{-1} \leq K \leq (D-1)^{-1}$

$$F_r(K) = \int_{x=d-R}^{R/K} f_{r_i}(x) \left[\int_{y=Kx}^{R} f_{r_s}(y)\, dy\right]dx$$

$$= \frac{4}{\pi R^2}\int_{d-R}^{R/K} x\left(1 - \frac{K^2x^2}{R^2}\right) \cos^{-1}\left(\frac{1}{2}\sqrt{\frac{(x+d+R)(x+d-R)}{xd}}\right)dx$$

$$= J(D-1, 1/K, K) \qquad \frac{1}{D+1} \leq K \leq \frac{1}{D-1} \qquad (4\text{-}55)$$

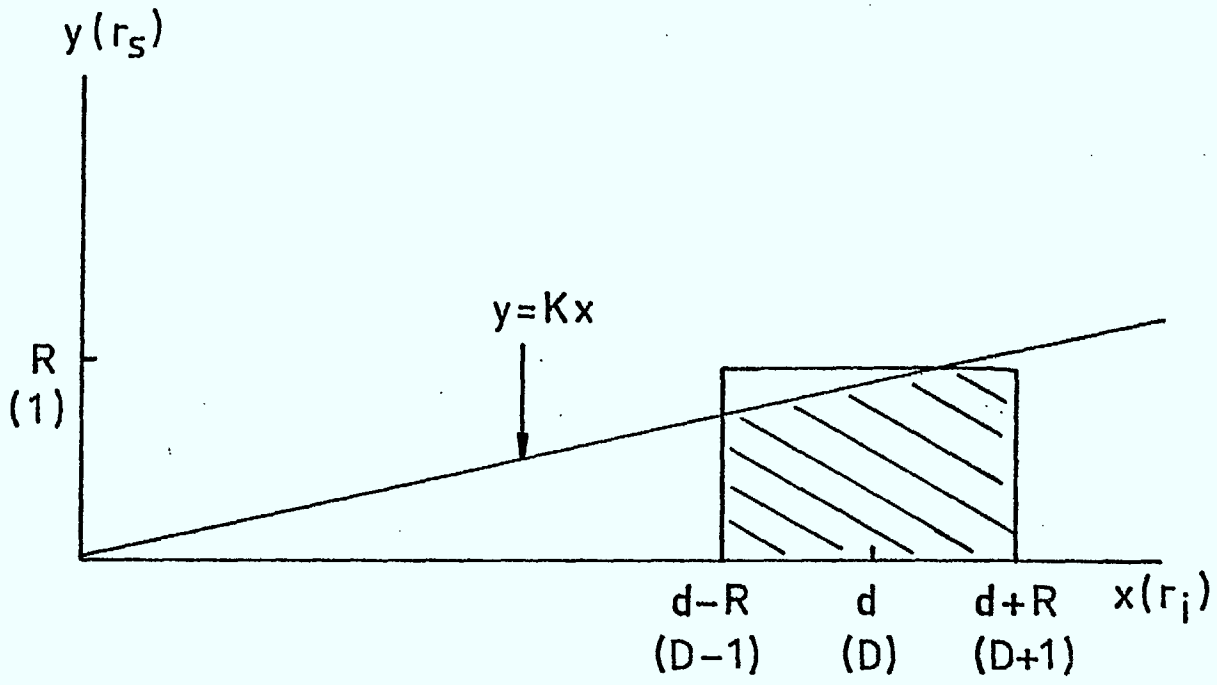

Fig. 4-8 Illustrating the calculation of distribution function $F_r(K)$.

In (4-55)

$$J(A,B,C) = \frac{4}{\pi} \int_A^B x(1-C^2x^2) \cos^{-1}\left[\frac{1}{2}\sqrt{\frac{(x+D+1)(x+D-1)}{xD}}\right]dx \qquad (4\text{-}56)$$

Finally,

$$F_r(K) = 1 \qquad K \geq \frac{1}{D-1} \qquad (4\text{-}57)$$

From the distribution function $F_r(K)$ one obtains the density function $f_r(K)$. Thus

$$f_r(K) = \begin{cases} 2KI(D-1,\ D+1) & 0 \leq K \leq \frac{1}{D+1} \\ 2KI(D-1,\ 1/K) & \frac{1}{D+1} \leq K \leq \frac{1}{D-1} \\ 0 & K \geq \frac{1}{D-1} \end{cases} \qquad (4\text{-}58)$$

Fig. 4-9 shows $f_r(K)$ for various values of D. Also shown is the function

$$g_r(k) = \begin{cases} 2D^2K & 0 \leq K < \frac{1}{D} \\ 0 & k > \frac{1}{D} \end{cases} \qquad (4\text{-}59)$$

As D increases, $g_r(K)$ becomes an increasingly better approximation to $f_r(K)$. This one expects, since a large value for D implies $d/R \gg 1$, which implies that $r_i \simeq d$ over the cell containing the wanted signal. In the case $d/R \gg 1$, (4-58) reduces to (4-15) with $\alpha = d^2K$.

We could now use (4-58) with r_s and r_i expressed in dB to obtain

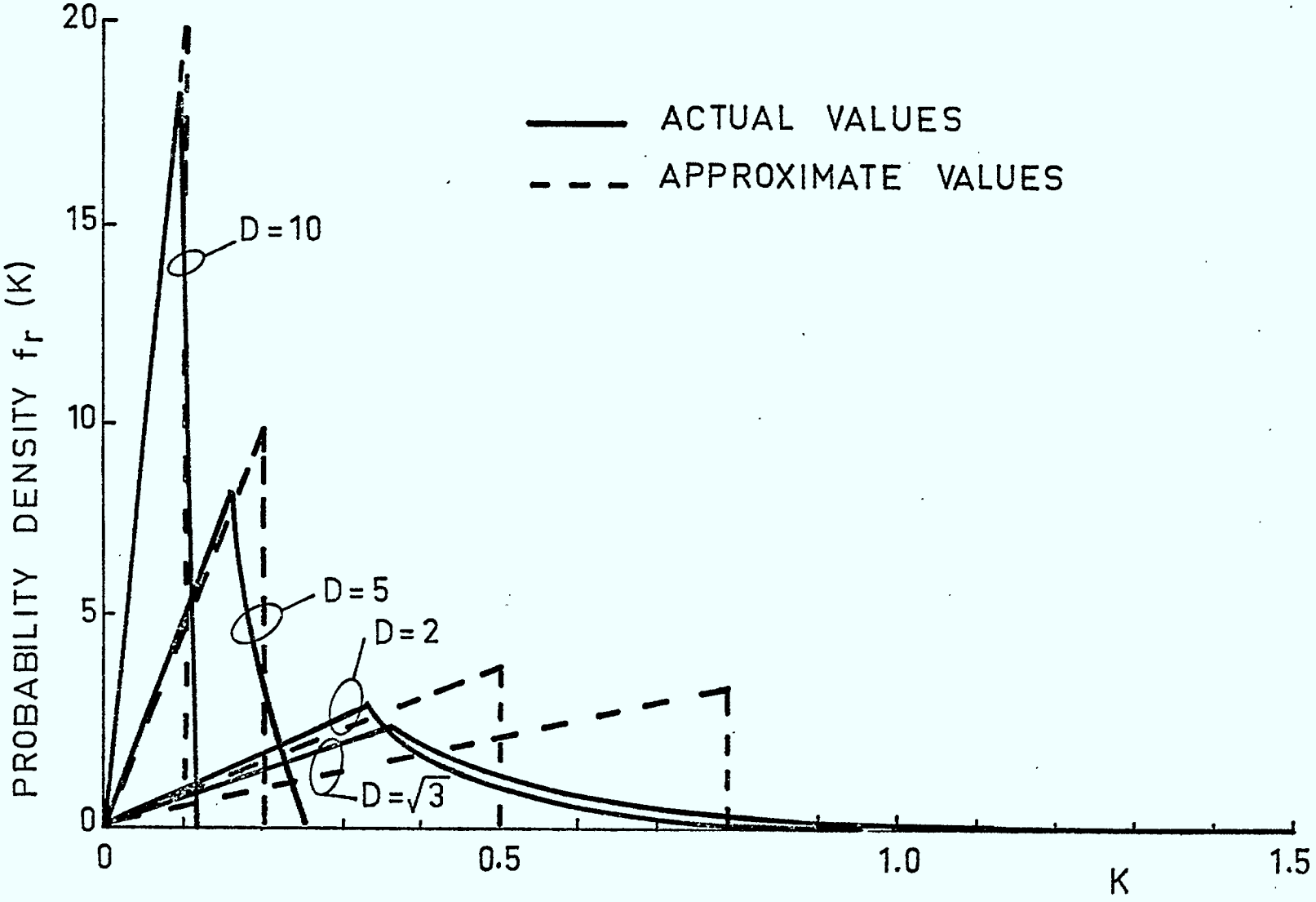

Fig. 4-9 Density function $f_r(K)$ for various D values.

$$f_r(\Gamma) = \frac{1}{2\sigma\sqrt{\pi}} \int_{-\infty}^{\infty} \exp\left[-\frac{\left(\frac{nK}{2} - \Gamma\right)^2}{4\sigma^2} \right] f_R(K)\,dK \qquad (4\text{-}60)$$

as in (4-39). From (4-60) the distribution function $F_I(\Gamma)$ could be obtained. The resulting variation in Γ would be less than for the single-cell case, and this variation would decrease as D increases, since the variation in the interference level decreases as D increases. The variation in Γ is less than in the multiple-interferer case considered next, however, since in that case only the signal is subject to distance and shadowing variations.

IV-4 Interference and Shadowing Variation of the Signal Only

When a channel is subject to interference from many cells, the variation of the bit-error probability is due primarly to the variation of the signal level. The signal level density function is given by (4-15) and the distribution function by

$$F_{r_s}(\alpha) = \begin{cases} 0 & \alpha \leq 0 \\ (\alpha/R)^2 & 0 \leq \alpha \leq R \\ 1 & R \leq \alpha \end{cases} \qquad (4\text{-}61)$$

We note immediately that (4-15) is identical in form to $g_r(K)$ in (4-59). This one expects, since (4-59) is based on the assumption of a large interference separation distance r_i which implies a virtually constant level of interference.

Let $\overline{N}$ be the (constant) noise-plus-interference level, averaged over any Rayleigh fading. The variation of the signal level over the coverage

area is readily obtained by expressing (4-15) in dB form and then proceeding as in Section 4-2. With

$$\overline{P}_s = 1_s^2 / r_s^n \tag{4-62}$$

with A and R_s given by (4-20) and (4-22), respectively, and with

$$R_{dB} = 20 \log_{10} R \tag{4-63}$$

$$P(\overline{N}-\overline{P}_s<\Gamma) = F_I(\Gamma)$$

$$= \int_{-\infty}^{\infty} G_I(\Gamma/R_s=K)\ f_{R_s}(K)dK \tag{4-64}$$

$$f_I(\Gamma) = \int_{-\infty}^{\infty} f_I(\Gamma|R_s=K)\ f_{R_s}(K)dK$$

$$f_{R_s}(K) = \begin{cases} c\ \exp[c(K-R_{dB})] & K \leq R_{dB} \\ 0 & K > R_{dB} \end{cases} \tag{4-65}$$

where c is given by (4-23b).

$$f_I(\Gamma/R_s=K) = (1/\sqrt{2\pi}\sigma)\ \exp\left[(\Gamma-m_d)^2/2\sigma^2\right] \tag{4-66}$$

where

$$m_d = \overline{N}-\overline{Q}_s+\frac{n}{2}K \tag{4-67}$$

In (4-67) $\overline{Q}_s$ is the mean signal power level in dB when $R_{dB} = 0$. Using the above results yields

$$f_I(\Gamma) = \frac{1}{\sqrt{2\pi}} \frac{c}{\sigma} \int_{-\infty}^{R_{dB}} \exp\left[-\frac{\left(\Gamma_1 - [\frac{n}{2}]K\right)^2}{2\sigma^2}\right] \exp\left[c(K-R_{dB})\right] dK \qquad (4\text{-}68)$$

where

$$\Gamma_1 = \Gamma - \overline{N} + \overline{Q}_s \qquad (4\text{-}69)$$

Equation (4-69) can be rewritten as follows:

$$f_I(\Gamma) = \frac{c}{n\sigma} \sqrt{\frac{2}{\pi}} \int_{-\infty}^{-\Gamma_2} \exp\left(\frac{-\beta^2}{2\sigma^2}\right) \exp\left(\frac{2c(\beta+\Gamma_2)}{n}\right) d\beta \qquad (4\text{-}70)$$

where

$$\Gamma_2 = \Gamma_1 - nR_{dB}/2$$

$$= \Gamma - \overline{N} + \overline{Q}_s - [nR_{dB}/2] \qquad (4\text{-}71)$$

$$\beta = (nK/2) - \Gamma_1 \qquad (4\text{-}72)$$

Note that $\overline{N} - \overline{Q}_s + [nR_{dB}/2]$ is the dB interference-to-signal power ratio at the cells radius R.

Function $f_I(\Gamma)$ is plotted in Fig. 4-10. The distribution function $F_I(\Gamma)$, obtained by integrating (4-70), and is shown in Fig. 4-11.

Variations in $f_I(\Gamma)$ when the interference level is constant are significantly less than when both signal and interference levels vary, as is seen by comparing Figs. 4-10 and 4-11 with Figs. 4-3 and 4-4. This statement is confirmed by Table 4-1, which shows standard deviations of the distributions $f_I(\Gamma)$ in Figs. 4-3 and 4-10. The entries in Table 4-1 also confirm that variations resulting from shadowing tend to be larger than do variations

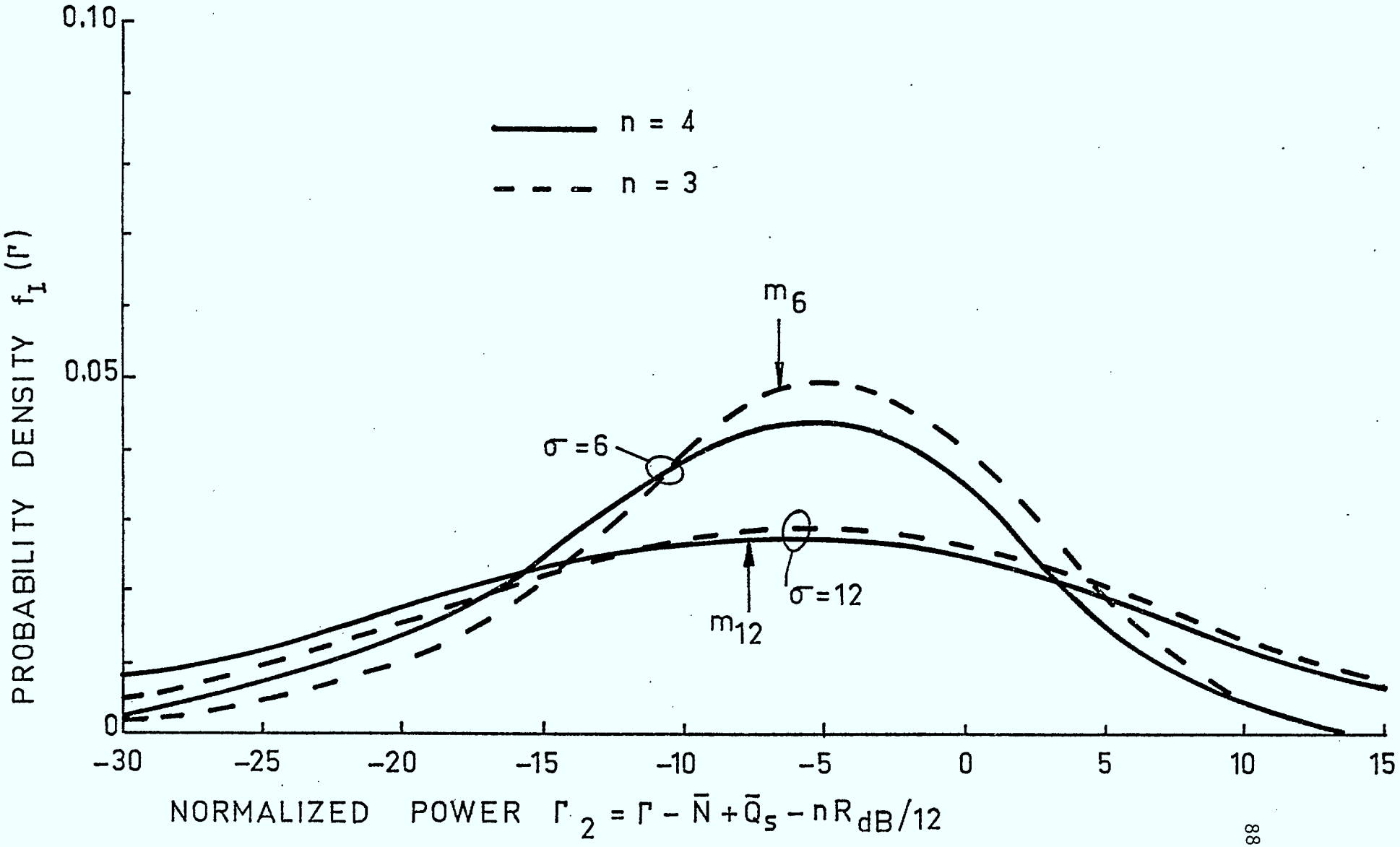

Fig. 4-10 Probability density $f_I(\Gamma)$ for constant interference; upstream interference.

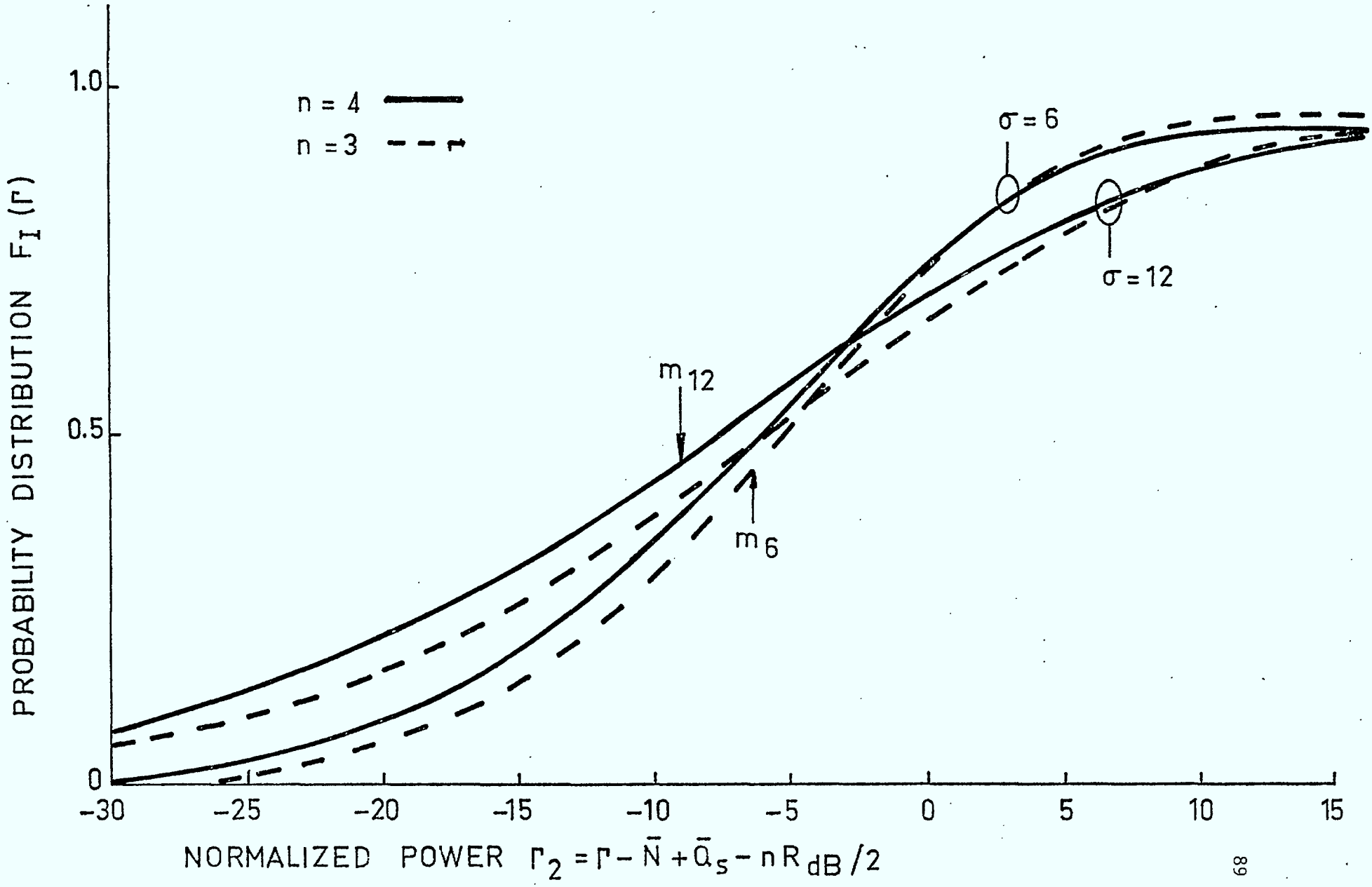

Fig. 4-11 Probability distribution $F_I(\Gamma)$ for constant interference; upstream interference.

n \ σ	0	6	12
0	0	8.5	17.0
3	9.2	12.6	19.4
4	12.3	15.0	20.9

(a)

n \ σ	0	6	12
0	0	6.0	12.0
3	6.5	8.9	13.7
4	8.7	10.6	14.8

(b)

Table 4-1 Standard deviations of the distributions $f_I(\Gamma)$ in Figs. 4-3 and 4-11
(a) Single-cell case: Fig. 4-3
(b) Signal-only variation: Fig. 4-11

resulting from mobile-to-base distance changes.

The entries in Table 4-1 are readily calculated by noting again that $f_I(\Gamma)$ is obtained by convolution of two density functions, one for shadowing and one for distance variation. Thus, the variance of $f_I(\Gamma)$ is the sum of the variances of these two densities. In the present case, where the interference level is constant, the component variances are σ^2 and $(n/2c)^2$. When the signal and interference levels vary as in the single-cell case, each of these variances is multiplied by $\sqrt{2}$, and the corresponding entries in Table 4-1 differ by $\sqrt{2}$.

The results in (4-70) and (4-71) are applicable in a variety of practical situations. For example, consider that $\overline{N}$ consists of n_i co-channel interfering signals, where n_i is sufficiently large that the variation of the interference is negligible in comparison with that of the signal. In this case (see Appendix I, or [F2,H1]),

$$\overline{N} = 10 \log_{10}[\phi n_i C_i(0)/d^n] + \overline{Q}_s + (\sigma^2/8.7)$$

$$= \overline{Q}_s + 10 \log_{10} \phi n_i C_i(0) - \frac{n}{2} d_{dB} + (\sigma^2/8.7) \qquad (4\text{-}73)$$

where

$$d_{dB} = 20 \log_{10} d \qquad (4\text{-}74)$$

In this case

$$\Gamma_2 = \Gamma - 10 \log_{10} \phi n_i C_i(0) + \frac{n}{2} D_{dB} - (\sigma^2/8.7) \qquad (4\text{-}75)$$

where

$$D_{dB} = 20 \log_{10}(d/R) \qquad (4\text{-}76)$$

IV-5 System Effects of Level Variations

Variations in signal and interference levels imply a variation in bit error probability $\overline{p}$, which depends on $\overline{P}_i/\overline{P}_s$ in an interference-limited system as explained in Chapter 3. Two systems with $\langle\overline{p}\rangle = 10^{-3}$, where $\langle\rangle$ denotes averaged over the shadowing and distance variations, may not be equally good if the variation in $\overline{p}$ about this average is different for the two systems. In single-cell systems, the variation in $\overline{p}$ is larger than in multiple-cell systems. As the number of interfering signals increases the variations in the interference level decreases.

Single-cell systems which are interference-limited could enjoy reduced variations in $\overline{p}$ if the base transceiver were located outside the actual coverage area, in which case variations in r_i and r_s would be reduced. Such a reduction could also be available to non-reuse systems with a few cells, in cases where location of the base transceiver outside of the coverage are is practical. Location outside the coverage area could also reduce variations from shadowing, in smaller urban areas.

Diversity also reduces variations due to shadowing and distance separation. The present results can be extended to include some diversity schemes, as explained in Chapter 5.

The distribution functions in Figs. 4-4 and 4-11 as well as others generated as explained earlier can be used to determine probability bounds on $\overline{p}$. For example, consider a cellular system which reuses channels, with normalized reuse distance D. Assume that system performance is limited by interference from six co-channel signals. Assume also that channel occupancy ϕ = 50% and that binary DPSK is used, and that $\overline{p}<10^{-2}$ is required with probability not less than 0.90. The curve in Fig. 4-11 enables the minimum value required for D to be determined.

For DPSK, $\overline{p}\simeq\Gamma$ (for $\overline{p}<<1$), which implies that $\Gamma\leq$-20dB with probability 0.9. Fig. 4-11 implies that for n=4 and σ=12, Γ_2=10 dB. For the present case n_1=6, ϕ=1/2, $C_1(0)$=1/3, $n_1\phi C_1(0)$=1 and $\sigma^2/8.7$=16.6 dB. It follows immediately from (4-75) that $D_{dB}=(2/n)(\Gamma_2-\Gamma+\sigma/8.7)=0.5(10-(-20)+16.6)=23.3$ dB. Consequently, it is required that D$\geq$14.8, which implies a system with a basic pattern of more than 63 cells (see Chapter 6). If σ=6, then Γ_2=5 dB, $\sigma^2/8.7$=4 dB, D_{dB}=0.5(29)=14.5 dB, and D$\geq$5.37, which implies a 9-cell pattern. Since the maximum throughput for the latter system is more than $63/9\simeq 7$ times that for σ=12, the benefits of a lower σ are clear.

If the propagation factor n=3, then D$\geq$35.5 for σ=12 and D$\geq$9.3 for σ=6. The D$\geq$35.5 value implies a >>63-cell pattern while D$\geq$9.3 implies a 31-cell system. The reduced value of n slightly reduces the variance of $f_I(\Gamma)$ in accordance with Table 4-1. However, this reduction does not compensate for the slower decrease in D^{-n}.

The effects of channel encoding can also be included in the above analysis. Consider for example the use of a (31,26) single-error FEC code, with sufficient interleaving to approximate memoryless channel behaviour.

over any Rayleigh fading. The decoded information bit error probability $\overline{p_i} \simeq 45(\overline{p})^2$, which implies $\bar{p}_i \simeq 4.5\times10^{-3}$ with 90% probability if $\Gamma \leq -20$ dB with 90% probability. As well, the distribution of $\bar{p}_i$ can be determined from that for $\bar{p}$, using standard mathematical techniques [P1].

The above example considers co-channel interference only on which designs are often based. Chapter 5 demonstrates how adjacent-channel interference should also be considered in determining $\overline{p}$.

VI-6 References for Chapter 4

[F1] R.C. French, "The effect of fading and shadowing on channel reuse in mobile radio", IEEE Trans. Veh. Technol., vol. VT-28, pp. 171-181, August 1979.

[F2] R.C. French, "Error rate predictions and measurements in the mobile radio data channel", IEEE Trans. on Veh. Technol., vol. VT-27, pp. 110-116, Aug. 1978.

[H1] F. Hansen and F.I. Meno, "Mobile fading - Rayleigh and lognormal superimposed", IEEE Trans. Veh. Technol., vol. VT-26, pp. 332-335, Nov. 1977.

[P1] A. Papoulis, Probability, Random Variables and Stochastic Processes. New York: McGraw-Hill, 1965.

V SPECTRUM EFFICIENCY FOR NARROWBAND DIGITAL TRANSMISSION

V-1 Spectrum Efficiency Determination

The following approach is used to determine the spectrum efficiency for land mobile radio systems operating over conventional circuit-switched narrowband channels.

1. For systems which reuse frequency channels, determine the reuse rate N/G and R/Δ such that $\langle\overline{p}\rangle$ is acceptable. For systems which do not reuse channels $N/G = 1$, but R/Δ must still be determined. In either case, some value must be assumed for ϕ. The choice $\phi \simeq 50\%$ is reasonable, and can be iteratively updated if desired.
2. Determine ϕ such that P_B (or d) is acceptable, given the number m of channels per mobile.
3. Determine Q as given by (2-4), assuming $(k/n) \cdot f \cdot g(\overline{P}_c) = 1$.

In executing the above procedure, N/G is controlled by co-channel interference levels, and R/Δ by adjacent-channel interference.

In order to complete step 1, it is first necessary to determine $\langle\overline{p}\rangle$, which represents an average over distance and shadowing variations. The next section illustrates this determination for systems where the large number of independent interfering signals supports the Gaussian interference assumption.

V-2 Bit-Error Probability Averaged Over Distance and Shadowing

The results in Sections 3-3 and 4-4 can be combined for calculation of the average bit-error probability $\langle\bar{p}\rangle$ when variation of the signal level from distance and shadowing is much greater than that of the interference. In this case

$$\langle\bar{p}\rangle = \int_{-\infty}^{\infty} \bar{p}(\Gamma) f_I(\Gamma) d\Gamma \tag{5-1}$$

where

$$\bar{p}(\Gamma) = \begin{cases} [2 + \exp(-c\Gamma)]^{-1} & \text{(DPSK)} \quad (5\text{-}2a) \\ [2 + \frac{1}{2}\exp(-c\Gamma)]^{-1} & \text{(FSK)} \quad (5\text{-}2b) \end{cases}$$

Note that $\gamma = e^{c\Gamma}$ is the interference-to-signal ratio, averaged over any Rayleigh fading. Equation (5-2a) also applies to SQPSK and to MSK with each data stream differentially detected.

A more convenient equation for $\langle\bar{p}\rangle$ is obtained by regarding f_I as a function of Γ_2 where

$$\Gamma_2 = \Gamma + \overline{SNR} \tag{5-3}$$

$$\overline{SNR}^{-1} = 10\log_{10}\phi\left[n_i C_d(0)(R/d_C)^n + \sum_i (R/d_A) C_d(\Delta T)\right] + (\sigma^2/8.7) \tag{5-4}$$

In (5-4) $d_C(d_A)$ denote the distance between the centre of the cell containing the signal and co-channel (adjacent-channel) interference.

From (5-3) $\Gamma = \Gamma_2 - \overline{SNR}$, and (5-1) and (5-2) can be rewritten as follows, where $\overline{SNR}$ in (5-4) is the same as (4-75) extended to include the effects of

any adjacent-channel interference.

$$\langle\overline{p}\rangle = \int_{-\infty}^{\infty} \overline{p}(\Gamma_2) f_I(\Gamma_2) d\Gamma_2 \qquad (5\text{-}5)$$

$$\overline{p}(\Gamma_2) = \begin{cases} \left[2 + \exp(-c(\Gamma_2 - \overline{SNR}))\right]^{-1} & \text{(DPSK)} \quad (5\text{-}6a) \\ \left[2 + \frac{1}{2}\exp(-c(\Gamma_2 - \overline{SNR}))\right]^{-1} & \text{(FSK)} \quad (5\text{-}6b) \end{cases}$$

Equations (5-5) and (5-6) now explicitly include the effects of channel occupancy, interference coefficients and distance separations d/R in $\overline{p}$. It is possible to rewrite (5-6b) as follows:

$$\overline{p}(\Gamma_2) = \left[2 + \exp(-c(\Gamma_2 - \overline{SNR} + 3))\right]^{-1} \qquad \text{(FSK)} \qquad (5\text{-}6c)$$

One sees that $\overline{p}$ for FSK and DPSK are identical if the average signal power $\overline{P}$ in FSK is twice (3 dB) that for DPSK, as explained in Seciton 3-3.

Fig. 5-1 shows $\langle\overline{p}\rangle$ vs. $\overline{SNR}$ for both DPSK and orthogonal coherent FSK for n = 3 and 4 and for σ = 0, 6, 9 and 12. Clearly variations in σ have a much greater effect on $\langle\overline{p}\rangle$ than do variations in n, for a given Γ_2 value. Note however that Γ_2 depends on both n and σ, in accordance with (5-4).

For large $\overline{SNR}$ values,

$$\langle\overline{p}\rangle \simeq e^{-c\cdot\overline{SNR}} \int_{-\infty}^{\infty} \overline{p}(\Gamma_2)\Big]_{\overline{SNR}=0} f_I(\Gamma_2) d\Gamma_2 \qquad (5\text{-}7)$$

Fig. 5-1, which shows $\langle\overline{p}\rangle$ in logarithmic co-ordinates vs. $\overline{SNR}$, places in evidence the linear relationship between $\log_{10}\langle\overline{p}\rangle$ and $\overline{SNR}$ in dB, when $\overline{SNR} >> 0$.

From Fig. 5-1 one can readily determine the $\overline{SNR}$ value required to yield a specified $\langle\overline{p}\rangle$ value. Fig. 5-1 is used to obtain these values, listed in

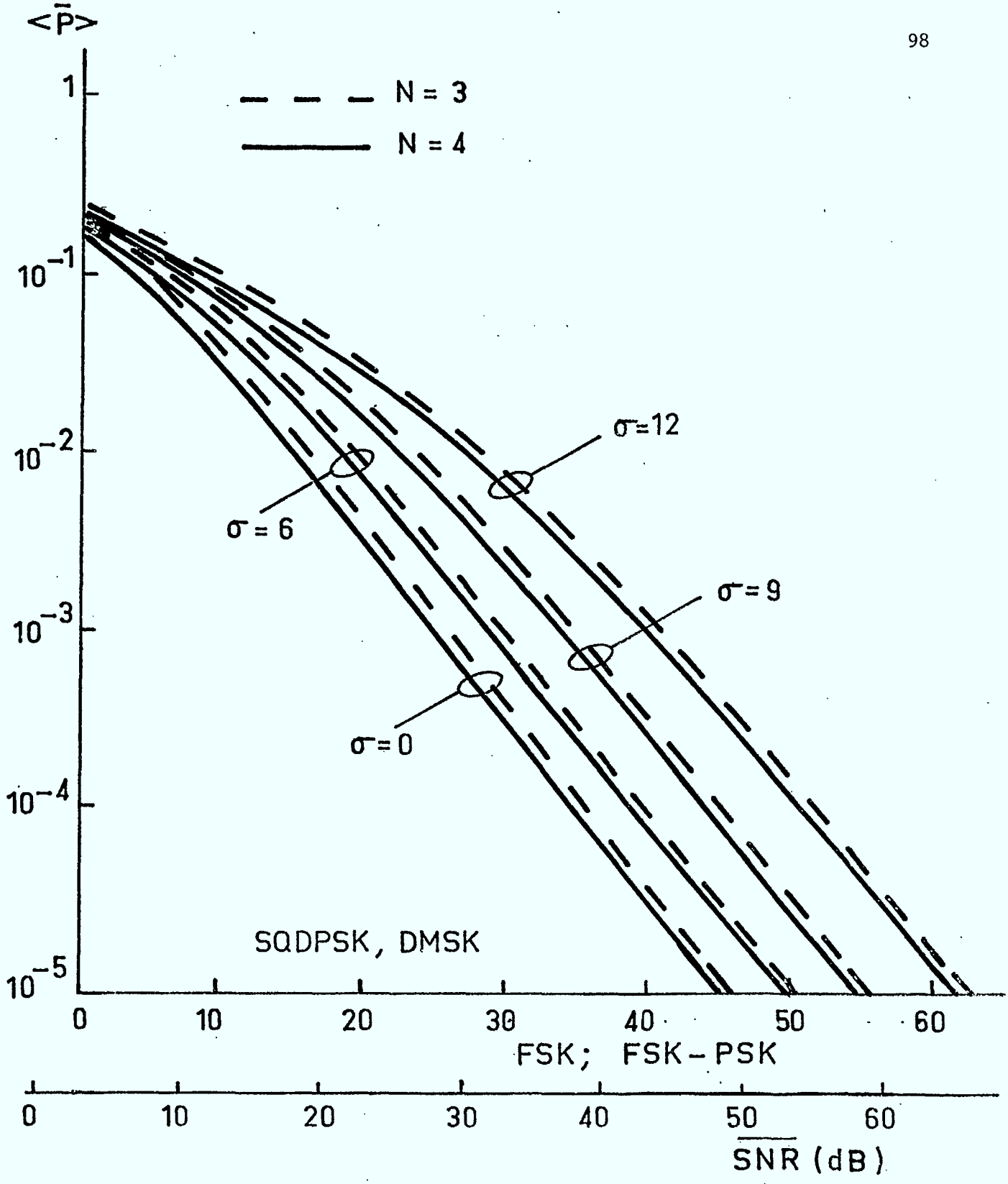

Fig. 5-1 Average bit-error probability $\langle \bar{p} \rangle$ for signal-only level variations.

Table 5-2. Table 5-2 is then used with (5-4) to obtain Table 5-3 which shows the required d/R values, assuming two co-channel and six adjacent-channel interfering signals of equal power. In obtaining Table 5-3 we used (5-8) below with $n_i = 6$ and $\phi = 0.5$.

$$10 \log_{10} n_i \phi C_i(0) = \begin{cases} \overline{3} & \text{SQDPSK} \\ 2.5 & \text{DMSK} \\ 4.0 & \text{FSK} \\ 0.4 & \text{FSK-PSK} \end{cases} \qquad (5\text{-}8)$$

The numbers in parentheses at the top of each column indicate the amount added to the column in Table 5-2, plus ($\sigma/8.7$) to obtain the corresponding column in Table 5-3. These numbers in parentheses are obtained by adding $\simeq 1$ dB to (5-8), to account for two adjacent-channel interferers ($10 \log_{10} 4/3 \simeq 1.25$). The minimum number of channel groups required to achieve d/R as shown in Table 5-3 are shown in Table 5-4; these are obtained with the help of Table 5-1.

Table 5-4 indicates that for cellular systems with an isotropic antenna at cell centre and $\sigma = 9$, $\langle \overline{p} \rangle \tilde{<} 3 \times 10^{-3}$ requires at least 43 groups of channels if $n = 4$ and more than 63 groups for $n = 3$. If $\sigma = 6$, $\langle \overline{p} \rangle \tilde{<} 3 \times 10^{-3}$ requires at least 13 channel groups for $n = 4$ and at least 43 groups for $n=3$.

No. of channel groups	D/r	$(D/r)^n$ n=3	(dB) n=4
3	3	14.3	19.1
4	3.46	16.2	21.7
7	4.58	19.8	26.4
9	5.2	21.5	28.6
12	6	23.3	31.1
13	6.24	23.9	31.8
16	6.93	25.2	33.6
19	7.55	26.3	35.1
21	7.91	27.0	36.0
25	8.66	28.1	37.5
27	9	28.6	38.1
28	9.17	28.9	38.5
31	9.6	29.5	39.3
36	10.4	30.5	40.7
37	10.5	30.6	40.9
39	10.8	31	41.3
43	11.4	31.7	42.3
44	11.5	31.8	42.4
48	12	32.4	43.2
49	12.1	32.5	43.3
57	13	33.4	44.6
61	13.5	33.9	45.2
63	13.7	34.1	45.5

TABLE 5-1 $(D/r)^n$ in dB vs. number of channel groups.

$\langle\bar{p}\rangle$	σ	SQDPSK; DMSK	PSK; FSK-PSK
	0	15.5	18.5
	6	19	22
10^{-2}	9	23	26
	12	28	31
	0	20	23
	6	24	27
3×10^{-2}	9	29	32
	12	35	38
	0	25.5	28.5
	6	29	32
10^{-3}	9	34	37
	12	40.5	43.5

TABLE 5-2 Required $\overline{SNR}$ values to achieve $\langle\bar{p}\rangle$ in Fig. 5-1.

$\langle\bar{p}\rangle$	σ	SQDPSK (4)	DMSK (3.5)	FSK (5)	FSK-PSK (1.5)
	0	19.5	19	23.5	20
	6	27	26.5	31	27.5
10^{-2}	9	36	35.5	40	36.5
	12	48.5	48	52.5	49
	0	24	23.5	28	24.5
	6	32	31.5	36	32.5
3×10^{-3}	9	48	41.5	46	42.5
	12	55.5	55	59.5	56
	0	29.5	29	33.5	30
	6	37	36.5	41	37.5
10^{-3}	9	47	46.5	51	47.5
	12	61	60.5	65	61.5

TABLE 5-3 Required values of D_{dB} to obtain values of $\langle\bar{p}\rangle$.

n=3

$\langle\bar{p}\rangle$	σ	SQDPSK	DMSK	FSK	FSK-PSK
	0	7	7	12	7
	6	21	19	39	25
10^{-2}	9	●	●	●	●
	12	●	●	●	●
	0	13	12	25	16
	6	48	43	●	48
3×10^{-3}	9	●	●	●	●
	12	●	●	●	●
	0	31	28	57	36
	6	●	●	●	●
10^{-3}	9	●	●	●	●
	12	●	●	●	●

n=4

$\langle\bar{p}\rangle$	σ	SQDPSK	DMSK	FSK	FSK-PSK
	0	3	3	7	4
	6	9	7	12	9
10^{-2}	9	21	21	36	25
	12	●	●	●	●
	0	7	7	9	7
	6	16	13	21	16
3×10^{-3}	9	43	43	●	44
	12	●	●	●	●
	0	12	9	16	12
	6	25	25	37	25
10^{-3}	9	●	●	●	●
	12	●	●	●	●

TABLE 5-4 Required number of channel groups G to achieve D_{dB} in Table 5-3. ● denotes $G > 63$.

V-3 Spectrum Efficiency of Cellular Systems with Isotropic Antenna at Cell-Centre

Figs. 5-2, 5-3, 5-4 and 5-5 show cellular systems, each based on a different basic pattern. All cells numbered i are assigned frequency channels from group i. The way in which the spectrum efficiency is determined is illustrated below for the 12-cell case.

The interference-to-signal ratio for the six co-channel and two adjacent-channel sources all with equal interference power is given by the following equation with $n_i=8$;

$$\overline{SNR}^{-1} = -10 \log_{10}(d_C/R)^n + 10 \log_{10} n_i \phi C_d(0) + (\sigma/8.7) \qquad (5\text{-}9)$$

For $\phi = 0.5$, $n = 4$ and $d_C/R = 6$,

$$\overline{SNR}^{-1} = -31.1 + 6.02 + C_d(0) + (\sigma/8.7) \simeq -27.7 \text{ dB} + (\sigma/8.7)$$

In obtaining $\overline{SNR}$ above, the median value $C_d \simeq -2.6$ from among the four modulation schemes was used. As shown on Fig. 3-3, $-4.43 \leq C_d(0) \leq -0.84$.

With $\sigma = 9$ dB, $\overline{SNR} = 18.4$ dB. Figure 5-1 shows $\langle\overline{p}\rangle = 10^{0.3} \times 10^{-2} = 2 \times 10^{-2}$ for SQDPSK and DMSK and 3×10^{-2} for FSK and FSK-PSK.

To ensure that interference from one co-channel and one adjacent-channel signal are equal requires that

$$C_d(\Delta T) - 10 \log_{10}(d_A/R)^n = C_d(0) - 10 \log_{10}(d_C/R)^n \qquad (5\text{-}10)$$

In the present 12-cell case, $d_A/R = 3$ (19.1 dB). With $C_d(0) \simeq -2.6$ $C_d(\Delta T) \simeq -2.5 + 19.1 - 31.1 = -14.6$ dB. From Fig. 5-1 the corresponding Δ/R values are obtained, as follows:

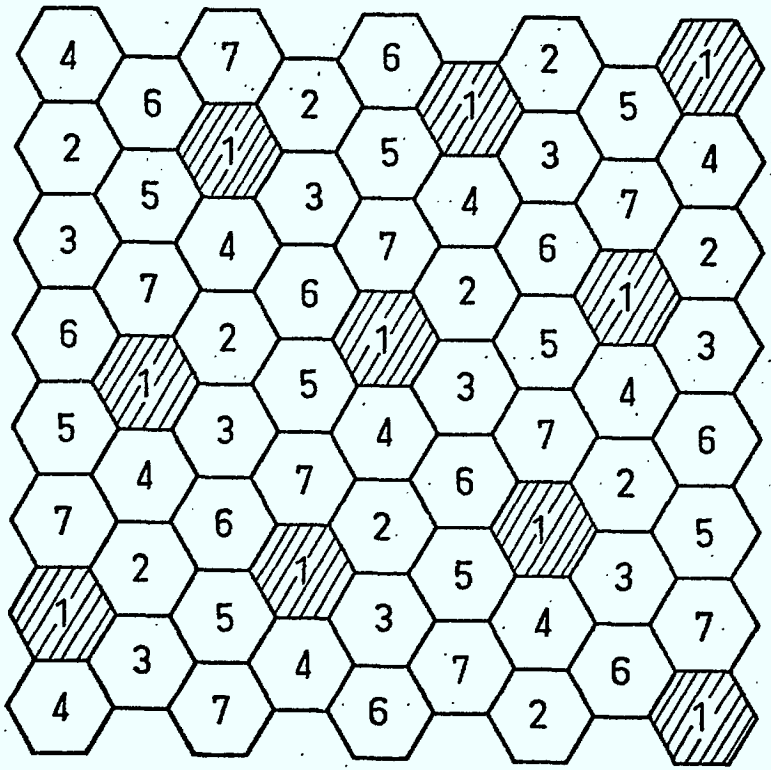

Fig. 5-2 Seven-Cell System Plan.

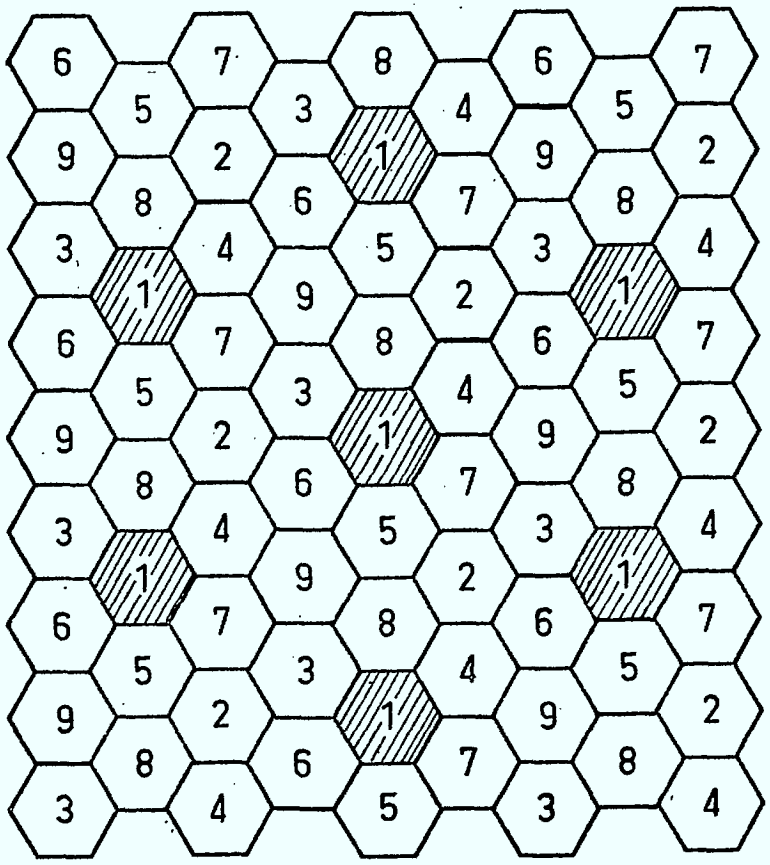

Fig. 5-3 Nine-Cell System Plan.

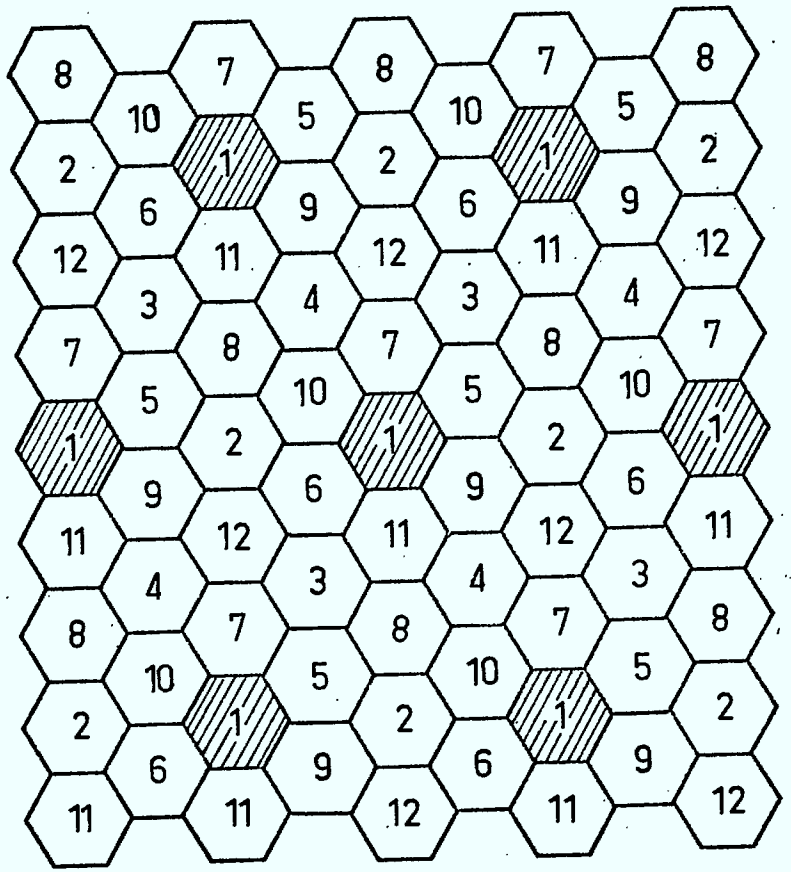

Fig. 5-4 Twelve-Cell System Plan.

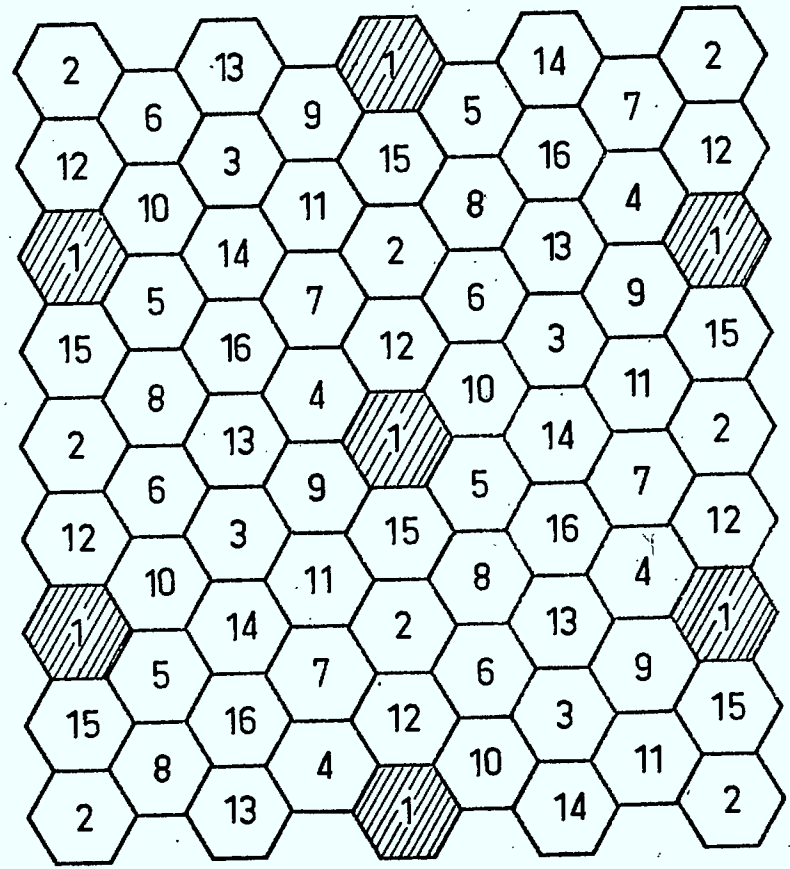

Fig. 5-5 Sixteen-Cell System Plan.

$$\Delta/R = \begin{cases} 0.85 & \text{SQDPSK} \\ 0.75 & \text{DMSK} \\ 1.25 & \text{FSK} \\ 1.0 & \text{FSK-PSK} \end{cases} \qquad (5\text{-}11)$$

From these Δ/R values the spectrum efficiency per cell is obtained from (5-12) below with G = 12.

$$Q/N = (R/\Delta)/G \qquad (5\text{-}12)$$

The spectrum efficiencies for the various signalling schemes, together with the average bit-error probabilities are listed in Table 5-5. From (2-4) one sees that this is the maximum possible efficiency.

The same approach is used to obtain results shown in Table 5-5 for the 7-, 9- and 16-cell systems. In the 7- and 9-cell systems $d_A/R = \sqrt{3}$ (9.5 dB), since the adjacent-channel signals are in either one or both adjacent cells.

In the 16-cell case $d_A/R \geq 2\sqrt{3}$ for many cells. If dynamic channel assignments [J1] could be used to ensure that $d_A/R \geq 2\sqrt{3}$ for all adjacent-channels, then ΔT could be reduced and Q/N increased for those modulation formats with fast ΔT roll-off rates. The results are shown in Table 5-5. Note that in the 16-cell results adjacent-cells with interference at $\pm 2\Delta$ actually limit R/Δ for SQDPSK and in the dynamic assignment case for FSK-PSK. The minimal improvement for dynamic channel assignment would not seem worthwhile here.

The $\langle\overline{p}\rangle$ values in Table 5-5 are nominal values and reasonably accurate for SODPSK and DMSK. The values for FSK and FSK-PSK are close to 1.65 times the values in Table 5-5.

N	σ	$\langle\bar{p}\rangle$	Q/N			
			SQDPSK	DMSK	FSK	FSK-PSK
7	0	1.6×10^{-3}	0.095	0.150	0.089	0.095
	6	10^{-2}				
	9	4×10^{-2}				
	12	1.4×10^{-1}				
9	0	10^{-3}	0.056	0.111	0.064	0.065
	6	7×10^{-3}				
	9	3×10^{-2}				
	12	10^{-1}				
12	0	6.3×10^{-4}	0.098	0.111	0.067	0.083
	6	4×10^{-3}				
	9	2×10^{-2}				
	12	8×10^{-2}				
16	0	3×10^{-4}	0.033†	0.078	0.045	0.039†
	6	2×10^{-3}		0.083**	0.050**	
	9	1.3×10^{-2}				
	12	6.3×10^{-2}				
21	0	2.5×10^{-4}	0.032‡	0.068	0.053	0.038‡
	6	2×10^{-3}				
	9	1.3×10^{-2}				
	12	6×10^{-2}				
7*	0	5×10^{-4}	0.204	0.204	0.119	0.159
	6	3×10^{-3}				
	9	2×10^{-2}				
	12	8×10^{-2}				

TABLE 5-5 Bit-error probability $\langle\bar{p}\rangle$ and maximum spectrum efficiency Q/N for cellular systems; σ=9, n=4.

* 120° sectoral illumination at cell corners.
** Dynamic channel assignments.
† Interference at ±2Δ limits R/Δ.
‡ Interference at ±3Δ limits R/Δ.

V-4 Twenty-One Cell System Performance

The procedure developed in the previous section can be applied to determine the spectrum efficiency of any cellular system. More complex examples are illustrated below and in the following section.

Figure 5-6 shows a 21-cell plan with channels assigned as indicated. The channels are divided into 21 groups which are subdivided further into three sets of seven subgroups each. Channels in the A set lie midway between close frequency neighbours in the B and C sets. Channels in subgroup i are separated from channels in subgroups i±1 by at least 3Δ Hz. Thus channels 4B and 4C are $\pm\Delta$ Hz away from frequency neighbours in group 4A, and group 4A channels are $\pm 3\Delta$ Hz from frequency neighbours in 5A and 3A. This channel assignment was proposed by Mikulski [M1] to replace what would be co-channel interference in a 7-cell system by adjacent-channel interference in a 21-cell system.

In Fig. 5-6, d/R = 7.9 for co-channel signals and 4.58 for signals separated by Δ Hz. For signals 2Δ Hz apart, $d/R \geq 3$, and for signals 3Δ Hz apart $d/R \geq \sqrt{3}$.

Again, we select ΔT such that one co-channel interference level equals or exceeds any adjacent-channel signal level. The following equations result, as in (5-10), with $C_d(0) = -2.6$ dB:

$$C_d(\Delta T) - 26.4 = C_d(0) - 36.0$$

$$C_d(\Delta T) = -12.2 \text{ dB} \qquad (5\text{-}13a)$$

$$C_d(2\Delta T) - 19.1 = -38.6$$

$$C_d(2\Delta T) = -19.5 \text{ dB} \qquad (5\text{-}13b)$$

$$C_d(3\Delta T) - 9.5 = -38.6$$

$$C_d(3\Delta T) = -29.1 \text{ dB} \qquad (5\text{-}13c)$$

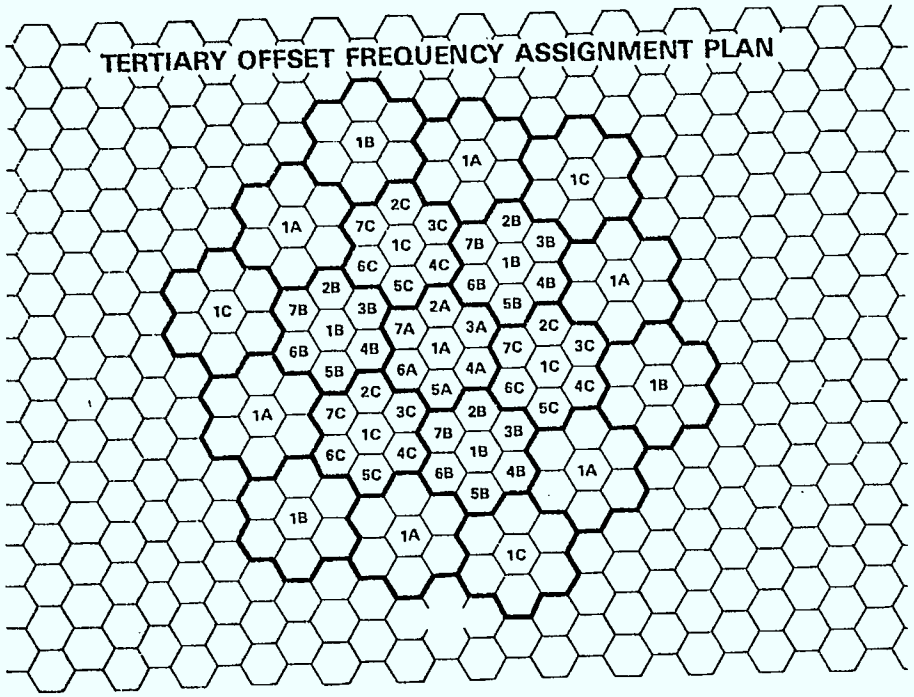

Fig. 5-6 Twenty-One-Cell System [M1].

Signalling Format	Channel Separation					
	3Δ		2Δ		Δ	
	3ΔT	ΔT	2ΔT	ΔT	ΔT	Q/N
SQDPSK	4.5	(1.5)	1.5	0.75	0.7	0.032
DMSK	1.4	0.47	0.95	0.48	(0.7)	0.068
FSK	2.5	0.83	1.5	0.75	(0.9)	0.053
FSK-PSK	3.75	(1.25)	1.5	0.75	1.2	0.038

TABLE 5-6 Determination of spectrum efficiency for 21-cell system. Limiting cases are circled.

With the help of Fig. 3-3, Table 5-6 results, which shows how each of the three constraints above limits ΔT. The largest value of ΔT in each line is the value chosen. It is seen that for SQDPSK and FSK-PSK, interference at $\pm 3\Delta$ from the adjacent cell determines ΔT. For FSK and DMSK interference from channels at $\pm\Delta$ Hz dominates. The difference here is a direct result of the differences in rate of decrease of $C_d(\Delta T)$ with ΔT.

If there are 12 equal-power interfering signals, then (5-9) yields

$$\overline{SNR}^{-1} = -35.9 + 7.8 - 2.6 + (\sigma/8.7)$$

$$= -30.7 \text{ dB} + (\sigma/8.7)$$

From Fig. 5-1 one obtains the nominal value $\langle\bar{p}\rangle \simeq 1.3 \times 10^{-2}$ for σ=9 dB. The actual value would vary a little from this value. For SQDPSK, from example, there are 8 rather than 12 dominant interfering signals which would increase $\overline{SNR}$ by 1.8 dB; however, $C_d(0) = -1.8$ rather than -2.6 which is an increase of 0.8 dB. The net reduction is 1.0 dB which implies $\langle\bar{p}\rangle \simeq 1.5 \times 10^{-2}$. For FSK, $\langle\bar{p}\rangle \simeq 2.5 \times 10^{-2}$ while for FSK-PSK $\langle\bar{p}\rangle \simeq 2 \times 10^{-2}$. For DMSK the nominal value is very close to the calculated value. The values for $\langle\bar{p}\rangle$ and O/N appear in Table 5-5.

V-5 Seven-Cell System with Bases at Cell Corners

It is desirable to maintain G small, while at the same time keeping interference levels to a minimum. The seven-cell pattern in Fig. 5-2 with 120° directional antennae is being tested by American Telephone and Telegraph [B1]. Here we extend our methods to determine spectrum efficiencies for this case.

In Figs. 5-7 and 5-8 the effective cell radius for the wanted signal is seen to equal R. For interference considerations, each cell is effectively divided into three disjoint diamond-shaped areas whose effective distance from interfering cell centres is determined with the help of Fig. 5-7.

The distance between each co-channel antenna which "sees" the signal cell is noted next to the antenna. Those antennae which see half of the signal cell are designated by (H). The average co-channel separation is 5.3 R, and since each antenna is active with probability 1/3, there are in effect $n_i = 2.5$ co-channel interferers.

Consider again the case $n = 4$ and $\phi = 0.5$. For the co-channel signals alone

$$-(n/2)D_{dB} + 10 \log_{10} n_i \phi C_d(0) = -29.0 + 1.0 + C_d(0)$$
$$= -28.0 + C_d(0) \qquad (5\text{-}14)$$

With $C_d(0) \simeq -2.6$ dB, (5-14) yields $\simeq -31$ dB for co-channel interference.

To determine adjacent-channel interference it is necessary to average in a meaningful way over the three diamond-shaped average areas in Fig. 5-8. For these areas, the averages are as follows:

$$-10 \log_{10}(d_A/R)^n + 10 \log_{10} n_i \phi: \quad \begin{cases} -19.0 - 0.4 = -19.4 \\ -12.0 - -1.8 = -13.8 \\ -17.9 - 3.8 = -21.7 \end{cases} \qquad (5\text{-}15)$$

The average of (5-15) over all three areas is -18.3 dB.

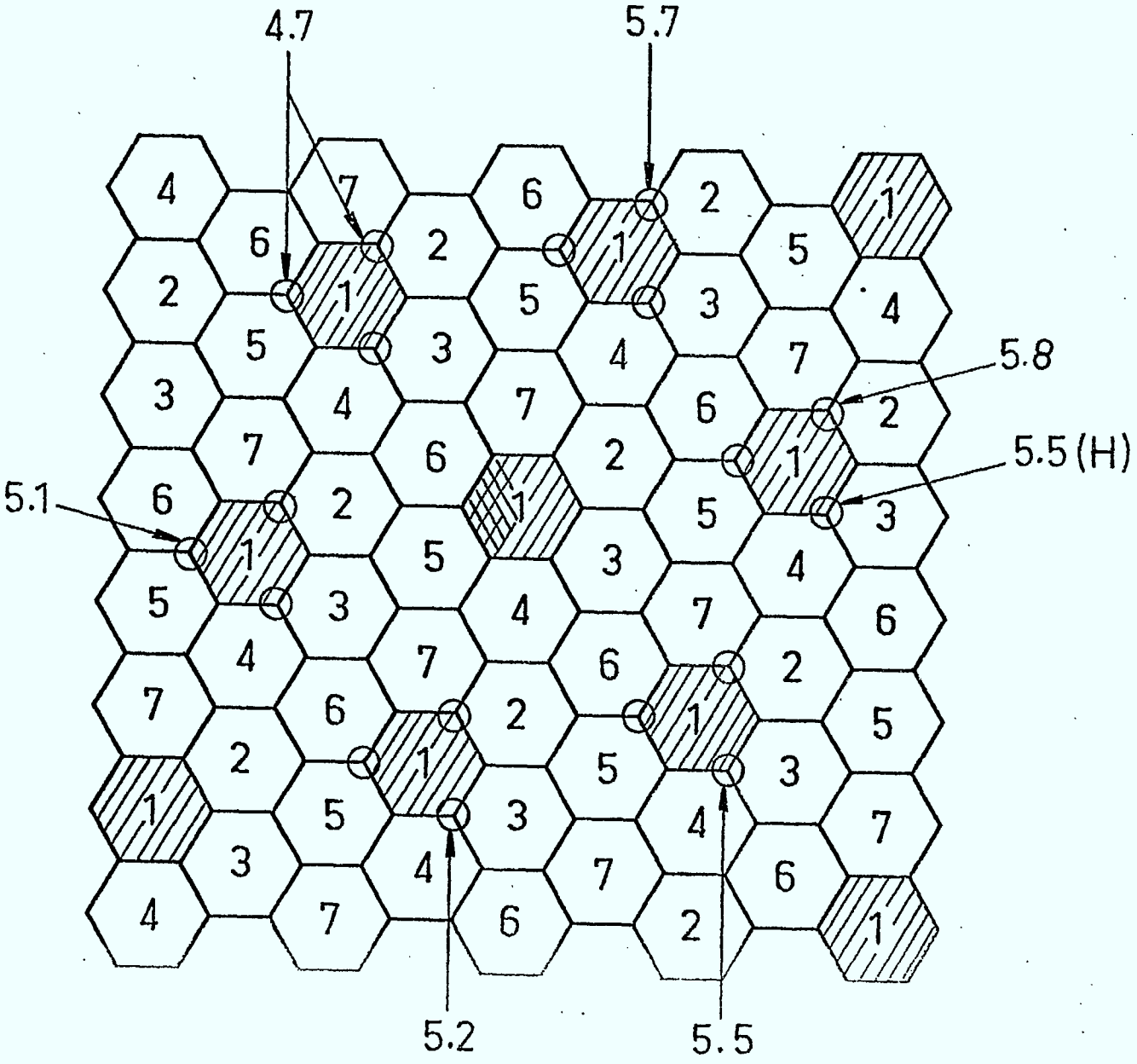

Fig. 5-7 Seven-cell system with 120° corner illumination; co-channel interference.

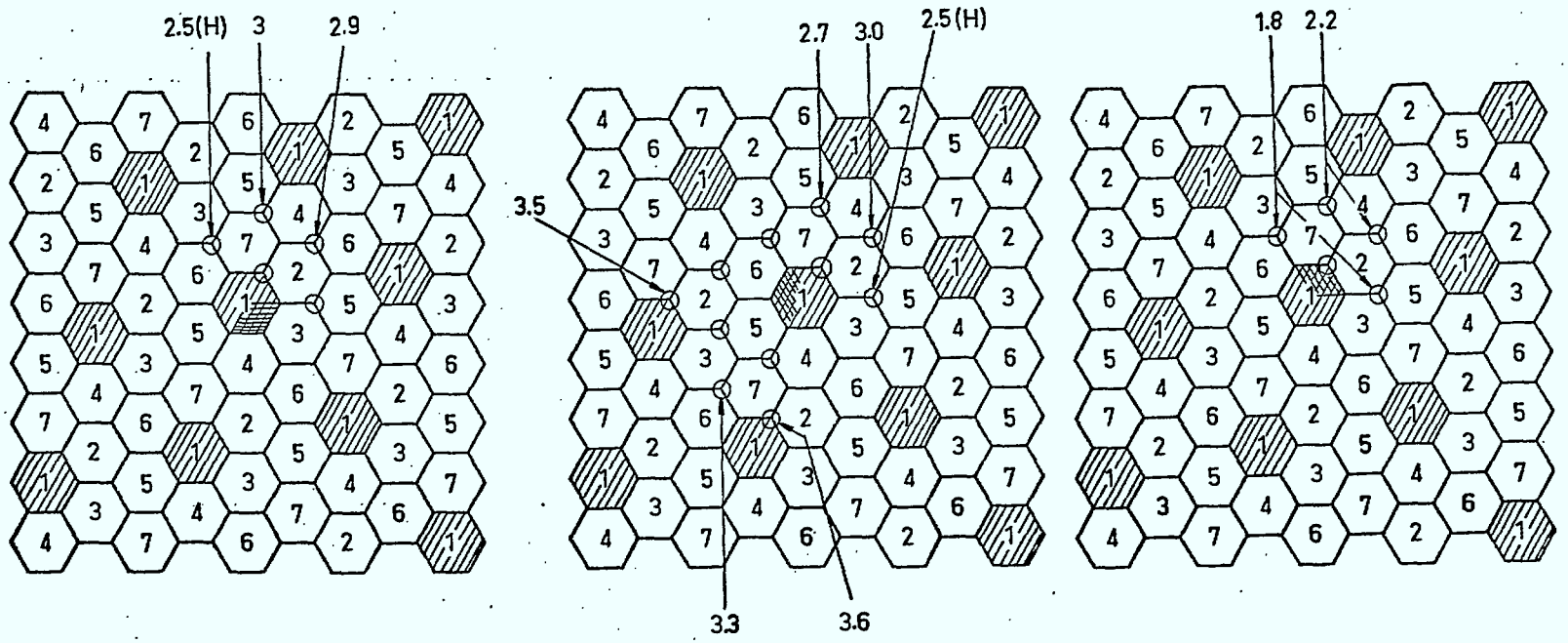

Fig. 5-8 Seven-cell system with 120° corner illumination; adjacent-channel interference.

If ΔT is selected such that the total co-channel interference equals the total adjacent-channel interference, then

$$C_d(\Delta T) - 18.4 = -31 \tag{5-16}$$

which yields $C_d(\Delta T) \simeq -12.6$ dB. The Δ/R values are as follows:

$$\Delta/R = \begin{cases} 0.75 & \text{SQDPSK} \\ 0.75 & \text{DMSK} \\ 1.20 & \text{FSK} \\ 0.95 & \text{FSK-PSK} \end{cases} \tag{5-17}$$

The corresponding maximum spectrum efficiencies in Table 5-5 are obtained from $Q/N = (R/\Delta)/7$.

The resulting $\overline{SNR} \simeq 28$ dB $- (\sigma/8.7)$; $\langle\bar{p}\rangle$ is as shown in Table 5-5.

The analysis here is not exact, particularly in determining adjacent-channel interference, since averaging dB levels does not yield the same result as first averaging power levels and then computing the dB result. However, the accuracy is probably adequate for our purposes.

Implementation costs for the system considered here would be comparable to those for systems with an isotropic antennae at cell centre, since there is in both cases one base per cell, on average.

V-6 Effects of Blocking Probability Requirements on Spectrum Efficiency

The O/N values in Table 5-5 are maximum spectral efficiences, under the condition that interference resulting from a co-channel signal is equal to a dominant adjacent-channel signal. These maximum values are based on ϕ=1. In an actual system, Fig. 2-4 or 2-5 must be used to determine the actual ϕ value, which depends on the number of channels per mobile per cell and on either P_B or d.

Consider again the 7-cell system with 120° directional antennae. Assume that each of the seven channel groups contains 96 channels and that 36 of these 96 channels are assigned to one directional antenna [B1]. In any cell not more than one of the 96 channels is active, which implies 96 channels per mobile per cell. Figure 2-4 can be used to obtain (ϕ, P_B) as follows: (0.85, 0.02), (0.90, 0.05), (0.96, 0.20), (0.99, 0.50). Because of the large number of channels per cell, ϕ is not degraded very much from its maximum possible value of unity.

If we consider a 40 channel system (rather than the above 672 channel system) then each cell is assigned 5.7 channels per cell, and (ϕ, P_B) are as follows: (0.35, 0.02), (0.43, 0.05), (0.65, 0.20), (0.84, 0.50). In this case the degredation resulting from the finite number of channels available is large, particularly when the blocking probability (or delay) is low.

In selecting the number of groups G of channels, or equivalently the number of cells in a basic cellular plan, G should be minimized subject to the required value of $\langle\bar{p}\rangle$ being achieved, in order that reductions from the value ϕ=1 be minimized.

V-7 Spectrum Efficiency with Channel Encoding

The techniques developed to this point can be extended, at least in principle to determine spectrum efficiencies when channel encoding is used for error detection, forward error correction or a combination of these. All that is needed is $\bar{p}_i$, the decoded bit-error probability in terms of $\bar{p}$, the uncoded bit error probability averaged over Rayleigh fading. This value of $\bar{p}_i$, expressed in terms of $\overline{SNR}$ in dB, is substituted into (5-5) in place of $\bar{p}$. In practice, determining $\bar{p}_i$ in terms of $\bar{p}$ is not easy for land mobile channels, unless interleaving is used to the extent that the memoryless channel assumption in (3-81) is reasonable.

If (3-81) is used, for example with a (31, 26) FEC code, and if bit-error probability $\bar{p}$ is small,

$$\bar{p}_i \simeq 45\ \bar{p}^2 \tag{5-18}$$

Small $\bar{p}$ implies $\overline{SNR}$ (dB) $\gg$ 0. For DPSK $\bar{p} \simeq e^{-c\ \overline{SNR}}$ and from (5-18) with A = 16.5

$$\bar{p}_i = e^{c(A-2\overline{SNR})} \tag{5-19}$$

Using (5-19) with $\overline{SNR}$ replaced by $2\overline{SNR}$ - 16.5 enables direct determination of $\langle\bar{p}_i\rangle$. The resulting spectrum efficiency must be multiplied by k/n = 0.84.

Consider again the 7-cell system with directional antennae at cell corners. In this case with σ = 9, $\overline{SNR}$ = 18.7 dB, $2\overline{SNR}$ - 16.5 = 20.9 dB, and for DMSK and SODPSK with n = 4 Fig. 5-1 yields $\langle\bar{p}_i\rangle \simeq 1.4\times10^{-2}$. The result in this case is a very small reduction in $\langle\bar{p}_i\rangle$ at the cost of a 15% reduction in

spectrum efficiency. If a (31,21) double-error-correcting code were used, $k/n = 0.68$ and

$$\bar{p}_i = 435\,\bar{p}^3 = e^{c(X-3\overline{SNR})} \qquad (5\text{-}20)$$

where X = 26.4 dB. Using 3(18.7) - 26.4 = 29.7 with Fig. 5-1 yields $\langle\bar{p}_i\rangle \simeq 3\times10^{-3}$. The result is an order of magnitude reduction in $\langle\bar{p}_i\rangle$ with a 33% reduction in spectrum efficiency.

If a (31, 26) code were used for error detection, then from the discussion in Section 3-4 it follows that the throughput reduction from coding is $(k/n)P_c \simeq 0.84(0.53) \simeq 0.45$. The decoded bit error probability with n = 31 and d = 3 is

$$\bar{p}_i \simeq 2^{-5}(d)(n-1)(n-2)\bar{p}^3/6 \simeq 13.6\,\bar{p}^3 \simeq e^{c(B-3\overline{SNR})} \qquad (5\text{-}21)$$

In (5-21) B = 11.3, and from Fig. 5-1 with $\overline{SNR}$ replaced by $3\overline{SNR}$ - B = 44.8, $\langle\bar{p}_i\rangle \simeq 10^{-4}$ for $\sigma = 9$. The result is a dramatic reduction in decoded bit error probability, which however is accompanied by a spectrum efficiency of 45% of that without coding and some delay which results from retransmission of blocks with detected errors.

V-6 Comments Regarding Cellular System Performance

Examination of Table 5-5 shows that for cellular systems having a single base at cell-centre, $\langle\bar{p}\rangle$ and O/N both decrease as the number of channel groups G increase. For a fixed number of channels per mobile m, the actual

Q/N value would decrease from the maximum shown, and the percentage reduction would increase with G.

Table 5-5 shows that DMSK modulation is always among the best, but that no one scheme is always worst in terms of spectrum efficiency. For the 7-cell system with directional antennae, SQDPSK and DMSK are best, with Q/N ≃ 0.20, while FSK has the lowest value ≃ 0.12. For the 21-cell system, however, SQDPSK and FSK-PSK give the lowest value; here Q/N ≃ 0.03 while DMSK and FSK give Q/N ≃ 0.07 and 0.05 respectively. In this latter case the differences in roll-off rates with ΔT become very important.

Channel encoding provides for substantial potential improvement in spectrum efficiency. Such improvement is based in part on the capability to interleave bits subject to deep fades with other bits having good $\overline{SNR}$ levels. Such a possibility has long been recognized [C1], and has proved viable in actual field tests [M2]. The determination of $\langle\bar{p}\rangle$ in an actual system requires an adequate model for bit-error dependencies as well as a tractable analytic or other approach, to determine bit-error probabilities following decoding.

The benefits associated directional antenna at cell corners is evident. The 7-cell system in Section V-5 gives the same nominal $\langle\bar{p}\rangle$ value as a 12-cell system with an isotropic base at cell-centre. However, there is a factor of two difference in maximum spectrum efficiency, and this difference would increase futher with a finite number of channels.

Recently, it has been proposed that <u>all</u> receivers at all three (alternate) corners of a cell be used for reception as well as for co-phased transmission to a mobile [H1]. This is diversity combining rather than selection

diversity, and would greatly reduce variations due to shadowing, distance separation and Rayleigh fading. Preliminary consideration has resulted in a 3-cell plan being proposed, which could considerably improve spectrum efficiency over that for the 7-cell system plan described earlier. To determine bit-error probability distributions as well as $\langle\bar{p}\rangle$ would require the distribution resulting from fading to be obtained (by convolution) and used to obtain $\bar{p}$. The distribution for $\bar{p}$ resulting from shadowing and distance separation would then have to be found (again by convolution), to determine $f_I(\Gamma)$ and $\langle\bar{p}\rangle$. The approach developed in this report is directly applicable.

Implementation of this new system is described elsewhere [H1]. Because any additional complexity is confined to base equipment, the system cost/benefit ratio might well be better than that of the seven-cell system with switched diversity. The need for accurate mobile location to facilitate co-phased transmission to mobiles would be one primary contributor to an increase in base costs, and would also cause some additional overhead in the data stream. As a final note, channel encoding would probably not be very effective in improving spectrum efficiency, since signal-to-interference level variations would be reduced by the inherent space diversity of the new system. A careful performance assessment of this system would be of interest.

V-9 References for Chapter 5

B1 F.H. Belcher, "Advanced mobile phone service", IEEE Trans. Veh. Technol., vol. VT-29, pp. 238-244, May 1980.

C1 D. Chase and L.J. Weng, "Multiple-burst correcting techniques for slowly fading channels", IEEE Trans. Inform. Theory, vol. IT-22, pp. 505-513, Sept. 1976.

H1 P.S. Henry and B.S. Glance, "A new approach to high-capacity digital mobile radio", Bell System Tech. J., vol. 60, pp. 1891-1904, Oct. 1981.

J1 W.C. Jakes, Microwave Mobile Communications. New York: Wiley, 1969.

M1 J.J. Mikulski, "A system plan for a 900-MHz portable radio telephone", IEEE Trans. on Veh. Technol., vol. VT-26, pp. 76-81, Feb. 1977.

M2 P.J. Mabey, "Mobile radio data transmission-coding for error control", IEEE Trans. Veh. Technol., vol. VT-27, pp. 99-110, Aug. 1978.

VI SPREAD SPECTRUM SYSTEMS

VI-1 Spread Spectrum System Alternatives

Digital transmission via spread-spectrum multiple access (SSMA) involves each user's data stream modulating a wideband carrier signal [D1,D2]. The carrier occupies the entire available bandwidth. Each user is identified by a unique code (called an address) which is used by the receiver for recovery, by correlation techniques, of the transmitted signal. Other users' signals act as wideband interference which is often approximated for analysis purposes as wideband Gaussian noise. A SSMA channel is shown in Fig. 6-1.

There are two approaches commonly used for addressing. One approach involves generation of a pseudorandom rectangular-wave address waveform. The data message is modulated onto this pseudorandom waveform, which then modulates a harmonic carrier for transmission. Demodulation is via correlation of the received signal and the pseudonoise carrier.

The second approach involves code-division multiple-access (CDMA) which is alternatively referred to as random address discrete access (RADA). In CDMA the address waveform consists of a sequence of tones, unique to each user. This sequence is then modulated by the data signal, and demodulated either by matched filtering (which is equivalent to correlation) or by incoherent filtering.

In conventional narrowband systems, transmission cannot begin unless an unused channel is available. Once a channel is secured, however, transmission of data begins almost immediately following a relatively short synchronization delay. In SSMA systems, the channel is always immediately acces-

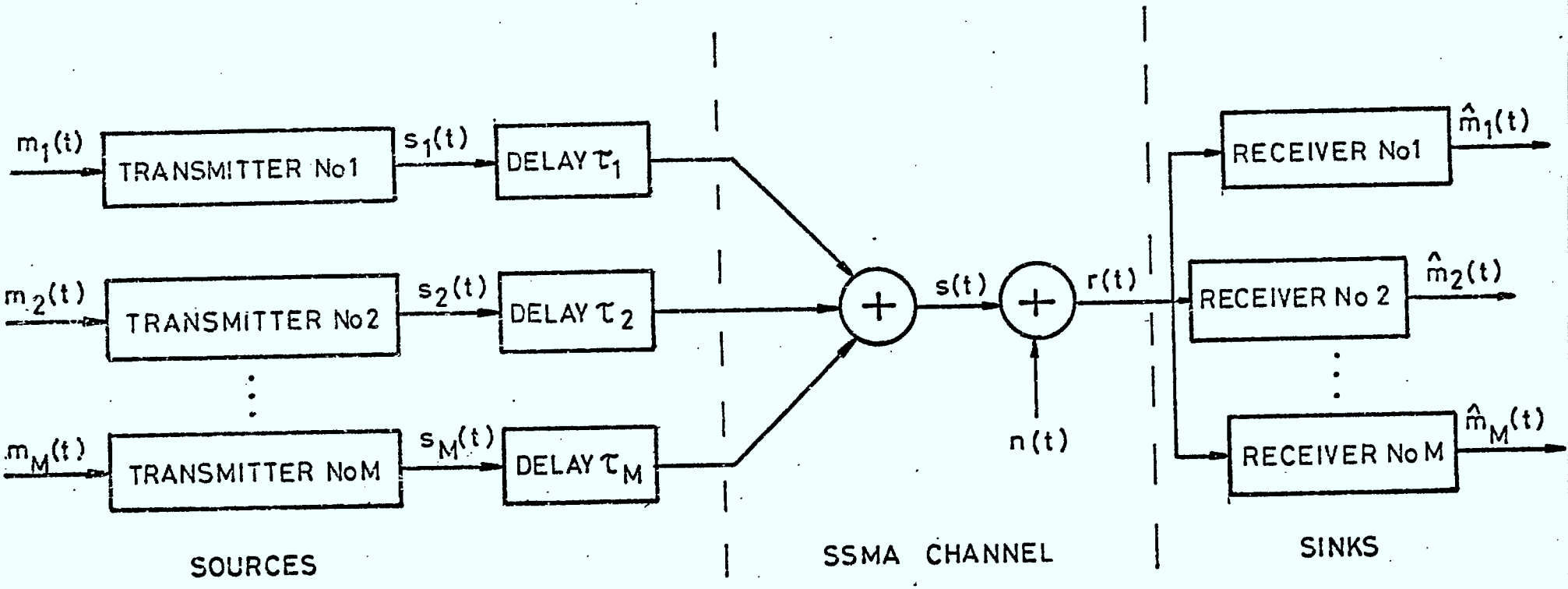

Fig. 6-1 SSMA channel.

sible. However, the carrier-to-noise ratio is well below unity and considerable time may be required for synchronization. In fact, when short interactive messages are being transmitted, the synchronization delay can be many times the time required for transmission of the actual message [L1]. In comparing SSMA and narrowband systems, the differences in synchronization performance is often overlooked.

Below is a summary, taken from [C1], which lists some advantages and disadvantages of SSMA for mobile communications:

Advantageous Features

1) The use of a large number of frequencies in each waveform results in a form of frequency diversity that significantly reduces the degradation in performance that normally arises from rapid fading.

2) Any user can access the system at any time without waiting for a free channel. Thus there are no blocked calls in the usual sense, although of course traffic will be ultimately limited by the available plant and its associated software.

3) There is no hard limit on the number of active users that can be handled simultaneously by the system. When the number of active users exceeds the design value, the result is a degradation of performance for all users rather than denial of access. This is usually referred to as "graceful degradation".

4) Since each potential user of the system is assigned a unique signal set, message privacy is achieved as a fringe benefit. This, of course, refers to privacy with respect to the casual listener

and does not preclude message interception by a properly equipped third party.

5) Because each user retains his unique signal set permanently, there is no channel switching or address changes as the user moves from cell to cell. Hence, the particularly objectionable characteristic of FM systems known as "forced termination", which occurs when a mobile crosses a boundary into a cell in which no channel is available, will not occur in this system.

6) Since all users occupy the same band, all user hardware is identical except for the filters associated with the unique signal set. (A recent feasibility study ... has shown that these receivers can be fabricated using existing CCD technology.)

7) Priority messages (e.g., public safety vehicles) can be accommodated in the system, even in the presence of system overload, without assigning dedicated channels or denying other users access to the system. This can be done either by increasing the power level, on an emergency basis, or by increasing the time-bandwidth product of the priority signal.

8) Under circumstances in which the full capacity of the system is not required, a spread-spectrum system may coexist in the same frequency band as conventional narrow-band systems without excessive mutual interference. This suggests the possibility that a spread-spectrum system could be phased into operation in a given geographical area without immediately obsoleting existing equipment operating in the same band. It is even possible that spread-

spectrum and narrowband schemes could coexist permanently, using the same band twice.

Disadvantageous Features

1) Effective power control is required in order to prevent users near the base station from overpowering more distant users. Preliminary studies indicate that a satisfactory power control system is realizable, however.

2) Message encoding and decoding is inherently more complex if full advantage of the available frequency diversity is to be achieved.

3) A vehicle-location technique, having modest accuracy, is required in order to adequately monitor the vehicle as it moves from cell to cell. However, some such facility is required of all the small-cell schemes that have been proposed; also, it is anticipated that location and power control circuitry will be essentially common in the receiver.

4) Fully coherent detection (i.e., true matched-filter detection) is not possible in a rapid fading environment.

5) The spread-spectrum approach does not appear to be particularly attractive for large-cell systems from the stand-point of cost-effectiveness. However, the operational advantages noted above would still apply in the large-cell case.

Another advantage, not specifically mentioned above is that shadowing, which has such an adverse effect on bit-error probability in conventional FDM systems is largely eliminated by the power control of mobile transmissions,

when transmission is from mobile to base. (In base-to-mobile transmission shadowing effects are less severe, since both signal and interference are subject to approximately the same shadowing variations, which are usually caused by objects near the mobile.) This power control compensates for level variations from shadowing and distance variations, but makes no attempt to adjust to the rapid changes in level due to Rayleigh fades.

The disadvantage of SSMA synchronization delay has already been discussed.

Some of the references at the end of this chapter include additional descriptions of SSMA systems.

VI-2 SSMA System Operation

Below we briefly describe the operation of frequency-hopped multilevel FSK (FH-MFSK). The description is taken directly from [G1]:

> The operation of the system may be understood by referring to Fig. 6-2. Every T seconds, K message bits are loaded into a shift register and transferred as a K-bit word X_m to the buffer. (The subscript m denotes one link in a multiuser sytem.) Assume for the moment that the modulo-2^K adder does nothing, so that X_m appears at the adder output, where it is used to select one of the 2^K different frequencies available from the tone generator. At the receiver, the spectrum of each T-second transmission is analyzed to determine which frequency, and hence which K-bit work X_m, is sent.
>
> The 2^K-ary FSK system just described is clearly not suitable for

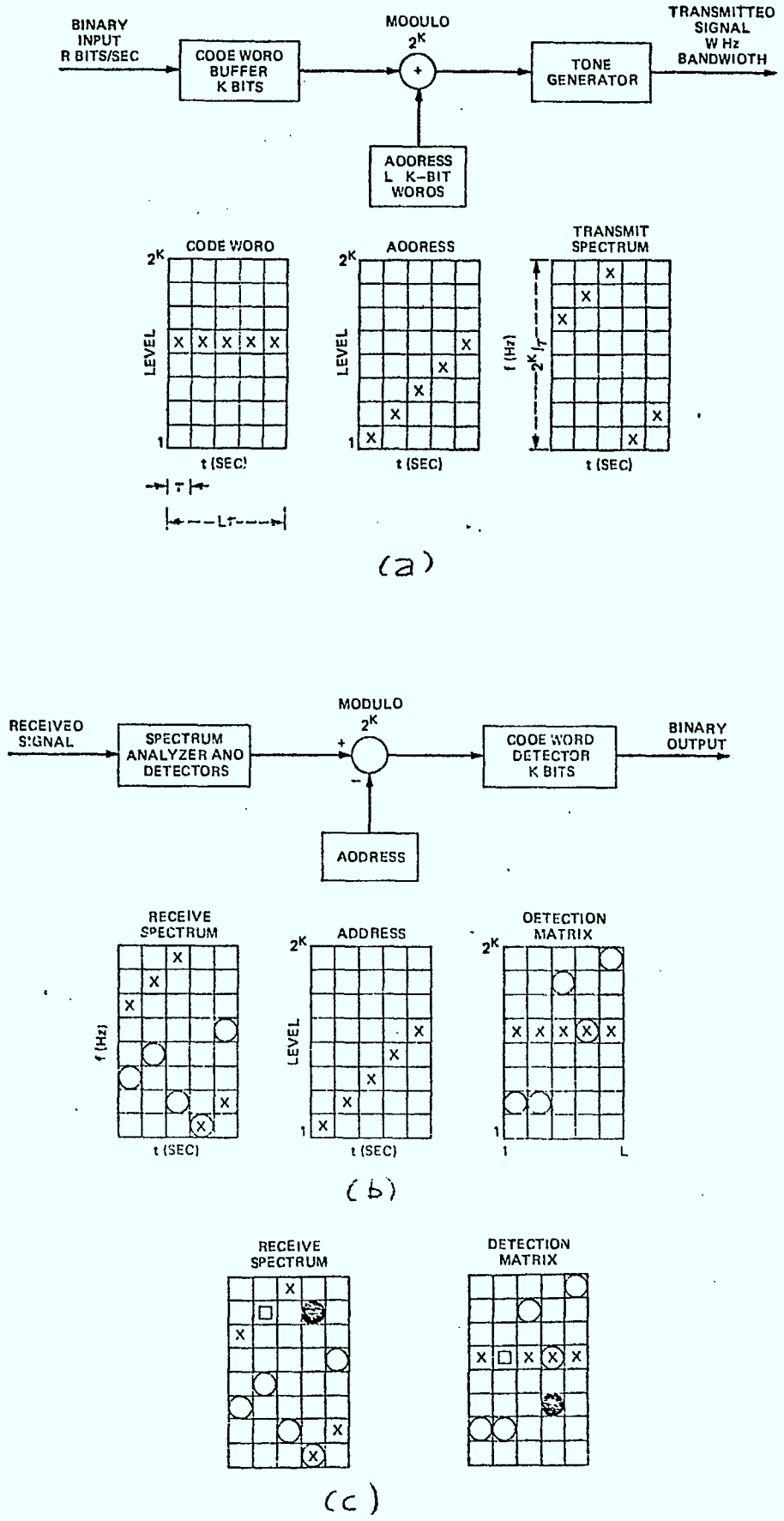

Fig. 6-2 FH-SSMA transceiver operations (from [G1]).
(a) Transmitter; (b) Receiver; (c) Detection.
● - denotes spurious entry. □ - denotes removal of X.
X - denotes signal.

multiple-user operation. If a second transmitter were to generate X_n, neither receiver m nor receiver n would know whether to detect X_n or X_m. However, by using address generators and modulo-2^K adders and subtractors, many links can share the same spectral band. Consider first an isolated link. During the basic signaling interval $T = L\tau$ seconds, an address generator in the transmitter generates a sequence of L numbers, each K bits long:

$$R_{m,1}, R_{m,2}, \cdots, R_{m,L} ,$$

at a rate of one number every $\tau = T/L$ seconds. Each $R_{m,1}$ is added modulo-2^K to X_m to produce a new K-bit number

$$Y_{m,1} = X_m \oplus R_{m,1}$$

which is used to select a transmitter frequency. (A circle around + (−) denotes addition (subtraction) modulo-2^K.) At the receiver, demodulation and modulo-2^K subtraction by the same number $R_{m,1}$ are performed every τ seconds, yielding

$$Z_{m,1} = Y_{m,1} \ominus R_{m,1} = X_m .$$

The sequence of operations is illustrated by the matrices of Fig. 6-2. Each matrix is either a sequency of K-bit numbers (code word, address, detection matrix) or a frequency-time spectrogram (transmit spectrum, receive spectrum). The matrices pertain to one link in a multiuser system. Crosses show numbers and frequencies generated in that link; circles show the contributions of another link.

If M links share the same frequency band, the detection and modulo-2^K subtraction produce extraneous entries in the 2^K-by-L

matrix of detected energy. Thus, as shown in Fig. 6-2, a word X_n transmitted over the nth link will be decoded by the receiver m as

$$Z'_{m,1} = X_n \oplus R_{n,1} \ominus R_{m,1} \quad .$$

When the address sequences $R_{n,1}$ and $R_{m,1}$ are distinct, the elements of $Z'_{m,1}$ are scattered over different rows. The desired transmission, on the other hand, is readily identified, because it produces a complete row of entries in the detection matrix. With many users, however, detection errors can occur in link m, even when all transmitted tones are received perfectly. This is because the tones of other users can combine to produce a complete row other than X_m in the detection matrix.

Noise and multipath propagation can influence the detection matrix by causing a tone to be detected when none has been transmitted (false alarm). In addition, the receiver can omit a transmitted tone from the detection matrix (miss). The effects of a false alarm and a miss are shown in Fig. 6-2. The squares indicate a missing tone in the transmitted code word; the solid circles indicate a false alarm. As shown, a miss can cause a detection matrix to have no complete row. To allow for this possibility, we use the majority logic decision rule: "Choose the code word associated with the row containing the greatest number of entries". Under this decision rule, an error will occur when insertions (tones due to other users and false alrams) combine to form a row with more entries than the row corresponding to the transmitted code word. An error can occur when insertions combine

to form a row containing the same number of entries as the row corresponding to the transmitted code word.

A spread-spectrum technique which uses PSK instead of FSK has also been proposed for mobile radio communication [C1,H1]. With this technique, each code word transmits K bits as a sequence of $L = 2^K$ tones. The preferred choice to date for K is K = 5. The user address is specified by the tone frequencies, and the source information is carried by the phases.

Figure 6-3 shows how a DPSK system might be implemented. A FSK implementation would be similar in complexity. However, the DPSK receiver's delay lines would be replaced by square-law devices, the N-chip delay would be removed from the transmitter, and an integrator would precede the binary phase modulator.

VI-3 SSMA System Performance

Because of power control at the mobile, all transmissions from within a cell arrive at the (central) base with equal power, averaged over Rayleigh level variations. All mobiles in other cells generate interference whose total power is approximately equal to that generated from within the cell [C1,C2].

Transmissions to any mobile from a base have the same average power level. However, mean signal levels from other bases vary with mobile location, due to changes in mobile-to-base distances. These level variations are moderate [H1,C1]; it is easy to show that over a cell's coverage area, the total interference power from six neighbouring base stations varies by a factor of 3 for n = 4 and 1.9 for n = 3. The effect of this variation is

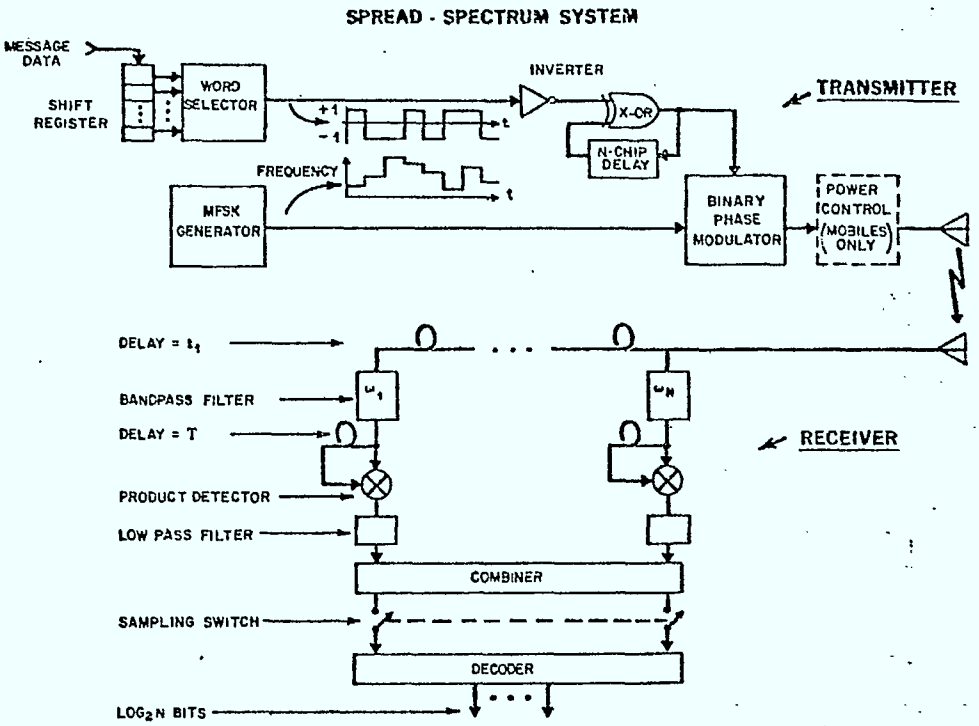

(a)

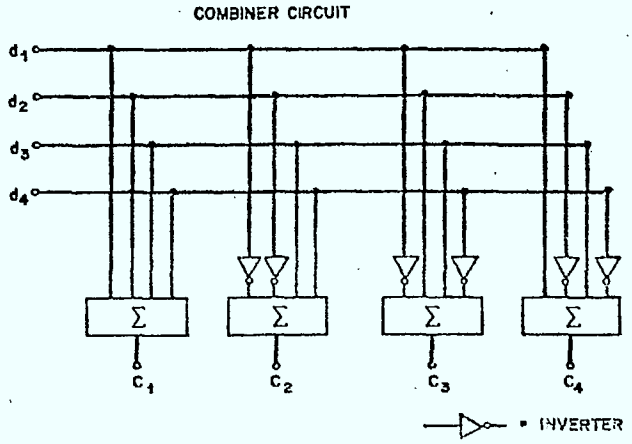

(b)

Fig. 6-3 FH-SSMA Implementation (from [H1]).

reduced by the (constant) interference level from the cell's own base. It has been shown that over 73% of a cell's service area upstream interference exceeds downstream interference, when this interference originates from outside the cell containing the wanted signal [C1,C2].

Two approaches have been used to obtain the SSMA bit-error probability [H1,G1]. One involves treating the interference as white Gaussian noise, to obtain the bit-error probability shown in Fig. 6-4, assuming K = 5 and L = 32 (see Fig. 6-2). In Fig. 6-4 ρ_f is the signal-to-interference ratio from the filters which detect each tone, assuming that all interference is from the cell containing the signal. In obtaining the FADE curve, each subchannel which transmits a tone chip was modelled as a narrowband Rayleigh channel of the type described in Chapter 2. Fading on each of these 2^K channels was assumed independent of that on other channels.

The spectrum efficiency O is obtained as follows, where K, L and τ are defined in Section 6-2, R is the bit rate, M the number of users per cell, and W the total system bandwidth [H1]:

$$R = K/L\tau \tag{6-1}$$

$$O = MR/W \tag{6-2}$$

$$= K/N\rho_f \tag{6-3}$$

From Fig. 6-4 one obtains $O \simeq 0.035$ for $\bar{p} \simeq 10^{-3}$ and $O \simeq 0.055$ for $\bar{p} \simeq 10^{-2}$. These values are entered in Table 6-1, and are for R = 32 kb/s.

An alternative approach was used by Goodman et al. [G1], which facilitated optimization of K and L. They found that in most situations $K \simeq \log_2(W/R)-1$, and that L was often best chosen to be less that the 2^K value used by Henry [H1] and Cooper and Nettleton [C1]. Goodman et al. stated [G1]:

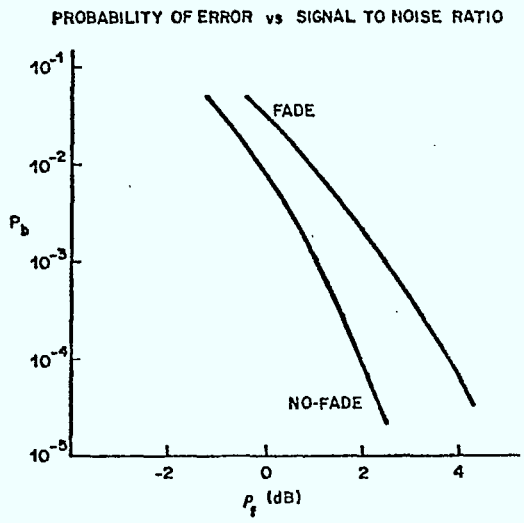

Fig. 6-4 Bit-error probability vs. matched-filter output signal-to-noise ratio (from [H1]).

			Narrowband		SSMA	
$\langle\bar{p}\rangle$	σ	ϕ*	16-cell (360° ill.)	7-cell (120° ill.)	FH-DPSK [H1]	FH-MFSK [G1]
10^{-3}	6	1.0	0.078	0.20	0.043	0.14
10^{-2}	9	"	"	"	0.063	0.17
10^{-3}	6	0.84/0.90	0.066	0.18	0.043	0.14
10^{-2}	9	"	"	"	0.063	0.17
10^{-3}	6	0.60/0.75	0.047	0.15	0.043	0.14
10^{-2}	9	"	"	"	0.063	0.17

* ϕ = 0.84/0.90 corresponds to a 625 channel system, with $P_B = 0.05$.
ϕ = 0.60/0.75 " " " 160 " " " " .
The / divides 16-cell result from 7-cell result.

Table 6-1 Spectrum Efficiency Comparisons.

"In fact, it would appear that the PSK system has been overdesigned in the sense that its redundancy allows it to perform adequately in poorer channels than might be expected in mobile radio. The price is an unnecessary limitation on user capacity."

These same comments would be applicable for the FSK system considered by Henry [H1].

Table 6-1 shows Q for the FH-MFSK system considered by Goodman, for the values K = 8 and L = 19, again with R = 32 kb/s. Each chip is sent via ON-OFF keying and detection is incoherent. For this system as well as for the one considered by Henry, the total bandwidth is W = 20 MHz. The results obtained by Goodman et al. are supported by Haskell [H1] who obtained Q ≃ 0.3, over a bandwidth range 1 < W < 35 MHz, for $\bar{p} \simeq 10^{-3}$. Haskell's results are based on all interference being from within the cell of the wanted signal, and would be reduced from this value for multiple-cell systems.

Table 6-1 shows that indeed, FH-MFSK with K = 8, L = 19 does result in threefold improvement in spectrum efficiency over the DPSK system with K = 5, L = 32.

VI-4 SSMA and Narrowband Transmission Compared

Table 6-1 indicates that for $\langle\bar{p}\rangle = 10^{-2}$ and $\langle\bar{p}\rangle = 10^{-3}$ efficiencies for SSMA with an isotropic base at cell centre and narrowband systems with 120° sectoral illumination are comparable. The SSMA results apply for R = 32 kb/s, and a change in R from this value may change Q.

It has been suggested that careful selection of SSMA address codes could improve O by 50% [G1]. Use of 120° sectoral illumination would also improve O threefold [C1,C2]. Use of switched diversity by multiple base sites for both reception and transmission would reduce signal level variations in narrowband systems, and would lead to improved spectrum efficiency. For example reduction in the shadowing variance from $\sigma = 12$ to $\sigma = 6$ dB reduces the bit error rate by a factor of ten (see Fig. 5-1). Channel encoding reduces the effects of Rayleigh fading, as explained earlier, unless the mobile is stationary in a deep fade location.

The spectrum efficiencies in Table 6-1 ignore the overhead involved in synchronization, retransmissions, sending of acknowledgements and in the case of narrowband channels, channel scanning. For direct-sequence SSMA, synchronization delay may be many times larger than the message duration [L1,L2], and this statement probably applies to FH-SSMA as well. The delay can be reduced by a parallel-search receiver, at the expense in receiver complexity [L1]. The synchronization delay for narrowband systems is normally much less than the message duration. A valid comparison of spectrum efficiencies requires a study of data transmission overheads, including SSMA synchronization delay. The statement that SSMA users gain immediate system access is somewhat misleading if synchronization first has to be established. The alternative of maintaining synchronization at all times is not very attractive, since the number of users in such a case would include the entire mobile population, even through only a small fraction would actually be transmitting message information. The result would be a very high level of interference.

The complexity and cost of SSMA systems would be much higher than the of narrowband systems, using present technology. Narrowband systems employ bit-by-bit transmission using FSK or DPSK. The receivers employ matched filters (DPSK) or envelope detectors (FSK). Synchronization circuitry is not complex. SSMA transmission involves grouping of K source information bits, modulo 2^K addition, and generation of tone sequences from a wideband frequency synthesizer. The receiver includes a wideband spectrum analyser, combining circuit, and a relatively complex decision device, together with complex synchronization circuitry. Power control at the mobile is required, and must operate over a very wide range to compensate for shadowing and distance changes. Both SSMA and narrowband systems require some mobile location capability.

Variations in average bit-error probability $\bar{p}$ are much less (ideally zero) for SSMA than for narrowband systems, because of mobile power control, and because of the large number of interfering signals. In practise, some limits on the range of mobile power variation would result, and some variation in $\bar{p}$ and some reduction in O would ensue. Notwithstanding, one of the positive benefits of SSMA is the minimal variation in $\bar{p}$.

Does SSMA provide for more flexibility than narrowband transmission? In transmission of voice, probably not. To accommodate alternative bit rates in narrowband transmission, different parts of the spectrum could be assigned different channel spacings. These channels could also be used for analog transmission whose spectral roll-off rate can be made comparable to that for MSK data transmission. In practise, two channel spacings Δ may be adequate, say 25 - 30 kHz and 10 - 15 kHz. In both cases $R \simeq \Delta$ (see Chapter 5). The

lower portion of the band could be for one spacing, with the remainder for the other spacing. The boundary could be moveable and set to encourage users to use the lower bit rate to obtain better service.

SSMA does permit a variation of rates along a continuum, and this feature may be useful for some data transmission applications. It is also possible to vary the rate to meet changing interference levels [C3], again at the cost of increased circuitry. However, narrowband systems also permit rate variation by changing the redundancy of a channel code, although the number of different rates possible here is somewhat restricted by decoder implementations; most multiple-error correcting decoders cannot be easily implemented. Again a few rates would be adequate in practise, and these could be realized using either SSMA or narrowband systems.

In summary, spectrum efficiencies for SSMA seem potentially higher than those for narrowband systems, because of constant average signal and interference levels. A more precise comparison requires careful study of data transmission overheads, including those related to SSMA synchronization. Present technology costs and complexity of SSMA implementation considerably exceed that for conventional narrowband systems, and it is not clear that future cost reductions would offset any operational advantages that SSMA may have.

VI-5 References for Chapter 6

C1 G.R. Cooper and R.W. Nettleton, "A spread spectrum technique for high-capacity mobile communications", IEEE Trans. Veh. Technol., vol. VT-27, pp. 264-275, Nov. 1978.

C2 G.R. Cooper and R.W. Nettleton, Spectral Efficiency in Cellular Land-Mobile Communications: A Spread Spectrum Approach. School of Elec. Eng. Tech. Rpt., Oct. 1978, Purdue Univ., W. Lafayette, Indiana, U.S.A.

C3 J.K. Cavers, "Variable rate transmission for Rayleigh fading channels", IEEE Trans. Commun., vol. COM-20, pp. 15-22, Feb. 1972.

D1 R.C. Dixon, Spread Spectrum Systems. New York: J. Wiley, 1976.

D2 R.C. Dixon, ed., Spread Spectrum Techniques. New York, IEEE Press, 1976.

E1 G. Einarson, "Address assignment for a time-frequency coded spread-spectrum system", Bell Syst. Tech. J., vol. 59, pp. 1241-1255, Sept. 1980.

G1 D.J. Goodman, P.S. Henry and V.K. Prabhu, "Frequency-hopped multilevel FSK for mobile radio", Bell Syst. Tech. J., vol. 59, pp. 1257-1275, Sept. 1980.

H1 P.S. Henry, "Spread spectrum efficiency of a frequency-hopped-DPSK spread-spectrum mobile radio system", IEEE Trans. Veh. Technol., vol. VT-28, pp. 327-332, Nov. 1979.

H2 B.G. Haskell, "Computer simulation results on frequency hopped MFSK mobile radio-noiseless case", IEEE Trans. Commun., vol. COM-29, pp. 125-132, Feb. 1981.

L1 V.C.M. Leung and R.W. Donaldson, "Confidence estimates for acquisition times and hold-in times for PN-SSMA synchronizer employing envelope correlation", IEEE Trans. Commun., vol. COM-30, Jan. 1982.

L2 V.C.M. Leung, Spread-Spectrum Multiple Access for Interactive Data Communications", Dept. of Electrical Engineering Ph.D. Thesis, University of British Columbia, Dec. 1981.

M1 L.B. Milstein, R.L. Pickholtz and D.L. Schilling, "Optimization of the processing gain of an FSK-FH system", IEEE Trans. Commun., vol. COM-28, pp. 1062-1079, July 1980.

M2 R.F. Mathis and R.F. Pawula, "A spread spectrum system with frequency hopping and sequentially balanced modulation - Part II: Operation in jamming and multipath", IEEE Trans. Commun., vol. COM-28, pp. 1785-1793, Oct. 1980.

P1 R.F. Pawula and R.F. Mathis, "A spread spectrum system with frequency hopping and sequentially balanced modulation - Part I: Basic operation in broad-band noise", IEEE Trans. Commun., vol. COM-28, pp. 682-688, May 1980.

S1 D.G. Schilling, L.B. Milstein, R.L. Pickholtz and R.W. Brown, "Optimization of the processing gain of an M-ary direct sequency spread spectrum communication system", IEEE Trans. Commun., vol. COM-28, pp. 1389-1398, Aug. 1980.

Y1 O-C. Yue, "Useful bounds on the performance of a spread spectrum mobile communication system in various fading environments", IEEE Trans. Commun., vol. COM-28, pp. 1819-1823, Oct. 1980.

Y2 O-C. Yue, "Frequency-hopping, multiple-access, phase-shift-keying system performance in a Rayleigh fading environment", Bell Syst. Tech. J., vol. 59, pp. 861-880, July-Aug. 1980.

APPENDIX - RELATIONSHIP BETWEEN MEAN AND MEDIAN SIGNAL LEVEL IN THE PRESENCE OF SHADOWING

The power, averaged over any Rayleigh fading, from a transmitted radio signal at distance r from the receiver is

$$\bar{P} = \ell^2/r^n \tag{A-1}$$

where ℓ^2 is the mean signal level. This level varies over a linear coverage range of approximately 50 cm. The level ℓ is lognormally distributed from the median level $\bar{Q}$, as follows.

$$L = 20 \log_{10} \ell \tag{A-2}$$

$$= 10 \log_{10} \ell^2 \tag{A-3}$$

$$\ell^2 = 10^{L/10} \tag{A-4}$$

$$= e^{cL} \tag{A-5}$$

$$c = \log_e 10/10 \tag{A-6}$$

The density function for L is

$$f_L(\Gamma) = \frac{1}{\sqrt{2\pi}\,\sigma} \exp\left[(\Gamma - \bar{Q})^2/2\sigma^2\right] \tag{A-7}$$

where σ is variance in dB. The mean signal level $\overline{\ell^2}$ is

$$\overline{\ell^2} = \int_{-\infty}^{\infty} e^{c\Gamma} f_I(\Gamma) d\Gamma \tag{A-8}$$

$$= \frac{1}{\sqrt{2\pi}\,\sigma} \int_{-\infty}^{\infty} e^{c\Gamma} \exp\left[-(\Gamma - \bar{Q})^2/2\sigma^2\right] d\Gamma \tag{A-9}$$

Completion of the square in the integrand's exponent yields

$$c\Gamma - (\Gamma - \bar{Q})^2/2\sigma^2 = -\frac{1}{2\sigma^2}\left[(\Gamma - \bar{Q})^2 - 2\sigma^2 c\Gamma\right]$$

$$= -\frac{1}{2\sigma^2}\left[(\Gamma - \bar{Q})^2 - 2\sigma^2 c(\Gamma - \bar{Q})\right] + c\bar{Q}$$

$$= -\frac{1}{2\sigma^2}(\Gamma - \bar{Q} - \sigma^2 c)^2 + c\bar{Q} + \frac{c^2\sigma^2}{2} \qquad \text{(A-10)}$$

Thus,

$$\overline{\ell^2} = \exp(c\bar{Q})\exp\left(\frac{c^2\sigma^2}{2}\right)\frac{1}{\sqrt{2\pi}\,\sigma}\int_{-\infty}^{\infty}\exp\left[\frac{-(\Gamma - \bar{Q} - \sigma^2 c)^2}{2\sigma^2}\right]d\Gamma$$

$$= \overline{q^2}\exp(c^2\sigma^2/2) \qquad \text{(A-11)}$$

where $\overline{q^2} = \exp(c\bar{Q})$. Clearly, only if $\sigma = 0$ does $\overline{\ell^2} = \overline{q^2}$.

Taking $10\log_{10}$ of each side of (A-11) yields

$$L/\bar{Q} = 10\log_{10}\exp\left[c(c\sigma^2/2)\right]$$

$$= 10\log_{10} 10^{(c\sigma^2/2)/10}$$

$$= \sigma^2/(2/c)$$

$$= \sigma^2/8.68 \qquad \text{(A-12)}$$

The following table shows the relationship between $\overline{\ell^2/q^2}$, $L/\bar{Q}$ and σ.

σ	$\overline{\ell^2/q^2}$	L/Q (dB)
0	1	0
3	1.27	1.04
6	2.60	4.15
9	8.57	9.33
12	45.6	16.6

Finally, consider n independent co-channel interfering signals with channel occupancy ϕ, interference coefficient $C_d(0)$, median (dB) power $\bar{Q}$, at separation distance d. Then the interference power

$$\overline{n^2} = \phi \sum_{i=1}^{n_i} (C_d(0)/d^n)\overline{\ell_i^2}$$

$$\bar{N} = 10 \log_{10} n^2$$

$$= 10 \log_{10} n_i \phi C_d(0) - 10 \log_{10} d^n + 10 \log_{10} \overline{\ell^2}$$

$$= 10 \log_{10} n_i \phi C_d(0) - 10 \log_{10} d^n + \bar{Q} + \frac{\sigma^2}{8.7} \qquad \text{(A-13)}$$

DONALDSON, ROBERT W.
--Frequency assignment for land mobile radio system in the 900 MHz band : suitability of new modulation techniques over land mobile channels.